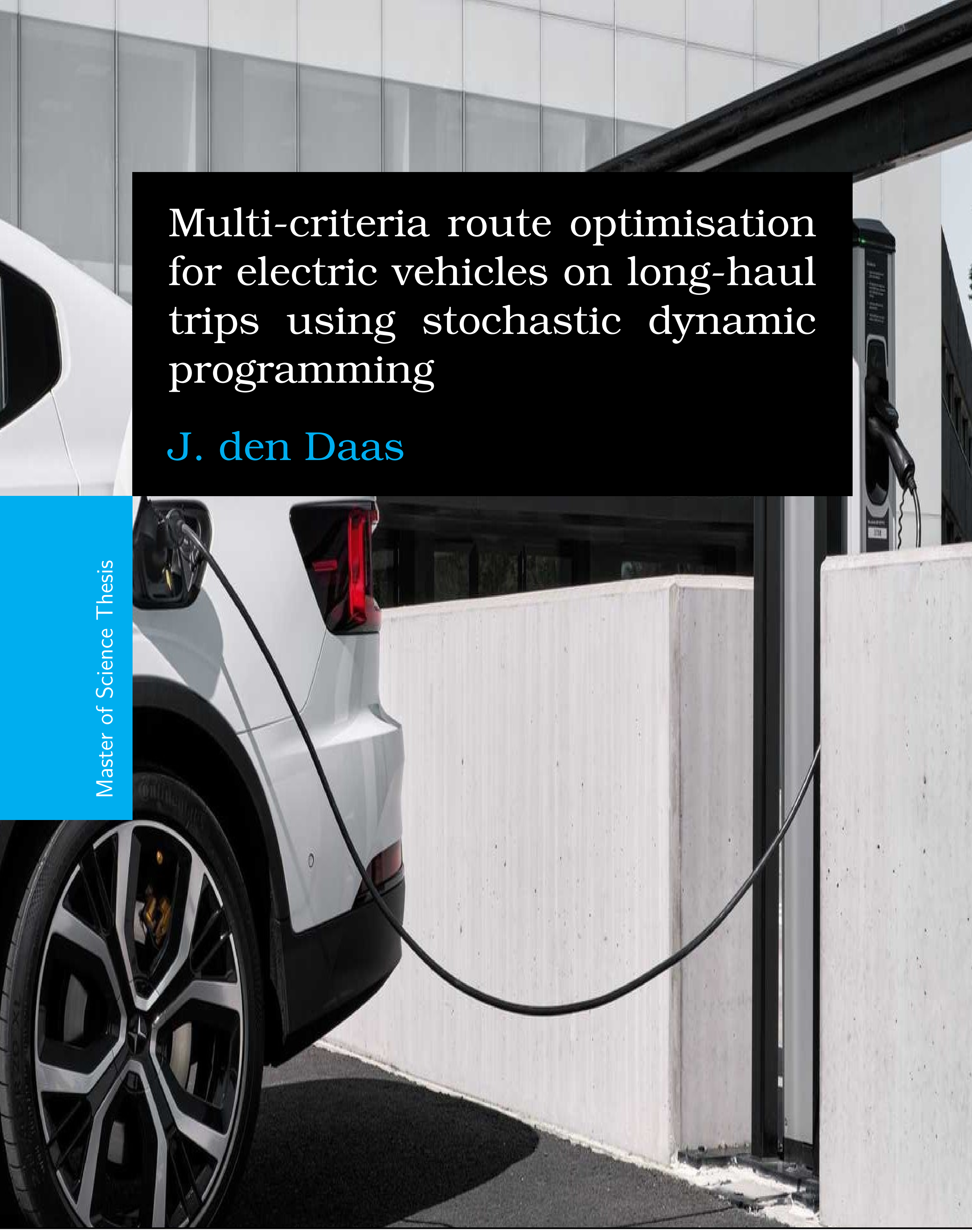

Multi-criteria route optimisation for electric vehicles on long-haul trips using stochastic dynamic programming

J. den Daas

Master of Science Thesis

Delft University of Technology

Delft Center for Systems and Control

Multi-criteria route optimisation for electric vehicles on long-haul trips using stochastic dynamic programming

Master of Science Thesis

For the degree of Master of Science in Systems and Control at Delft University of Technology

J. den Daas

February 11, 2022

Faculty of Mechanical, Maritime and Materials Engineering (3mE) · Delft University of Technology

Abstract

Stochastic Dynamic Programming (SDP) has shown promising results for sequential decision problems of the route optimisation for an Electric Vehicle (EV) with the presence of stochastic variables in the travel cost. However, in studies, the optimisation problem formulation for EVs has been lacking in detail. For example, possible waiting times at a Charging Station (CS) have been neglected. This thesis uses SDP to formulate a more holistic optimisation problem for EVs moving through a road network where travel speeds and charging station availability are stochastic. The goal is to optimise the travel costs, which consists of, e.g., the journey time and the charging cost, for an EV on long-haul trips.

In this thesis, four simulation-based case studies are conducted: (1) comparison of conventional navigation system with the proposed method; (2) speed optimisation in order to improve the travel costs; (3) charging platform selection in order to improve the travel cost; (4) uncertainty influence on the travel costs. The case studies are conducted to create insight into how the travel costs of an EV can be optimised. In these case studies, the influence of multiple factors has been taken into account and investigated. For example, cabin climate control, which is dependent on the ambient temperature, has a significant influence on the energy consumption of the EV resulting in higher travel costs.

The simulation results have shown interesting results. Compared to a Min algorithm, which uses a strategy to minimise the travel and charging time, the proposed method can find an optimal policy that is in some cases 5% shorter in terms of journey time. It is profitable for certain ambient temperatures and maximum allowable driving speeds in terms of journey time and charging cost to optimise the driving speed below the maximum allowed driving speed on highways. This results in a shorter journey time and saving charging costs. For example, for a maximum speed of 120 (km/h) and an ambient temperature of 20 °C, 3% of journey time advantage can be achieved by optimising the driving speed.

Table of Contents

List of Figures

List of Tables

Acknowledgements

This thesis has not been as expected due to the ongoing Corona pandemic. Being forced to work from home instead of on the Faculty of Mechanical Engineering has most definitely asked for a certain change in my mentality. This makes me even more proud of the final result, and therefore I would like to thank some people who have helped me along the way.

First of all, I would like to thank my supervisor Azita Dabiri for asking critical questions during our meetings, providing helpful feedback and insights on my work, thinking along, and pushing me in the right direction when needed.

Also, I would like to thank Viktor Larsson and Mitra Pourabdollah from Volvo for their support, feedback, insights from the field and our interesting discussions on the topic of electric vehicles. My final result would have never been so applicable without you.

Thanks to Jaap, Roel, Cas, Bart and Floris for spending all this time at home with me, having coffee breaks, a good laugh and all other distractions at home during the thesis.

I want to thank Charlotte, Laura and in particular my parents, Paul and Marian, for their unconditional support, enabling me to make my own choices, and for keeping me motivated. Without you, I would have never written this thesis or completed my studies. Thank you.

> "Education is the most powerful weapon which you can use to change the world."
>
> — *Nelson Mandela*

Delft, University of Technology — J. den Daas
February 11, 2022

Chapter 1

Introduction

Dependence on petroleum contributes to severe environmental and energy problems. One of the significant contributors to energy consumption and greenhouse gas emissions is the transportation sector. A study from the International Energy Agency indicates that the transportation sector contributes 28% of global energy consumption and 23% of global greenhouse gas emissions [18]. A promising solution lies in the usage of EVs since these have better characteristics compared to conventional Internal Combustion Engine Vehicles (ICEV) such as high energy efficiency and emission reduction, which both can contribute to reduced global warming. Primarily if the energy used for the charging of EVs is obtained from renewable energy sources, their usage can make a significant impact [21].

However, one of the challenges that have to be overcome for the stimulation of EV adaption is range anxiety [2, 17, 22, 4]. Range anxiety refers to EV drivers concerned about running out of battery energy on trips, or that much charging is required during the travel. The lack of charging infrastructure strengthens this range anxiety while not offering charging security. Moreover, the charging time associated with EV driving also leads to range anxiety. For example, if someone is in a hurry to reach a specific destination and has to charge the battery of the EV to reach the destination. The charging time could lead to the destination not being reached in time. To overcome range anxiety, route planning for EVs is of high importance. With accurate route planning, the charging processes can be included, and the EV driver will be given detailed instructions for reaching the destination, lowering the range anxiety.

The route planning for EVs is much more challenging than for ICEV. Due to the lacking charging infrastructure for EVs, the energy consumption of the EV is of much higher importance compared to ICEV. EVs will deliberately have to plan where to charge since, in contrast to ICEV, battery recharging takes significantly more time than refuelling. On top of that, because there is a lack of charging infrastructure for EVs, many EVs will arrive at the same CS, which can lead to charging poles being taken. Since the charging process takes at least 30 minutes to charge from 20% State of Charge (SoC) to 80% SoC [13, 7], this can cause waiting times to arise at CSs. The selection of a CS can therefore have a high impact on the travel time of an EV and is thus a delicate problem.

The route guidance systems for the EV have evolved over the years. The systems mainly differ in the way the traffic information, such as the traffic speed and density or the waiting times at a CS, is handled. The proposed approaches in the literature all seem to share a similar objective function, reaching the destination of the EV with minimal travel costs. The travel costs are, however, formulated differently among the presented literature. For example, in [28], the used energy of the EV en route is minimised, while in [27], the travel costs consisting of the travel time, energy consumption and charging costs, are minimised.

The literature shows the most significant distinction in how CS characteristics are modelled, such as charging costs, charging time, and charging demand. Since the charging demand of EVs has a stochastic nature, the literature seems to find it hard to incorporate this demand in their methods. Historical data has the disadvantage that it can be temporary and spatially bounded, which makes it unusable for a general case. Therefore, some literature assumes that some of these essential characteristics are a fixed variable or do not take these characteristics into account. For example, in [12], only the selection of a CS with a specific charging efficiency is taken into account. The method does not provide any information on the CS properties, such as the energy price or the waiting time at the CS. To simulate the amount of EVs present in a CS for charging, the method presented in [27], makes use of a fixed arrival rate of EVs at a CS. In this way, the method includes the waiting time at a CS in their solution. The more recent literature tackles the problem of charging demand with real-time communication systems. With the use of an Intelligent Transportation Systems (ITS), EVs and CSs can communicate with each other. Due to this communication, the EVs can reserve a charging spot at a CS for a specific moment, such as in [10], or the EV driver can see the current waiting time at a CS, such as presented in [7]. The latter has a disadvantage that if a disturbance occurs on the way to the CS, which will impact the arrival time at the CS, the reservation of a charging spot or the expected waiting time at arrival has become useless.

To solve the route guidance problem of EVs Dynamic Programming (DP) is one of the methods that is mainly used. In specific, problems that encounter stochastic variables use SDP. SDP has shown excellent results in providing route guidance for EVs in, for example, [9, 14] it is used to find an optimal route for EVs. It is a promising control method for the route guidance of EVs since: (1) it can coordinate and control multiple control objectives at the same time, which makes it able to control, e.g., both the amount of energy to be charged at a CS and the following link the EV will travel; (2) constraints can be added, such that the solution is feasible, e.g. the EV will not run out of energy during the route; (3) it allows stochastic variables in the optimisation, e.g., stochastic driving speeds and waiting times can be used.

1-1 Problem statement

In recent studies, the focus lies on lowering the travel costs, such as the driving, charging and travel time [12, 27, 10, 7, 9, 14] in order to overcome range anxiety; however, these studies have overlooked the characteristics of CSs such as possible waiting times and the significant impact of the charging process and its role in the route planning problem. Since most EV drivers make use of charging recommendations, such as in [22], or routing and charging point reserving systems, such as in [4], EV clustering at CSs can take place. This causes long waiting times at CSs, contributing to overall travel time. However, the lack of charging infrastructure combined with busy CSs at specific times of the day results in a long waiting time at CSs.

In this thesis, the expected travel costs of an EV moving from origin to destination will be minimised. The novelty of this thesis lies in the approach regarding the waiting times at CSs and the inclusion of all aspects that influence the travel costs of an EV, which will be discussed later.

SDP has proven to be an effective algorithm to solve decision-making problems under different circumstances. These circumstances are related to the available traffic information, which can be deterministic, using DP, but for SDP methods, this information can be stochastic as well. The main goal of this thesis will be to investigate how the travel costs of an EV can be minimised. This goal will be reached by answering the following main research question:

> How can the travel cost of an electric vehicle on long haul trips, with historical charging occupancy information and historical average road network travel speeds, be minimised?

The following sub-questions are used to answer the main research question:

1. *What factors influence the travel costs of the Electric Vehicle on long-haul trips?*

   Which factors are important for the travel costs that the EV incurs during a long-haul trip. Next to the obvious costs, such as the charging cost, are there any factors that have a significant influence on the travel costs or certain decisions that have to be made during the navigation of EVs on long-haul trips?

2. *How can Stochastic Dynamic Programming be used to optimise the travel costs of an Electric Vehicle?*

   What possibilities arise using SDP to further optimise the EV's travel costs on long-haul trips. Are there new insights that can be created regarding the costs that influence the route optimisation of EVs, which potentially could change the way it is now, in general, looked at the way the optimal route for an EV is created?

1-2 Thesis outline

The outline of this thesis is as follows. The used electric vehicle model and all of its components are explained in Chapter 2. In Chapter 3, the road network and charging infrastructure model will be discussed. This includes all the costs that are incurred for an EV during the route. Next, the methodology concerning SDP will be presented in Chapter 4. In Chapter 5, parameter sensitivity studies will be executed as well as verification of the proposed method and validation of the suggested simplification. The conducted case studies will be elaborated in Chapter 6, among the results is comparing the performance of the proposed method with a conventional method to optimise the travel costs of EVs. This thesis is concluded with an overall discussion, conclusions, and suggestions for future work in Chapter 7.

Chapter 2

Electric Vehicle Model

In this chapter, the EV model will be discussed. It will be discussed what parts the energy consumption of an EV consists of and how this is modelled in the thesis. Multiple factors influence energy consumption, e.g., cabin climate control and the propulsive power demand.

Moreover, it will be discussed how the charging time of an EV is modelled. For the charging time, various factors influence this process, e.g., the battery temperature and the available charging power.

Lastly, it will be discussed how the battery temperature is modelled. The battery temperature is of importance, while it has numerous effects. Among these effects is that the temperature can influence the charging speed. However, it also affects the safety of EV passengers. High battery temperatures can cause thermal runaway and an explosive battery fire in the worst case. However, high battery temperatures are generally avoided because this decreases the battery lifetime. Therefore, the battery temperature must be incorporated in the model and the possibility to heat or cool the battery if required. In this chapter, the used battery thermal model and the battery's thermal heating and thermal cooling are discussed.

2-1 Energy Consumption

Many factors influence the energy consumption of an EV. The prediction of energy consumption is important because this influences the moment and place for the charging process. In this section, the factors that contribute to the energy consumption of the EV will be elaborated.

First, there is the propulsive power demand. This is the energy that is required to move the EV. Multiple aspects affect the propulsive power demand required to move the EV. For example, during the acceleration of the EV, there is more propulsive power demand required compared to the situation where the EV is driving at a constant speed. Moreover, if there are elevation differences on the road segment, this can impact the propulsive power demand to keep the same speed for the EV. For simplicity, it is assumed that there are no elevation

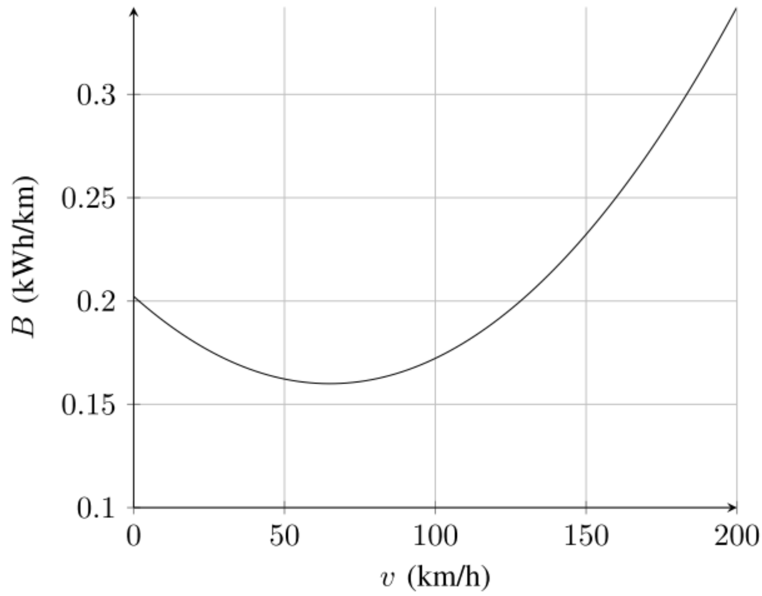

Figure 2-1: Example of energy consumption B_{v} based on driving speeds v_{ij} [23].

differences and that the EV is driving at a constant speed. Therefore, a relation between the average driving speed and the energy consumption for the propulsive power demand is used. An example of such a relation is given in Figure 2-1.

For each speed, a specific energy consumption B_{v} is present. This energy consumption represents the number of kWh per driven km. To determine the energy that is required for the propulsive power demand to advance over a segment, denoted by e_{p}. The length of this segment has to be multiplied with the energy consumption rate based on the driving speed given by:

$$e_{\mathrm{p}} = d * B_{\mathrm{v}}, \tag{2-1}$$

where d the length of the segment, and:

$$B_{\mathrm{v}} = f_{\mathrm{e}}(v). \tag{2-2}$$

In Eq. (2-2), the function $f_{\mathrm{e}}(v)$ gives the energy consumption rate B_{v} based on the driving speed.

Aside from the propulsive power demand, there is also energy consumption because the cabin climate has to be regulated. The cabin climate control energy consumption is quite substantial on the total energy consumption [19]. The amount of energy spent on the cabin climate control depends on the ambient temperature and the time the cabin climate control is active. More cabin climate control is required for very cold and very hot ambient temperatures. An example of a relation between the ambient temperature and the power for the cabin climate

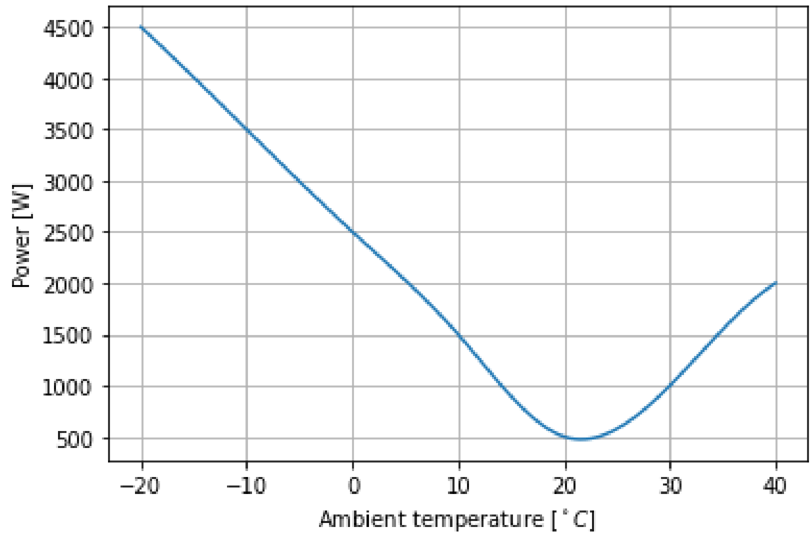

Figure 2-2: Relation between the ambient temperature and the power required for the cabin climate control.

control is given in Figure 2-2. The required energy for the cabin climate control during a time period τ is given by:

$$e_{\mathrm{cc}} = \tau * B_{\mathrm{cc}}, \tag{2-3}$$

where B_{cc} is the cabin climate control rate and is given by:

$$B_{\mathrm{cc}} = f_{\mathrm{cc}}(T_{\mathrm{ambient}}). \tag{2-4}$$

In Eq. (2-4), $f_{\mathrm{cc}}(T_{\mathrm{ambient}})$ is a function that gives the energy consumption rate for the cabin climate control based on the ambient temperature.

Next to the cabin climate control, there is also the energy required for the thermal heating and cooling of the battery, which will be explained in detail in Section 2-3. This heating or cooling of the battery is present while driving. Therefore, the energy consumption for the heating or cooling of the battery is given by:

$$e_{\mathrm{B}} = \tau * B_{\mathrm{b}}, \tag{2-5}$$

where τ is a given time period and B_{b} is the cooling or heating rate of the battery.

Lastly, there is base-load present due to the auxiliary energy consumption, for example, for all electronics on board of the EV. The energy consumption for a given time period due to this base-load is given by:

$$e_{\mathrm{a}} = \tau * B_0, \tag{2-6}$$

where B_0 is the base-load.

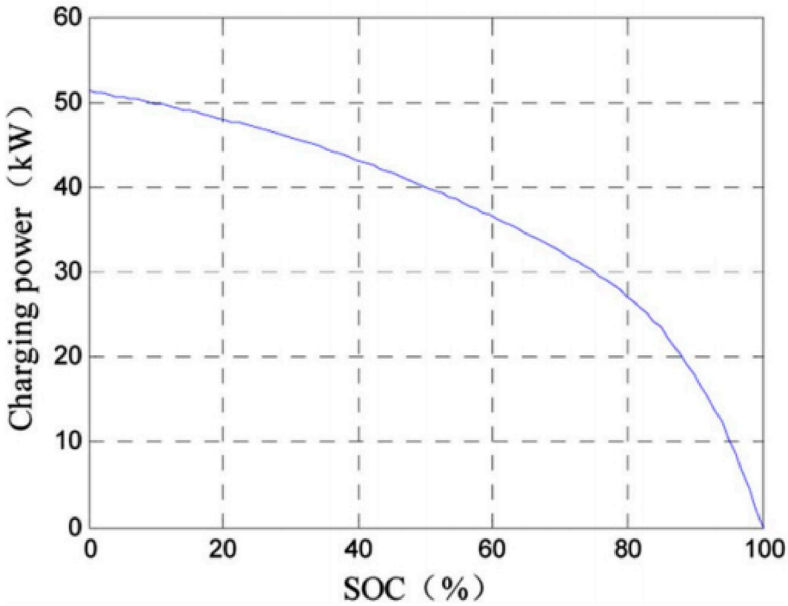

Figure 2-3: Charging profile of a Nissan Altra EV [3].

2-2 Charging Time

When an EV is about to run out of battery energy capacity, the battery has to be recharged. In contrast to ICEV, this process takes much longer. The charging takes place at a CS, where the EV driver must plug in their EV to a charging pole. The charging time depends on multiple factors. In this section, it will be explained how this charging time can be calculated.

The amount of energy to be charged depends on the arrival energy at the CS of the EV, which is given by e. The departure energy of the EV at the CS is denoted by e'. Therefore the amount of energy that is charged, denoted by Δe, is equal to:

$$\Delta e = e' - e. \tag{2-7}$$

The energy to be charged is linked to a certain charging time, denoted by τ_c. The temperature of the battery upon arrival at the CS, denoted by T, has a big influence on this charging time since the battery temperature influences the charging speed that can be achieved. For example, a very cold battery (0 °C) charges much slower than a warm battery (30 °C). Furthermore, the charging speed also depends on the State of Charge (SoC), the battery capacity level, of the battery. A low SoC battery charges faster than a high SoC battery. The SoC namely influences what the maximum effective charging power, denoted by p_cs, can be. The higher the SoC, the lower the maximum effective charging power. An example of a charging speed profile is shown in Figure 2-3. In this figure, it can be seen that the maximum effective charging power drops fast when reaching high SoC. This means that the charging speed decreases if the SoC increases.

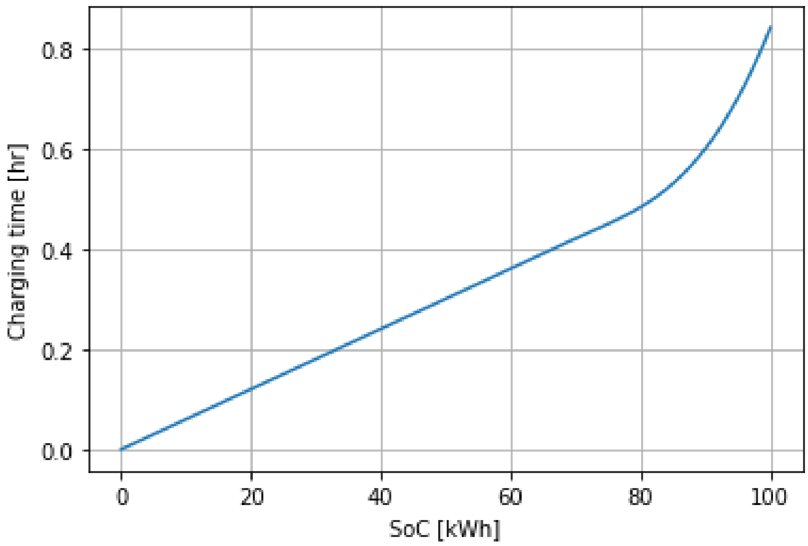

Figure 2-4: Charging time relation with SoC.

An example of the relation between the charging time, depending on the departure energy and the arrival energy, is given in Figure 2-4. One can calculate the charging time with this relation by subtracting the required charging time of the departure SoC with the required charging time of the arrival SoC. This charging time model, based on [23], assumes a linear charging time up to 80 % SoC, where after the charging time becomes non-linear. In Figure 2-4 a charging speed of 40 kW is used as example. An example of the charging speed, of which the function is denoted by $f_\mathrm{c}(\Delta e)$, in relation to the SoC, is given by:

$$f_\mathrm{c}(\Delta e) = \begin{cases} \Delta e/p_\mathrm{cs} & \text{if } \ 0 < \mathrm{SoC} \leq 80, \\ 1.25 * \Delta e/p_\mathrm{cs} & \text{if } 80 < \mathrm{SoC} \leq 90, \\ 1.75 * \Delta e/p_\mathrm{cs} & \text{if } 90 < \mathrm{SoC} \leq 100, \end{cases} \tag{2-8}$$

where p_cs is the charging power provided by the CS. The charging time is also dependent on the battery temperature, an example of the relationship between the charging time and battery temperature is given by:

$$\tau_\mathrm{c} = \begin{cases} \infty, & \text{if } T \leq 0, \\ (T_\mathrm{min}/T) * f_\mathrm{c}(\Delta e), & \text{if } 0 < T < T_\mathrm{min}, \\ f_\mathrm{c}(\Delta e), & \text{if } T \geq T_\mathrm{min}. \end{cases} \tag{2-9}$$

From Eq. (2-9) it can be seen that for battery temperatures lower than or equal to 0 degrees Celsius the charging time becomes infinity. For temperatures lower than T_min, which is a temperature that can be set arbitrary, the charging time increases with a factor $T_\mathrm{min}/T > 1$.

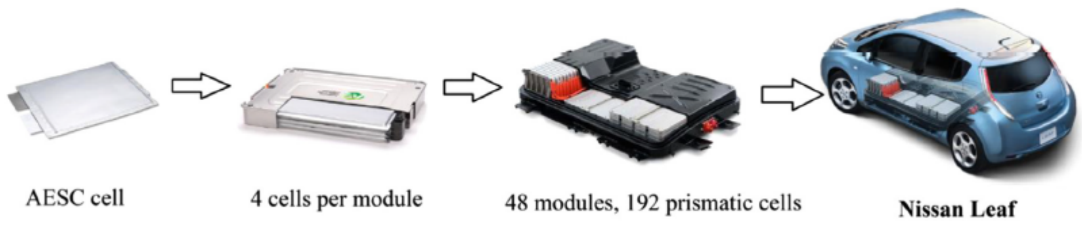

Figure 2-5: Lithium-ion battery cell-, module-, and pack-level of a Nissan Leaf [26].

2-3 Battery Thermal Model

To control the battery temperature, a battery thermal model can be used. There are various thermal modelling approaches, such as a lumped capacitance thermal approach, numerical and analytical thermal models and equivalent circuit thermal models. In [24] the advantages, disadvantages and recommended applications of these modelling approaches have been investigated. Considering the scope of this research and taking in mind the recommended applications described in [24], the lumped capacitance thermal approach will be used. Mainly the fact that a fast processing time can be achieved using this model while at the same time the model can predict the thermal behaviour of the battery in a satisfactory manner gives rise to picking this sort of model.

With the lumped thermal capacity model, it is assumed that the battery remains at a uniform temperature while undergoing a transient thermal response. We may ignore minor differences in temperature within the battery. The assumed uniform temperature of the battery can be specified in terms of changes in the internal energy of the battery. The heat transfer from the battery to the surroundings and vice versa might happen via conduction, radiation, or convection. To model the battery temperature of the EV, we start with the energy balance of the battery, which is given by:

$$m_{\mathrm{b}} C_{\mathrm{p}} \frac{dT}{dt} = Q_{\mathrm{in}}(t) - Q_{\mathrm{out}}(t), \tag{2-10}$$

where m_{b} is the battery mass, C_{p} is the specific heat capacity, T is the battery temperature, $Q_{\mathrm{in}}(t)$ is the heat generated at time t and $Q_{\mathrm{out}}(t)$ is the heat dissipation from the battery at time t. The battery mass consists of the mass of all cells that are present within the battery. In Figure 2-5, one can see that a battery pack consists of multiple modules and the modules consist of a number of cells. Therefore, the battery mass, denoted by m_{b}, is given by:

$$m_{\mathrm{b}} = n_{\mathrm{m}} * n_{\mathrm{c}} * m_{\mathrm{cell}}, \tag{2-11}$$

where n_{m} represents the number of modules contained in a battery pack, n_{c} is the number of cells present in a module and m_{cell} is the mass of a single battery cell. In the following of this section, it will be discussed how the heat generation and heat dissipation at time t are defined and how the battery can either be cooled or heated.

In the case of having a battery temperature that is lower than the desired temperature, one would like to heat the battery. Looking at Eq. (2-10), in order to achieve a battery heat increase, the heat generation Q_{in} has to be larger than the heat dissipation Q_{out} at time t.

Figure 2-6: Example of an air controlled battery pack temperature regulator [8].

There are multiple ways to create an external heat dissipation into the battery. Examples of this kind of heating system are air heating systems or refrigerated heating systems. An example of an air heating system is given in Figure 2-6, in this figure, one can see that ambient air is blown through a Heat, Ventilation and Air Conditioning (HVAC) system, which can heat the air. This hot air can then be used to heat the cabin and the battery pack.

When the battery temperature is higher than the desired temperature, active cooling of the battery has to occur. Eq. (2-10), in order to achieve a battery heat decrease, the heat generation Q_{in} has to be smaller than the heat dissipation Q_{out} at time t. When cooling the battery, there is passive cooling and active cooling. Passive cooling of the battery takes place due to, for example, convection and radiation. However, this passive cooling might not be sufficient to cool the battery down to the desired temperature within a certain time period. Active cooling might then be required from an external source. This external cooling can, for example, be the same as in Figure 2-6, where instead of heating the ambient air, the ambient air is cooled down such that the battery pack loses heat.

2-4 Conclusions

In this chapter, the EV model has been discussed. The energy consumption consists of the propulsive power demand, which depends on the driving speed, the cabin climate control, which depends on the ambient temperature, and the auxiliary load. Together, these factors determine the energy consumption of an EV while driving.

The charging time is dependent on the amount of energy to be charged, the available charging power, the SoC at the start and end of the charging process, and the battery temperature at the start of the charging process. A non-linear relation is used in order to determine the charging time.

The battery temperature can affect the travel cost for an EV, while too low temperatures have a negative effect on the charging process. However, also too high temperatures can impose safety dangers. Therefore, the heating or cooling of the battery is required to guarantee a safe trip or to optimise the travel cost of an EV. The thermal model presented in this chapter can be used to model the battery temperature and the cooling or heating of the battery to the extent required for this purpose.

Chapter 3

Road Network and Charging Infrastructure Model

This chapter will discuss the model for the road network and charging infrastructure. The costs incurred for an EV during the route will be explained. These costs consist of costs that are incurred at a CS but also of costs that are incurred while driving from a CS to another CS. First, it will be explained how a network for the optimisation is constructed, and then the specific costs will be discussed.

3-1 The Network

The route optimisation takes place between an *origin* and *destination*. It is assumed that this origin and destination, referred to as o and d subsequently, are both present in a network with *directed* edges. These directed edges connect the nodes, representing either a single CS or a cluster of CSs. The edges represent roads, which can, for example, be highways or provincial roads that connect the CSs. Since the edges are directed, the road can only be used in one direction. For example, in Figure 3-1 one can travel from origin o to CS 1, but not from CS 1 to origin o.

We assume that a network is defined as a directed graph $G = (\mathcal{N}, \mathcal{A})$. Nodes in the network are given by $i \in \mathcal{N}$, whereas an arc between node i and j is given by $(i, j) \in \mathcal{A}$. Each CS in the network represents a decision point, the decision that can be made consists of multiple criteria. Each edge in the network has a certain cost attached to it. This cost of an edge can have both deterministic and stochastic parts. In the remainder of this section, these costs will be elaborated.

3-2 Edge Cost

First, the edge cost will be discussed. This is the cost incurred when travelling from one node to another node. Essential for the edge cost are the edge length, the driving speed, the energy

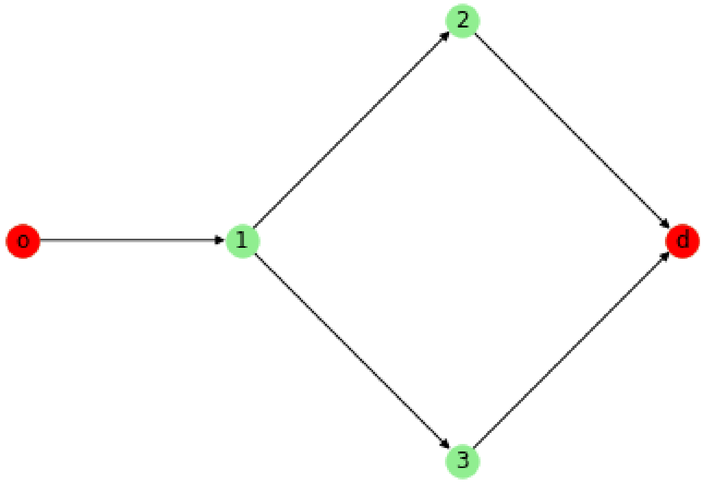

Figure 3-1: Example of a network with directed edges and nodes.

consumption and the travel time, which will be explained in the following.

3-2-1 Edge Length

Each edge in the network has a specific length, denoted by d_{ij} (km). This length is deterministic and will not change. It represents the distance between node i and node j. The length of each edge is contained in set D, such that $d_{\mathrm{ij}} \in D$. Possible elevation in link segments is neglected.

3-2-2 Driving Speed

Next to the length of each edge, a certain driving speed is present. This driving speed is assumed to be the average driving speed for the whole edge length. However, this driving speed is not deterministic. It is only possible to predict a certain driving speed incurred for a certain edge at a specific time. Therefore, each edge has a certain probabilistic driving speed, which is dependent on the time, denoted by t. The expected driving speed, denoted by $\bar{v}_{\mathrm{ij}}$ (km/h), of an edge with probability distribution $P_v(t)$ is given by:

$$\bar{v}_{\mathrm{ij}} = E\{v_{\mathrm{ij}}(t)\}, \tag{3-1}$$

where:

$$E\{v_{\mathrm{ij}}(t)\} = \sum_{i=1}^{n} v_{\mathrm{i}} p_{\mathrm{i}} \in P_{\mathrm{v}}(t) = v_1 p_1 + v_2 p_2 + \ldots + v_{\mathrm{n}} p_{\mathrm{n}}. \tag{3-2}$$

In Eq. (3-2), the expectation of v_{ij} is expressed as the weighted sum of the possible speeds, denoted by v_{i}, with their probabilities to occur, denoted by p_{i}, as weights. Since $p_1 + p_2 +$

$... + p_{\mathrm{n}} = 1$, this weighted sum can be used. However, this only holds if the random variable, denoted by v_{ij}, has a finite number of outcomes. The probability distribution $P_{\mathrm{v}}(t)$ depends on the time t, while for different time intervals the expected speed can differ severely. For example, during rush hour the expected speed can be lower than during hours outside the rush hour.

3-2-3 Travel Time

The travel time between node i and node j, denoted by τ_{ij}, is dependent on the expected driving speed. Therefore, the travel time can change based on the time of day. The travel time is the drive time between the two charging stations and thus represents the time spent from leaving node i and arriving at node j. This travel time is given by:

$$\tau_{\mathrm{ij}} = \frac{d_{\mathrm{ij}}}{\bar{v}_{\mathrm{ij}}}. \tag{3-3}$$

3-2-4 Energy Consumption

Based on the expected driving speed, the energy consumption for the propulsive power demand of an edge should be calculated. The expected driving speed is used because the energy consumption differs for different driving speeds, as discussed in Section 2-1. The energy consumption of an edge is denoted by e_{ij} [kWh], based on the expected driving speed the share of energy consumption for the propulsive power demand is equal to:

$$e_{\mathrm{ij}} = d_{\mathrm{ij}} * B_{\mathrm{v}}, \tag{3-4}$$

This energy consumption is based on the expected driving speed. Therefore the energy consumption per edge can be different based on the time. Next to the propulsive power demand, there is also energy consumption because the cabin climate has to be regulated, the battery is actively heated or cooled, and an auxiliary load is present. All of these energy consumption's are present while driving. Therefore the energy consumption has to be multiplied by the travel time, described in Eq. (3-3). The total energy consumption between node i and node j is given by:

$$e_{\mathrm{ij}} = d_{\mathrm{ij}} * B_{\mathrm{v}} + \tau_{\mathrm{ij}} * (B_0 + B_{\mathrm{c}} + B_{\mathrm{b}}), \tag{3-5}$$

3-3 Node Cost

Next to the edge cost, there is also the node cost. This is the cost that is incurred at a node in the network. For the node cost, essential factors are the waiting time, the charging time and the charging cost, which will be discussed in the following.

3-3-1 Charging Time

Each node in the network represents a decision point. For example, a decision regarding the amount of energy charged in the current node and to which node is travelled next has to be taken. The amount of energy to be charged depends on the arrival energy at node i, which is given by e. To arrive at the next node j, the energy of departure at node i, denoted by e', has to be higher than e_{ij} such that the EV does not run out of battery. This would cause the travel cost to increase severely since one would need to be towed to the nearest CS. The energy to be charged is linked to a certain charging time at a CS, denoted by τ_{i}.

If the arrival energy is sufficient to reach the next CS at node j, it is an option to refrain from charging. The departure time at node i is then equal to the arrival time. However, if charging takes place, a charging penalty time, denoted by t_{p}, has to be added. This penalty is present because the EV has to leave the road it is currently driving on, set up the charging process and get back on the road again. Therefore, the charging time τ_{i} is defined as

$$\tau_{\mathrm{i}} = \begin{cases} 0, & \text{if } \Delta e = 0, \\ \tau_{\mathrm{i}} + t_{\mathrm{p}}, & \text{otherwise.} \end{cases} \tag{3-6}$$

3-3-2 Waiting Time

Because the charging infrastructure is limited, waiting times at charging stations can be present. This could be the case, especially during hours when many people want to charge their EV. Unfortunately, this waiting time is not known. Therefore, a probability distribution can model the waiting time at a CS. Based on a probability distribution $P_{\mathrm{w}}(t)$, which is dependent on the time of the day, t, the expected waiting time, denoted by $\bar{w_{\mathrm{i}}}$, at node i is given by

$$\bar{w_{\mathrm{i}}} = E\{w_{\mathrm{i}}(t)\}, \tag{3-7}$$

where the expected value is calculated by:

$$E\{w_{\mathrm{i}}(t)\} = \sum_{\mathrm{i}=1}^{\mathrm{m}} w_i p_i \in P_w(t) = w_1 p_1 + w_2 p_2 + ... + w_m p_m. \tag{3-8}$$

This expected waiting time is incurred before the charging takes place. However, if no charging occurs, there is also no waiting time incurred.

3-3-3 Charging Cost

Finally, the energy that is charged is not cost-free. A dynamical pricing model is used for the energy costs, denoted by $c_{\mathrm{p}}(t)$, representing different energy prices based on the time of day and day in the week. This cost is based on the time of arrival at CS at node i and the amount of energy that is charged and is given by:

$$c_{\mathrm{e}} = c_{\mathrm{p}}(t) * \Delta e. \tag{3-9}$$

3-4 Conclusions

In this chapter, the model for the road network and charging infrastructure has been discussed. This model describes the costs incurred for an EV during the route. These costs consist of the edge cost and the node cost. The edge cost gives the cost required to travel from node i to node j. This cost depends on the expected driving speed, the energy consumption, which also depends on the driving speed, the required energy consumption for the cabin climate control and the required energy for the cooling or heating of the battery. The travel time between two nodes depends on the edge distance and the expected driving speed.

The cost incurred at a node is given by the charging time, depending on the amount of energy charged, the battery temperature at arrival, the SoC at arrival and the charging power that the CS can deliver. Other costs incurred at a node are given by the waiting time and the price for the charging event.

Now that the edge cost and node cost are clearly defined, we can elaborate on the used methodology to find an optimal policy for the EV in a network. The used methodology is explained in the next chapter.

Chapter 4

Stochastic Dynamic Programming

In this chapter, the used methodology of SDP will be discussed in detail. It will be elaborated on how the travel costs of an EV can be minimised using SDP. A simplification to improve the computation time of the method while having the same optimal policy, as a result, will be discussed. First, a general explanation of SDP will be given, followed by a more tailored method for the optimisation problem of the route guidance of an EV on long-haul trips.

4-1 An Introduction to Stochastic Dynamic Programming

DP can be used for problems in many settings. These problems often consist of optimisation problems that evolve over time. The problems range from the control of heating systems to managing entire economics. Examples of similar optimisation problems are scheduling problems, selling assets, investing money in portfolios, purchasing new equipment, forecast problems, or simply playing a game of backgammon. All these problems have in common: they involve making decisions, then observing information, after which more decisions are taken, and so on. Such problems are known as *sequential decision problems*. These problems might be straightforward to formulate, however solving them is another matter.

This is where DP comes into play. With DP, problems are broken down into smaller sub-problems using recursive equations that depend on a state variable to find the optimal solutions to the sub-problems iteratively—ultimately leading to the overall optimal solution.

With DP problems, specific control actions generate a sequence of states from a discrete-time dynamic system [1]. If the system evolves over a finite number of N steps, the problem is said to be a finite horizon problem. The state and control at time k are denoted by x_{k} and u_{k} respectively.

For stochastic finite horizon optimal control problems the evolution of state x_{k} is influenced by a random disturbance w_{k}, which is characterised by a probability distribution $P_{\mathrm{k}}(\cdot|x_{\mathrm{k}}, u_{\mathrm{k}})$ that may depend explicitly on x_{k} and u_{k}, but not on values of prior disturbances $w_{\mathrm{k}-1}, ..., w_0$. The states of the system evolve according to the following equation:

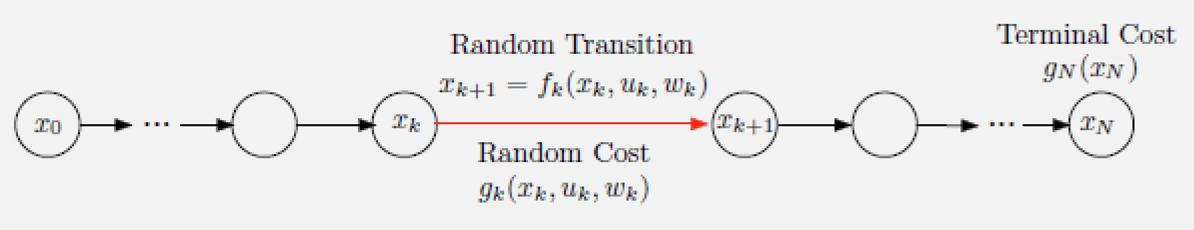

Figure 4-1: Illustration of an N-stage stochastic optimal control problem [1]

$$x_{\mathrm{k}+1} = f_{\mathrm{k}}(x_{\mathrm{k}}, u_{\mathrm{k}}, w_{\mathrm{k}}), \qquad k = 0, 1, ..., N-1, \tag{4-1}$$

where k is the time index, x_{k} is the state of the system, an element of some space, u_{k} is the selected control variable at k from some given set $U_{\mathrm{k}}(x_{\mathrm{k}})$, w_{k} is a random disturbance, f_{k} is a function of $(x_{\mathrm{k}}, u_{\mathrm{k}}, w_{\mathrm{k}})$ that describes the mechanism by which the state is updated from time k to time *k+1* and N is the horizon or number of times control is applied.

The stochastic finite horizon optimal control problem involves a cost function that is additive in the sense that the cost incurred at time *k*, denoted by $g_{\mathrm{k}}(x_{\mathrm{k}}, u_{\mathrm{k}}, w_{\mathrm{k}})$, accumulates over time. The cost incurred at time k is referred to as the stage cost. An illustration of how the stage cost, starting from state x_{k} under control variable u_{k}, develops for a N-stage stochastic optimal control problem is shown in Figure 4-1.

An important difference with deterministic DP is that the optimisation for SDP does not optimise over control sequences but rather over policies. These policies consist of a sequence of functions, where μ_{k} maps states x_{k} into controls $u_{\mathrm{k}} = \mu_{\mathrm{k}}(x_{\mathrm{k}})$, and also satisfies the control constraints, such that $\mu_{\mathrm{k}}(x_{\mathrm{k}}) \in U_{\mathrm{k}}(x_{\mathrm{k}})$. In the presence of stochastic uncertainty, policies can result in improved cost since they allow choices of controls u_{k} that incorporate knowledge of the state x_{k}. Suppose there is no knowledge present on the effect of the disturbance on the state x_{k}. In that case, the controller cannot adapt appropriately to unexpected values of the state, which can adversely affect the cost. This is a fundamental difference between deterministic and stochastic optimal control problems.

Evaluating various quantities such as cost function values for stochastic problems involves forming expected values, which is another important distinction between deterministic and stochastic optimal control problems. With an initial state x_0 and policy $\pi = \{\mu_0, ..., \mu_{\mathrm{N}-1}\}$, the future states x_{k} are defined through the following system equation:

$$x_{\mathrm{k}+1} = f_{\mathrm{k}}(x_{\mathrm{k}}, \mu_{\mathrm{k}}(x_{\mathrm{k}}), w_{\mathrm{k}}), \qquad k = 0, 1, ..., N-1. \tag{4-2}$$

Thus, for given functions g_{k}, $k = 0, 1, ..., N-1$, the expected cost of π starting at x_0 is:

$$J_\pi(x_0) = E\Big\{g_{\mathrm{N}}(x_{\mathrm{N}}) + \sum_{\mathrm{k}=0}^{\mathrm{N}-1} g_{\mathrm{k}}(x_{\mathrm{k}}, \mu_{\mathrm{k}}(x_{\mathrm{k}}), w_{\mathrm{k}})\Big\}, \tag{4-3}$$

where $E\{\cdot\}$ represents the expected value operator over all the random variables w_{k} and x_{k}. An optimal policy π^* is one that minimises the expected cost, given in Eq. (4-3), i.e.:

$$J_{\pi^*}(x_0) = \min_{\pi \in \Pi} J_\pi(x_0), \tag{4-4}$$

where Π is the set of all admissible policies. The optimal cost depends on x_0 and is denoted by $J^*(x_0)$, given by:

$$J^*(x_0) = \min_{\pi \in \Pi} J_\pi(x_0). \tag{4-5}$$

The function in Eq. (4-5) can be seen as a function that assigns the optimal cost $J^*(x_0)$ to each initial state, such that $J^*(x_0)$ can be seen as the optimal cost function. The optimal policy for SDP problems can then found by starting with:

$$J^*_\mathrm{N}(x_\mathrm{N}) = g_\mathrm{N}(x_\mathrm{N}), \tag{4-6}$$

where $g_\mathrm{N}(x_\mathrm{N})$ is a terminal cost incurred at the end of the process. For $k = 0, ..., N-1$, let:

$$J^*_\mathrm{k}(x_\mathrm{k}) = \min_{\mathrm{u_k \in U_k(x_k)}} E\Big\{ g_\mathrm{k}(x_\mathrm{k}, u_\mathrm{k}, w_\mathrm{k}) + J^*_{\mathrm{k+1}}\Big(f_\mathrm{k}(x_\mathrm{k}, u_\mathrm{k}, w_\mathrm{k})\Big)\Big\}. \tag{4-7}$$

Then, if $u^*_\mathrm{k} = \mu^*_\mathrm{k}(x_\mathrm{k})$ minimises the right side of Eq. (4-7) for each x_k and k, the policy $\pi^* = \{\mu_0, ..., \mu^*_{\mathrm{N}-1}\}$ is optimal.

4-2 Stochastic Dynamic Programming Formulation

In the following, it will be discussed how our problem is formulated as an SDP problem. This will involve describing the state variables, the control variables, state transition functions and other vital parts of the methodology.

4-2-1 State Variables

As described, x_k is the state of the system. In our case, this system is the EV. The physical system is characterised by a set of parameters called the state variables. The state of the system can influence the possible control decisions. The set of all possible states at time k is called the *state space*, and denoted by S_k. In our research, it is assumed that the state variable is defined as follows:

$$x_\mathrm{k} = (i, e_\mathrm{k}, t_\mathrm{k}, T_\mathrm{k}), \tag{4-8}$$

where i is the CS, e_k is the SoC, t_k is the time and T_k is the battery temperature. The system's state influences the control decision set presented during the optimisation—for example, the amount of energy that the EV can charge at a CS.

4-2-2 Control Variables

As stated in Section 4-1, during the optimisation, an optimal policy is sought such that the expected costs with the initial state, denoted by x_0, are minimised. This optimal policy is a function of the state x_k. For this optimisation problem, the control actions consist of (i) which charging station should be travelled to next (ii) the amount of energy to be charged (iii) the amount of cooling or heating of the battery during the driving. Hence, the control action is given by:

$$u_\mathrm{k} = (j, \Delta e_\mathrm{k}, q_\mathrm{k}), \tag{4-9}$$

where j is the next node, q_k is the heating or cooling rate between node i and node j, and Δe_k is the amount of energy to be charged. The amount of energy to be charged is given by:

$$\Delta e_\mathrm{k} = e'_\mathrm{k} - e_\mathrm{k}, \tag{4-10}$$

where e'_k is the departure energy. Upon arrival at each node, whether charging takes place or not, a decision has to be taken as to which node to travel next. This decision depends on the state x_k. Take the network given in Figure 4-2 as an example, where an optimal policy is sought between origin o and destination d. It is straightforward to see the fact that at the origin o only one decision is optimal regarding which node to travel next to since the only node which can be travelled next to is node 1. However, upon arrival at node 1, the EV can either travel to node 2 or node 3, respectively. This decision is dependent on state x_k, while this state can influence the associated cost to travel to node 2 and node 3, which makes one node favourable, in terms of cost, to travel to the next over the other node.

A node is said to be reachable, meaning one can travel from the current node to the node in question, if the edge between the two nodes is contained in set $\mathcal{A}$, given by:

$$(i, j) \in \mathcal{A}. \tag{4-11}$$

The nodes that can be reached from node i are contained in set $\mathcal{N}^+$ and satisfy the condition given in Eq. (4-11). Therefore the possible set of nodes to travel next to, denoted by $U_\mathrm{j}(x_\mathrm{k})$, when in node i is given by:

$$U_\mathrm{j}(x_\mathrm{k}) = \{j \in \mathcal{N}^+\}. \tag{4-12}$$

Next to deciding to which node to travel next to also a decision has to be made regarding the amount of energy that is charged at node i. Therefore a charging control decision set, $U_\mathrm{e}(x_\mathrm{k})$, is presented. This charging control decision set is dependent on state x_k, while it describes the amount of energy to be charged, which is dependent on the arrival energy. The charging control decision set is equal to:

$$U_\mathrm{e}(x_\mathrm{k}) = \{0 \le \Delta e_\mathrm{k} \le e_\mathrm{c} - e_\mathrm{k}\}. \tag{4-13}$$

In Eq. (4-13), it can be seen that the minimum of the charging control decision set is equal to zero. This is a particular case where no charging takes place. In the case that charging does

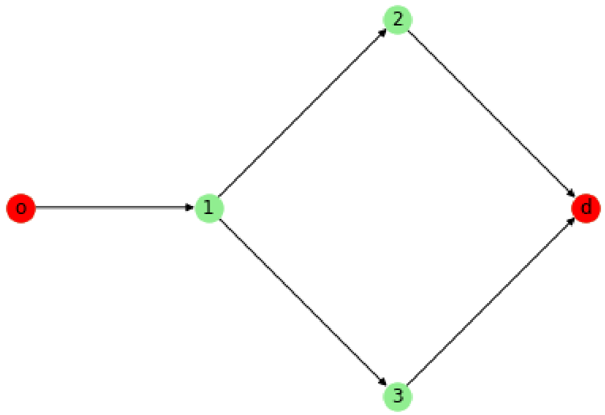

Figure 4-2: Example network to illustrate control variable *j*.

take place, the amount of charged energy depends on the state x_k. The maximum amount of energy to be charged is the battery capacity, denoted by e_c, minus the arrival energy, which means that the charging process can go to a maximum of 100% SoC.

Finally, there is a control variable that controls the heating or cooling of the battery. As stated in Section 3-3, the battery temperature influences the charging time. Therefore, it is desired that the battery temperature upon arrival at a CS is higher or equal to T_min and lower or equal to T_max, for safety reasons. The control variable q_k, which controls the cooling or heating rate of the battery is chosen from the set $U_\mathrm{q}(x_\mathrm{k})$ which is dependent on the predicted battery temperature upon arrival at the next charging station, denoted by $T_\mathrm{p,k+1}$. This control variable should be contained in the set, $q_\mathrm{k} \in U_\mathrm{q}(x_\mathrm{k})$, given by:

$$U_\mathrm{q}(x_\mathrm{k}) = \begin{cases} Q_\mathrm{heat}, & \text{if } T_\mathrm{p,k+1} < T_\mathrm{min}, \\ 0, & \text{if } T_\mathrm{min} \leq T_\mathrm{p,k+1} \leq T_\mathrm{max}, \\ Q_\mathrm{cool}, & \text{if } T_\mathrm{p,k+1} > T_\mathrm{max}, \end{cases} \tag{4-14}$$

where Q_heat and Q_cool are variables that can be optimised and T_min and T_max are temperature values that can be set for the optimal charging of the battery as well as the safety for the EV drivers respectively. The predicted temperature of the battery upon arrival of the next charging station can be calculated using Eq. (2-10) described in Section 2-3.

4-2-3 Random Disturbances

There are two random disturbances present that influences the system's dynamics. The first disturbance influences the waiting time at a CS, while this waiting time is not known until arrival at the CS. The disturbance on the waiting time at stage k is denoted by $w_\mathrm{w,k}$ and is dependent on the arrival time at the CS. The second disturbance influences the driving speed between two nodes. The driving speed between nodes is random, while this depends on multiple factors, such as the weather, traffic density and possible accidents. The disturbance in the driving speed, on the edge between node i and node j respectively, is denoted by $w_\mathrm{v,ij}$.

There is a given collection of probability distributions $P_{w_{\mathrm{w,k}}} = \{P_{w1}, ..., P_{wm}\}$, corresponding to m possible distributions describing the probability for the disturbance $w_{\mathrm{w,k}}$ to occur. In a distribution, the probability for a certain disturbance to take place is described. The arrival time at a certain CS, determines which probability distribution will be used to describe the set of disturbances $w_{\mathrm{w,k}}$. Therefore, this is described by the conditional probability $P_{w_{\mathrm{w,k}}}(w_{\mathrm{w,k}}|x_{\mathrm{k}})$.

For the disturbance on the driving speed, also a given set of probability distributions $P_{w_{\mathrm{v,ij}}} = \{P_{v1}, ..., P_{vn}\}$, corresponding to n possible distributions is present. The probability distribution for the distribution on the travel speed depends on the state, the control action, and the waiting time disturbance, and is defined by $P_{w_{\mathrm{v,ij}}}(w_{\mathrm{v,ij}}|x_{\mathrm{k}}, u_{\mathrm{k}}, w_{\mathrm{w,k}})$.

As can be seen, the probability distribution of the travel speed can be affected by a control input. However, the evolution of the component $w_{\mathrm{w,k}}$ cannot be affected by control, except indirectly through x_{k}. Since the random disturbance $w_{\mathrm{w,k}}$ influences the arrival state of our system, we have to include this random event in our state. Therefore, the augmented state of our system is given as:

$$\tilde{x}_{\mathrm{k}} = (x_{\mathrm{k}}, w_{\mathrm{w,k}}). \tag{4-15}$$

4-2-4 State Transition Function

Based on the current state, the control policy and the random disturbances, the evolution of the main state component x_{k} is defined in the following way:

$$x_{\mathrm{k+1}} = f_{\mathrm{k}}(x_{\mathrm{k}}, u_{\mathrm{k}}, w_{\mathrm{w,k}}, w_{\mathrm{v,ij}}), \tag{4-16}$$

where $f_{\mathrm{k}}(\cdot)$ is a non-linear function obtained from Algorithm 1.

Algorithm 1 function $f_{\mathrm{k}}(x_{\mathrm{k}}, u_{\mathrm{k}}, w_{\mathrm{w,k}}, w_{\mathrm{v,ij}})$

1: $\tau_{\mathrm{i}} = f_{\mathrm{c}}(e'_{\mathrm{k}}, e_{\mathrm{k}}, T_{\mathrm{k}})$ ▷ Charging time
2: $\tau_{\mathrm{ij}} = d_{\mathrm{ij}}/(\bar{v}_{\mathrm{ij}} + w_{\mathrm{v,ij}})$ ▷ Driving time
3: $e_{\mathrm{ij}} = d_{\mathrm{ij}} * f_{\mathrm{e}}(\bar{v}_{\mathrm{ij}} + w_{\mathrm{v,ij}}) + \tau_{\mathrm{ij}} * (B_0 + B_{\mathrm{c}} + B_{\mathrm{b}})$ ▷ Energy consumption

4: **if** $\Delta e_{\mathrm{k}} \mathrel{!=} 0$ **then**
5: $\quad\tau_{\mathrm{i}} = \tau_{\mathrm{i}} + t_{\mathrm{p}}$

6: $e_{\mathrm{k+1}} = e'_{\mathrm{k}} - e_{\mathrm{ij}}$ ▷ Arrival energy
7: $T_{\mathrm{k+1}} = f_{\mathrm{T}}(e_{\mathrm{ij}}, B_{\mathrm{c}}, \tau_{\mathrm{ij}}, T_{\mathrm{k}}, T_{\mathrm{ambient}})$ ▷ Arrival battery temperature
8: $t_{\mathrm{k+1}} = t_{\mathrm{k}} + w_{\mathrm{w,k}} + \tau_{\mathrm{i}} + \tau_{\mathrm{ij}}$ ▷ Arrival time
9: $x_{\mathrm{k+1}} = (j, e_{\mathrm{k+1}}, t_{\mathrm{k+1}}, T_{\mathrm{k+1}})$ ▷ Next state
return $x_{\mathrm{k+1}}$

The first line in Algorithm 1, calculates the charging time, denoted by τ_{i}, which is dependent on the energy e'_{k}, when leaving the charging station, the energy when arriving at the charging station denoted by e and the battery temperature upon arrival at charging station i, denoted by T_{k}. The driving time between the two charging stations is calculated in the second line. This is done by dividing the distance d_{ij} between the two charging stations by the expected driving speed, which is disturbed by the driving speed disturbance. The required energy to travel between charging station i and j is given by e_{ij}.

In line 5, a charging penalty, t_{p}, is added if charging takes place. This penalty is present because the EV has to leave the road it is currently driving on, set up the charging process and get back on the road again. One can then calculate the energy level upon arrival at the next charging station with line 6. The temperature upon arrival at the next charging station is calculated by function $f_{\mathrm{T}}(e_{\mathrm{ij}}, B_c, \tau_{\mathrm{ij}}, T_{\mathrm{k}}, T_{\mathrm{ambient}})$. The arguments of this function include the required energy to travel from charging station i to charging station j, the required time to travel between these two charging stations, the energy required for the cooling or heating of the battery, the battery temperature upon arrival at charging station i and the ambient temperature. Moreover, the arrival time at the next station will be updated according to line 8. This concludes the calculation of the next state $x_{\mathrm{k}+1}$, given by Algorithm 1.

4-2-5 Stage Cost

The stochastic optimal control problem is finite since the system evolves over a N finite number of stages, which are the nodes within the network. At each stage, a stage cost $g_{\mathrm{k}}(x_{\mathrm{k}}, u_{\mathrm{k}}, w_{\mathrm{w,k}}, w_{\mathrm{v,ij}})$ is incurred. The stage cost $g_{\mathrm{k}}(\cdot)$, consists of the cost for the charging and the cost for time, defined as:

$$g_{\mathrm{k}}(x_{\mathrm{k}}, u_{\mathrm{k}}, w_{\mathrm{w,k}}, w_{\mathrm{v,ij}}) = c_{\mathrm{p}}(t_{\mathrm{k}}) * \Delta e_{\mathrm{k}} + \alpha\Big(w_{\mathrm{w,k}} + \tau_{\mathrm{i}} + \frac{d_{\mathrm{ij}}}{(\bar{v}_{\mathrm{ij}} + w_{\mathrm{v,ij}})}\Big), \tag{4-17}$$

the cost for the charging process is given by the charging price at the arrival of the CS, given by $c_{\mathrm{p}}(t_{\mathrm{k}})$, multiplied with the amount of energy that is charged, denoted by Δe_{k}. Moreover, parameter α can change the relative importance of the charging cost to the time cost. The influence and appliance of this parameter will be discussed in Chapter 6. The time cost is given by the total amount of time spent between arriving at node i to arriving at node j. The stage cost depends on both the disturbance on the driving speed $w_{\mathrm{v,ij}}$, and the disturbance concerning the waiting time $w_{\mathrm{w,k}}$.

In the stage cost function, α can be used to set different navigation modes; α has an influence on the relative impact of the charging cost and the elapsed time. The charging cost is given by the first term in Eq. (4-17), which describes the cost for the charging process, given by:

$$c_{\mathrm{charging}} = c_{\mathrm{p}}(t_{\mathrm{k}}) * \Delta e_{\mathrm{k}}, \tag{4-18}$$

where c_{charging} stands for the charging cost. The second term of Eq. (4-17), gives the cost for the elapsed time. The elapsed time is the time required to travel from the current charging station to the next charging process at the next CS, measured from the moment of arrival at the current charging station. This time cost is given by:

$$c_{\mathrm{time}} = w_{\mathrm{w,k}} + \tau_{\mathrm{i}} + \frac{d_{\mathrm{ij}}}{(\bar{v}_{\mathrm{ij}} + w_{\mathrm{v,ij}})}. \tag{4-19}$$

Such that the stage cost is given by:

$$g_{\mathrm{k}} = c_{\text{charging}} + \alpha * c_{\text{time}}. \tag{4-20}$$

4-2-6 Recursive Value Iteration

Now that the stage cost and evolution of the main state component is defined, the optimal cost-to-go at a specific stage k and the augmented state $(x_{\mathrm{k}}, w_{\mathrm{w,k}})$ is defined as follows:

$$J^*_{\mathrm{k}}(x_{\mathrm{k}}, w_{\mathrm{w,k}}) = \begin{cases} \min\limits_{u_{\mathrm{k}} \in U_{\mathrm{k}}(x_{\mathrm{k}}, w_{\mathrm{w,k}})} \quad \underset{w_{\mathrm{v,ij}}}{E} \Big\{ g_{\mathrm{k}}(x_{\mathrm{k}}, u_{\mathrm{k}}, w_{\mathrm{w,k}}, w_{\mathrm{v,ij}}) & \\ \quad + \sum_{w=1}^{m} p_w \quad J^*_{k+1}\Big(f_{\mathrm{k}}(x_{\mathrm{k}}, u_{\mathrm{k}}, w_{\mathrm{w,k}}, w_{\mathrm{v,ij}}), w\Big) \Big| w_{\mathrm{w,k}} \Big\}, & \text{if } k < N, \\ \min\limits_{u_{\mathrm{k}} \in U_{\mathrm{k}}(x_{\mathrm{k}}, w_{\mathrm{w,k}})} \quad \underset{w_{\mathrm{v,ij}}}{E} \Big\{ g_{\mathrm{k}}(x_{\mathrm{k}}, u_{\mathrm{k}}, w_{\mathrm{w,k}}, w_{\mathrm{v,ij}}) \Big| w_{\mathrm{w,k}} \Big\}, & \text{if } k = N. \end{cases} \tag{4-21}$$

Where p_{w} is the probability that the next disturbance $w_{\mathrm{w,k+1}}$ is selected according to probability distribution $P_{w_{\mathrm{w,k}}}$.

4-2-7 Uncontrollable State Components

It is possible to see $w_{\mathrm{w,k}}$ as a disturbance, but there is a difference: $w_{\mathrm{w,k}}$ is observed before we apply control u_{k}, while $w_{\mathrm{v,ij}}$ occurs after applying u_{k}. Therefore, $w_{\mathrm{w,k}}$ is an uncontrollable state component. Which means that we can simplify our method by averaging out the uncontrollable component $w_{\mathrm{w,k}}$ and we execute the DP algorithm over the controllable component x_{k}. To do so, let $J^*_{\mathrm{k}}(x_{\mathrm{k}}, w_{\mathrm{w,k}})$ denote the optimal cost-to-go at stage k and state $(x_{\mathrm{k}}, w_{\mathrm{w,k}})$, and define:

$$\hat{J}_{\mathrm{k}}(x_{\mathrm{k}}) = \underset{w_{\mathrm{w,k}}}{E} \Big\{ J^*_{\mathrm{k}}(x_{\mathrm{k}}, w_{\mathrm{w,k}}) | x_{\mathrm{k}} \Big\}. \tag{4-22}$$

We will derive a DP algorithm that generates $\hat{J}_{\mathrm{k}}(x_{\mathrm{k}})$, starting with

$$\begin{aligned} \hat{J}_{\mathrm{k}}(x_{\mathrm{k}}) = \underset{w_{\mathrm{w,k}}}{E} \Bigg\{ & \min_{u_{\mathrm{k}} \in U_{\mathrm{k}}(x_{\mathrm{k}}, w_{\mathrm{w,k}})} \quad \underset{w_{\mathrm{v,ij}}, x_{\mathrm{k+1}}, w_{\mathrm{w,k+1}}}{E} \Big\{ g_{\mathrm{k}}(x_{\mathrm{k}}, u_{\mathrm{k}}, w_{\mathrm{w,k}}, w_{\mathrm{v,ij}}) \\ & + J^*_{\mathrm{k+1}}(x_{\mathrm{k+1}}, w_{\mathrm{w,k+1}}) | x_{\mathrm{k}}, u_{\mathrm{k}}, w_{\mathrm{w,k}} \Big\} \Big| x_{\mathrm{k}} \Bigg\}, \end{aligned} \tag{4-23}$$

which can be rewritten as:

$$\begin{aligned} \hat{J}_{\mathrm{k}}(x_{\mathrm{k}}) = \quad & \underset{w_{\mathrm{w,k}}}{E} \Bigg\{ \min_{u_{\mathrm{k}} \in U_{\mathrm{k}}(x_{\mathrm{k}}, w_{\mathrm{w,k}})} \quad \underset{w_{\mathrm{v,ij}}, x_{\mathrm{k+1}}}{E} \Big\{ g_{\mathrm{k}}(x_{\mathrm{k}}, u_{\mathrm{k}}, w_{\mathrm{w,k}}, w_{\mathrm{v,ij}}) \\ & + \underset{w_{\mathrm{w,k}}}{E} \Big\{ J^*_{\mathrm{k+1}}(x_{\mathrm{k+1}}, w_{\mathrm{w,k+1}}) | x_{\mathrm{k+1}} \Big\} | x_{\mathrm{k}}, u_{\mathrm{k}}, w_{\mathrm{w,k}} \Big\} \Big| x_{\mathrm{k}} \Bigg\}, \end{aligned} \tag{4-24}$$

and finally:

$$\begin{aligned}\hat{J}_{\mathrm{k}}(x_{\mathrm{k}}) = \underset{w_{\mathrm{w,k}}}{E}\Bigg\{ \min_{u_{\mathrm{k}}\in U_{\mathrm{k}}(x_{\mathrm{k}})} \underset{w_{\mathrm{v,ij}}}{E}\Big\{ & g_{\mathrm{k}}(x_{\mathrm{k}}, u_{\mathrm{k}}, w_{\mathrm{w,k}}, w_{\mathrm{v,ij}}) \\ & + \hat{J}_{\mathrm{k}+1}\Big(f_{\mathrm{k}}(x_{\mathrm{k}}, u_{\mathrm{k}}, w_{\mathrm{w,k}}, w_{\mathrm{v,ij}})\Big)\Big\}\Big| x_{\mathrm{k}}\Bigg\}.\end{aligned} \tag{4-25}$$

The advantage of this equivalent DP algorithm is that is executed over a significantly reduced state space [1]. For example, if x_{k} takes n possible values and $w_{\mathrm{w,k}}$ takes m possible values, then DP is executed over n states instead of nm states.

4-3 Conclusions

In this chapter, the methodology of SDP has been introduced and discussed. It is well known that DP offers a good framework for sequential decision problems [20]. Therefore, SDP is well suited to find the optimal policy in a road network where travel speeds and charging station availability are stochastic for an EV. The control actions for our problem will consist of (i) the next node to travel to (ii) the amount of charging that takes place (iii) the amount of cooling or heating of the battery is applied.

A simplification is suggested in Section 4-2-7, with respect to the uncontrollable state component $w_{\mathrm{w,k}}$, the waiting time. With the presence of an uncontrollable state component, the DP algorithm can be simplified considerably and executed over the state's controllable components.

In the next chapter, the proposed method will be verified, the simplification will be validated, and parameter sensitivity analyses will be performed.

Chapter 5

Parameter Sensitivity Studies

This chapter will discuss the verification of the proposed method and parameter sensitivity analyses. The sensitivity analyses are executed to test the influence of specific parameters on the proposed method. The verification of the proposed method is executed to check the validity of the proposed method. First, the simulation setup will be discussed, followed by the verification and sensitivity analyses.

5-1 Simulation Setup

In this section, the simulation setup used during the case studies will be discussed. First, the networks used for the case studies will be described. Then, it will be discussed how the random disturbances are modelled, followed by elaborating on the battery thermal model specifics.

5-1-1 Case Networks

There will be three networks on which the case studies are performed. The topology of these networks are adapted from [15] and are given in Figure 5-1, accompanied by their number of nodes and links. As shown in the figure, the network is a directed network. The arrows are pointing from node to node represent in which direction the car can travel. Moreover, as can be seen in Figure 5-1, there is a difference between the networks. The first and second networks have the same amount of links; however, the number of nodes, representing either a single CS or a cluster of CSs, is different. The second and third networks do not have the same amount of links but do have the same amount of nodes. For each of the networks, the first node, denoted by node 1, is the origin node o and the last node is the destination node d, which is node 10 in the first case and node 12 in the second and third case.

At the beginning of each simulation, the distance of the links in the network is randomly distributed between [100km, 120km]. Therefore, the distance between the origin and destination nodes lies between 500-600 kilometres, which causes the fact that the EV will have to charge at least once, and the trip is considered a long-haul trip.

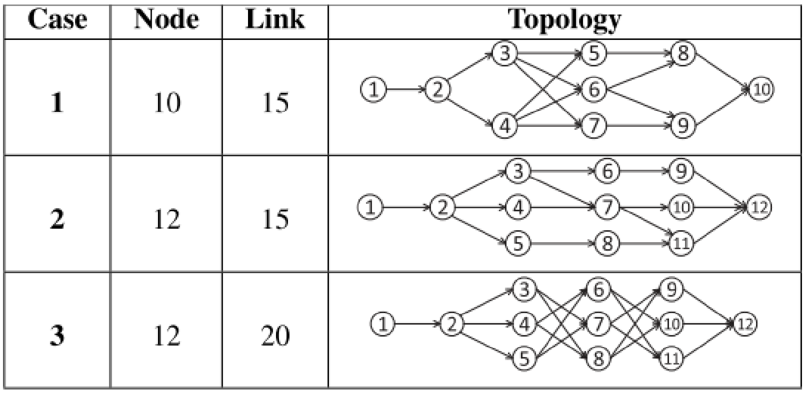

Case	Node	Link	Topology
1	10	15	
2	12	15	
3	12	20	

Figure 5-1: Three networks [15].

Table 5-1: Division of the day.

Time Interval	Peak	Intermediate	Base
00:00-06:59			X
07:00-09:59	X		
10:00-14:59		X	
15:00-18:59	X		
19:00-23:59			X

5-1-2 Random Disturbances

A set of probability distributions is present for the travel speed between the nodes. This set is denoted by $P_{w_{\mathrm{v,k}}}$. For the creation of the travel speed distributions, a difference is made between peak-hours, intermediate-hours, and base-hours. To be more specific, a day is split up into time intervals assigned to the specific mean travel speed group. The division of the daytime is given in Table 5-1.

For each of the peak-hours, intermediate-hours, and base-hours a different probability distribution is present. Intuitively, one can understand that during peak hours, the chance of running into a traffic jam is more significant than during base hours. This is since the traffic density is, in general, higher during peak-hours, which increases the probability of accidents happening and a higher probability of a lower average driving speed. The probability distributions are normally distributed, which can be described by $N(\mu, \sigma^2)$, where μ is the mean and σ^2 is the variance. Without loss of generality, let us assume that the peak-hours, intermediate-hours, and base-hours can be described by:

$$N(\mu, \sigma^2) = \begin{cases} N(\mu = 60,\ \sigma^2 = 5), & \text{Peak,} \\ N(\mu = 80,\ \sigma^2 = 3), & \text{Intermediate,} \\ N(\mu = 100,\ \sigma^2 = 1), & \text{Base.} \end{cases} \tag{5-1}$$

The distributions in Eq. (5-1), describe the probability for a particular mean travel speed to occur. During the peak-, and intermediate hours there is a higher variance present, meaning

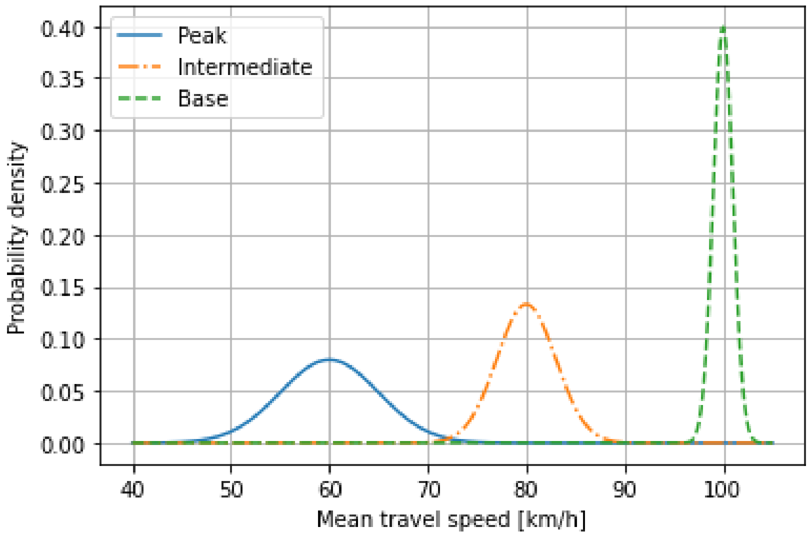

Figure 5-2: Realisations of the Probability Density Function (PDF) of the different mean travel speed groups.

that there is a bigger chance of having a mean travel speed that varies from the mean of the distribution, shown in Figure 5-2.

As discussed in Section 3-2, the propulsive energy consumption on a link l_{ij} depends on the mean travel speed, which gives a specific energy consumption B per kilometre. In this base case study, the relation between energy consumption per driven kilometre and the mean travel speed, presented in Figure 2-1 is used. The available charging power of each CS is set to be equal to 50 kW, there is no spatial or temporal dependency of this charging power. This means that the available charging power in each node, representing a CS, is the same. The charging price, denoted by c_p, depends on energy demand, hence the time of the day. The charging price is given by:

$$c_{\mathrm{p}}(t_{\mathrm{k}}) = \begin{cases} 0.42\,(\mathrm{EUR/kW}), & \text{if } t_{\mathrm{k}} \in t_{\mathrm{peak}}, \\ 0.40\,(\mathrm{EUR/kW}), & \text{if } t_{\mathrm{k}} \in t_{\mathrm{intermediate}}, \\ 0.35\,(\mathrm{EUR/kW}), & \text{if } t_{\mathrm{k}} \in t_{\mathrm{base}}, \end{cases} \tag{5-2}$$

where t_{peak}, $t_{\mathrm{intermediate}}$, and t_{base} represent the set of all time intervals belonging to the corresponding group and t is the arrival time at the CS. It is assumed that the charging price is fixed during the charging period. This charging price is determined based upon the arrival time of the EV at a CS.

As described in Section 3-3, at each node, if charging takes place, a waiting time is incurred. One can imagine that this waiting time depends on the demand for charging at a specific time. Therefore, similar to the mean travel speed, a division during the day is made, separating the expected waiting times. This separation is made based on [6] and [25], who have researched the usage of fast charger behaviour of EV drivers in Norway and The Netherlands, respectively. A result from [25], is presented in Figure 5-3 showing the distribution of fast charge events throughout the day in The Netherlands. Based on these studies, a differentiation is made

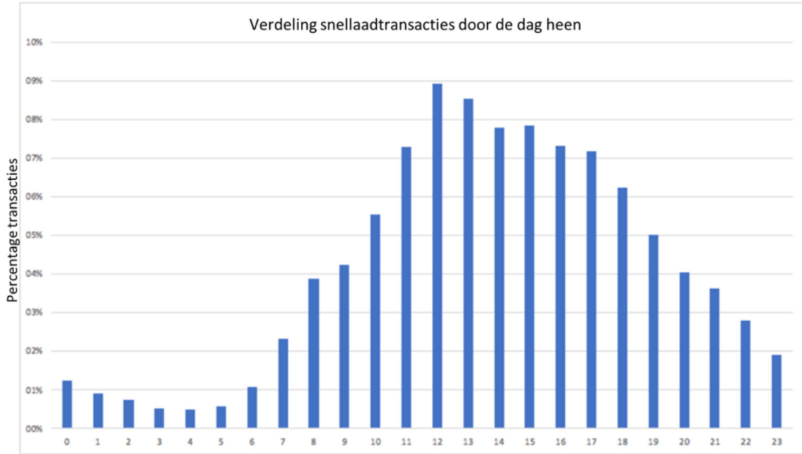

Figure 5-3: Distribution of fast charger events throughout the day in The Netherlands [25].

Table 5-2: Division of the day accompanied with belonging waiting time group.

Time Interval	Peak	Intermediate	Base
00:00-06:59			X
07:00-09:59		X	
10:00-14:59	X		
15:00-18:59	X		
19:00-23:59		X	

between peak-, intermediate-, and base hours with respect to the charging demand. The result is shown in Table 5-2.

The waiting times are described with a half-normal distribution to avoid negative waiting times. The half-normal distribution is a normal distribution that is folded about the origin, that is obtained by left-truncating $N(0, \sigma^2)$ below zero [11]. The probability distribution for the peak-, intermediate-, and base waiting time groups can be described by:

$$N(\mu, \sigma^2) = \begin{cases} N(\mu = 0,\ \sigma^2 = 0.75), & \text{Base}, \\ N(\mu = 0,\ \sigma^2 = 1.50), & \text{Intermediate}, \\ N(\mu = 0,\ \sigma^2 = 3.00), & \text{Peak}. \end{cases} \tag{5-3}$$

The corresponding half-normal probability distributions to Eq. (5-3) are shown in Figure 5-4. The waiting time at a CS is expressed in minutes, and obviously, the waiting time cannot become negative.

5-1-3 Battery Thermal Model Specifics

As discussed in Section 3-3, the battery temperature is important for the charging efficiency. The lower optimal battery temperature is assumed to be equal to 25 $°C$. For safety reasons, as discussed in Section 2-3, the maximum battery temperature is assumed at a temperature of 35 $°C$ [16]. This implies that the EV will have optimal charging if the battery temperature

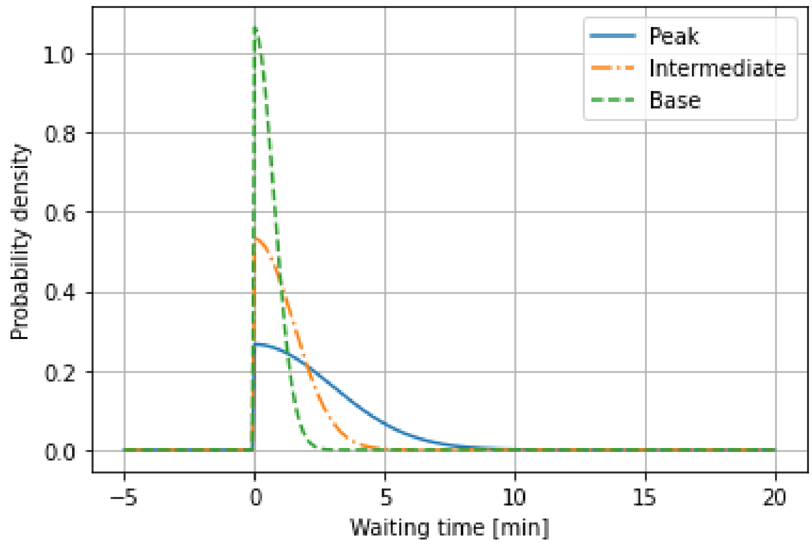

Figure 5-4: Realisations of PDF of the different waiting time groups.

remains between 25 °C and 35 °C. While the maximum battery temperature is a strict constraint, the battery temperature is allowed to be lower than the minimum optimal battery temperature of 25 °C.

For the battery thermal heating and cooling, multiple assumptions are made. It is assumed that a maximum heating rate of 7 kW can be present for thermal heating. It is also assumed that the efficiency from electric power to heat is equal to 100 %, since heat losses can be captured and used to heat the battery. The resistive battery heat losses are assumed to be equal to 4 % of the propulsive wheel power. This passive heat heats the battery while driving. Therefore Q_{in} in Eq. (2-10) is given by:

$$Q_{\text{in}} = 0.04B + Q_{\text{h}}, \tag{5-4}$$

where Q_h is the heating rate from an external source. Furthermore, it is assumed that the battery can be cooled with the HVAC system at a maximum rate of 5 kW. The efficiency of the electric power to cooling power is assumed to be equal to 80 %. The battery is assumed to be only passively cooled by convection since the radiation cooling is negligible. Therefore Q_{out} in Eq. (2-10) is given by:

$$Q_{\text{out}} = hA(T - \text{T}_{\text{ambient}}) + Q_{\text{c}}, \tag{5-5}$$

where Q_c is the cooling rate from an external source. The parameters describing the set from which the cooling and heating rate can be chosen and the mechanism for this cooling or heating are shown in Table 5-3.

Important battery parameters, such as the number of modules, the battery weight and specific heat, are given in Table 5-4.

Table 5-3: Cooling and heating mechanisms.

Heating/Cooling mechanism	Rate	Efficiency
High Voltage Coolant Heater	0-7(kW)	100 %
HVAC	0-5(kW)	80 %

Table 5-4: Battery parameters.

Parameter	Value	Description
e_c	65 kWh	Battery capacity of the EV
n_m	12 (−)	Number of modules in the battery pack
n_c	6 (−)	Number of cells per module
m_b	450 (kg)	Battery mass
C_p	1100 (J/kg/K)	Specific heat capacity of the battery
A	0.28 (m^2)	Battery module surface area
h	4 (W/m^2/K)	Natural heat convection constant

Now that all essential parameters and probability distributions are known, the algorithm verification and sensitivity analyses can be conducted. First, we will examine the algorithm's sensitivity concerning the charging granularity.

5-2 Verification and Sensitivity Analyses

In this section, the verification of the method and the sensitivity analyses will be performed and discussed. The goal of the verification is to see whether the proposed method works. The sensitivity analyses are performed to test the influence of multiple parameters and test the method's robustness. First, the simplification will be verified, after which the sensitivity and influence of multiple parameters will be investigated.

5-2-1 Verification of Simplification

In Section 4-2-7, a simplification is made regarding the uncontrollable state component $w_{\mathrm{w,k}}$, which is the waiting time disturbance. This uncontrollable state component can be averaged out such that the DP algorithm is executed over a significantly reduced state space. With the simplification the DP algorithm is executed over the state space of x_k rather than over the state space of x_k and $w_{\mathrm{w,k}}$.

Therefore, in this section, the validity of the simplification will be verified. In order to do so, 100 simulations of network 1 will be held, both for the method with simplification and the method without simplification. All parameters will be the same for both methods, and the only difference is the made simplification. To show the validity of the simplification, three simulations will be discussed to a profound extent. In these three simulations, the found optimal policies of the method without simplification and the method with simplification will be compared. If the simplification is valid, we expect to see no difference between the optimal policies found by the method without simplification and the method with simplification.

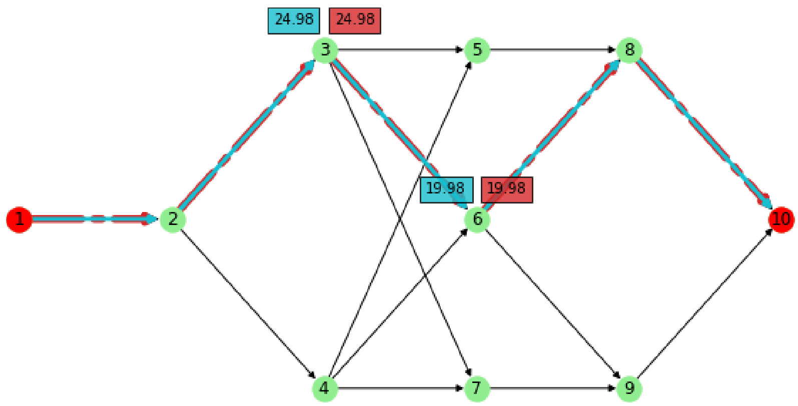

Figure 5-5: First result of the optimal policies of one simulation for the method with simplification (cyan) and the method without simplification (red) for network 1.

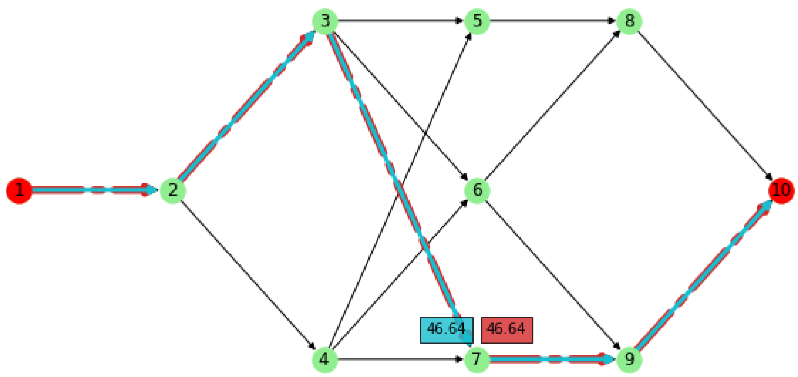

Figure 5-6: Second result of the optimal policies of one simulation for the method with simplification (cyan) and the method without simplification (red) for network 1.

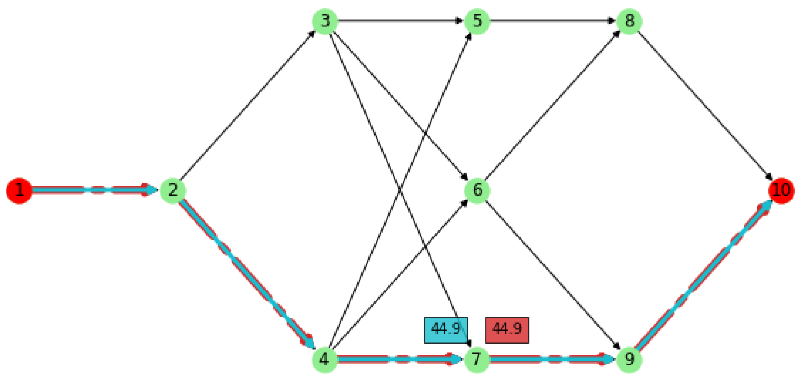

Figure 5-7: Third result of the optimal policies of one simulation for the method with simplification (cyan) and the method without simplification (red) for network 1.

Table 5-5: Mean running time of 100 simulations of the method without simplification an the method with simplification.

Method	Without simplification	With simplification
Running time [s]	46.7	0.180

In Figure 5-5, Figure 5-6, and Figure 5-7 the results of three simulations with the optimal policies found by the method without simplification, given by the red line, and by the method with simplification, given by the cyan line are shown. In these figures, it can be seen that the optimal policy found by the method without simplification and the method with simplification are the same. While the found path is the same for both methods and also the location and the amount of charge is the same. The difference, however, is present in the running time of the algorithm. For the first simulation, the method without simplification needs 43.8 seconds to find the optimal solution and the method with simplification needs only 0.156 seconds to find the optimal solution. A vast difference is present because with the simplification, the algorithm is only executed over the state space of x_{k} and not the state space of x_{k} and $w_{\mathrm{w,k}}$.

Therefore, it is safe to say that the method with simplification can find the same optimal policy as the method without simplification. The fact that with the simplification, the algorithm is only executed over the controllable components makes this method much faster in terms of running time while finding the same policy as the method without simplification. In order to show the difference in running time for both the methods in Table 5-5 the mean running times for both methods for 100 simulations are shown.

To conclude, we have shown that the suggested simplification is valid. It gives the same optimal policy but with a much lower running time. Therefore, only the method with simplification will be used in the remaining simulations.

5-2-2 Sensitivity to Charging Granularity

We will start by investigating the sensitivity of the proposed method with respect to the charging granularity. The charging granularity has an influence on the charging decision control set $U_{\mathrm{e}}(x_{\mathrm{k}})$. This charging decision control set holds all possible charging amounts for a given state x_{k}. The charging granularity influences how big this set is going to be. A high granularity means that there are a lot of possible charging amounts. If the charging granularity becomes lower, the number of possible charging amounts decreases. The charging granularity is determined with the parameter δ_{e}, and at state x_{k}. If the arrival energy is equal to e_{k}, then the first possibility for the amount of charging besides from 0, which corresponds to no charging, is given by:

$$\Delta e_{\mathrm{k}} = \delta_{\mathrm{e}}, \tag{5-6}$$

the second option for the amount of charging is given by:

$$\Delta e_{\mathrm{k}} = 2\delta_{\mathrm{e}}, \tag{5-7}$$

Table 5-6: Parameters for simulations of the charging granularity.

Parameter	i [-]	e_0 [kWh]	t_0 [hr]	T_0 [°C]	T_{ambient} [°C]
Value	Node 1	65	$\Omega \rightarrow [0, 20]$	20	20

and so on. However, if the amount of charging is bigger than the amount of charging that can be accepted before reaching a full battery capacity, given by:

$$\Delta e_{\text{k}} > e_{\text{c}} - e_{\text{k}}, \tag{5-8}$$

then this amount of charge will not be accepted to the charging control decision set $U_{\text{e}}(x_{\text{k}})$. Therefore, the amount of charge required to reach a full battery capacity is always present in the charging control decision set, even if this is not a multiplier of δ_{e}. In terms of δ_{e} the charging decision control set can be expressed as:

$$U_{\text{e}}(x_{\text{k}}) = [0, \delta_{\text{e}}, 2\delta_{\text{e}}, ..., e_{\text{c}} - e_{\text{k}}]. \tag{5-9}$$

One can understand that the bigger δ_{e} is, the smaller the charging control decision set $U_{\text{e}}(x_{\text{k}})$ will be. To investigate the influence of the charging granularity on the performance of the proposed method, each network that is presented in Figure 5-1 will be simulated 100 times. In each simulation, the link distances will remain the same. However, the charging granularity will be changed. Each simulation represents the optimisation of the expected costs for each presented charging granularity. The parameter δ_{e} that will be tested, which determines the charging granularity's, is given by:

$$\delta_{\text{e}} = [5.0, 7.5, ..., 20.0] * (e_{\text{c}}/100) \text{ (kWh)}, \tag{5-10}$$

representing 5.0 %, ..., 20 % of the battery capacity, which in this simulation setup is equal to 65 kWh. The smallest δ_{e} is equal to 5.0 per cent, which means that the EV has to charge at least 3.25 kWh if it decides to go for charging. Lower charges are assumed to be unlikely and therefore not incorporated. The bigger δ_{e} becomes, the lower the charging granularity becomes as well, the highest charging granularity is achieved for $\delta_{\text{e}} = 5.0$.

It is to be expected that the algorithm's running time will decrease if the charging granularity decreases. This is because the size of state space S_{k} will grow if the charging granularity becomes bigger. More states have to be checked to generate the optimal policy. The question, however, is how the expected costs will change with the decrease of the charging granularity. In each simulation, the same initial state is used. Parameters that determine the initial state are the starting node, the initial SoC, initial battery temperature and time of departure. The parameters of the starting state and the ambient temperature used during the optimisation are summarised in Table 5-6. The initial state x_0 is given by:

$$x_0 = \{i, e_0, t_0, T_0\}. \tag{5-11}$$

In Figure 5-8a, the results with respect to the run time versus the parameter δ_{e} are shown. The figure shows the mean run times of 100 simulations. As expected, we can see that the

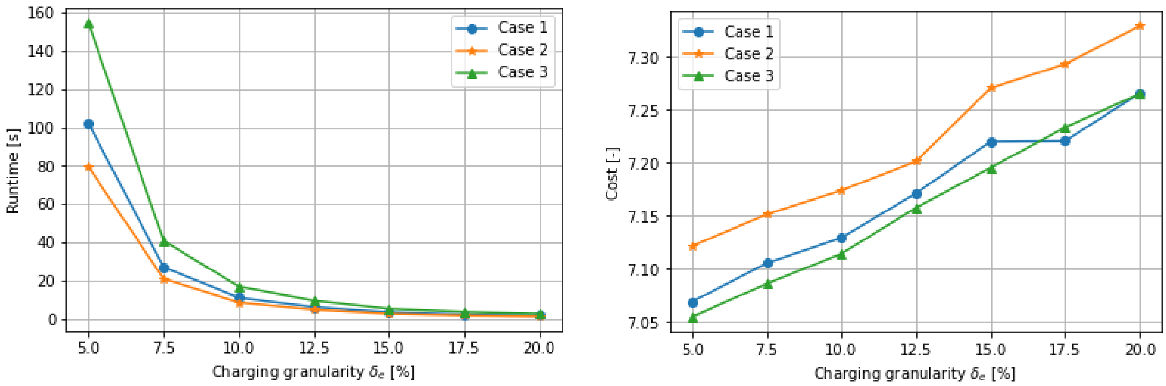

(a) Run time.

(b) Cost.

Figure 5-8: Influence of charging granularity on run time and cost.

run time decreases if the charging granularity decreases. This holds for each of the three networks, while the running time is different for each network. The run time comes closer to each other if the charging granularity increases.

In Figure 5-9, the run time decrease compared to the previous run time per increase in parameter δ_e is shown for all three cases. It can be seen that there is a certain non-linear trend present that is independent of the cases, while this holds for each of the three cases. This non-linear trend is given by the run time decrease combined with a charging granularity decrease. Furthermore, it can be seen in Figure 5-9, that the biggest decrease in run time is achieved when the parameter δ_e is changed from 5.0 % to 7.5 %. As the charging granularity decreases, the run time decrease also decreases. Meaning that if the parameter δ_e keeps on getting bigger, the run time will at a certain point stay unchanged. This can be explained by the charging control set reaching a minimum size at a certain point. This minimum size of the charging set is equal to:

$$U_e(x_k) = [0, e_c - e_k], \tag{5-12}$$

which is given by the minimum charged energy and maximum charged energy. This minimum size of the set is reached if Eq. (5-8) holds, and no other amount of charges are accepted to the charging control decision set. The larger δ_e becomes, more often will Eq. (5-8) hold and therefore the minimum size set described in Eq. (5-12) will occur more. Therefore the run time decreases if δ_e becomes bigger.

In Figure 5-8b, the mean expected cost calculated according to Eq. (4-25) for 100 simulations for each parameter δ_e for each of the three cases is shown. In the figure, we can see that there is an increase in the mean of the expected costs with the decrease of the charging granularity. This can be explained because a more appropriate energy level for the EV at departure at a CS can be chosen with a higher granularity. Because there are more options for the amount of charge that is chosen, resulting in an optimal policy where there is no unnecessary charging, i.e., charging more energy than required to reach the destination, that takes place.

Looking at the results presented in Figure 5-8, we can conclude that the charging granularity influences the outcome of the expected cost and the running time. In the figure, it can be seen

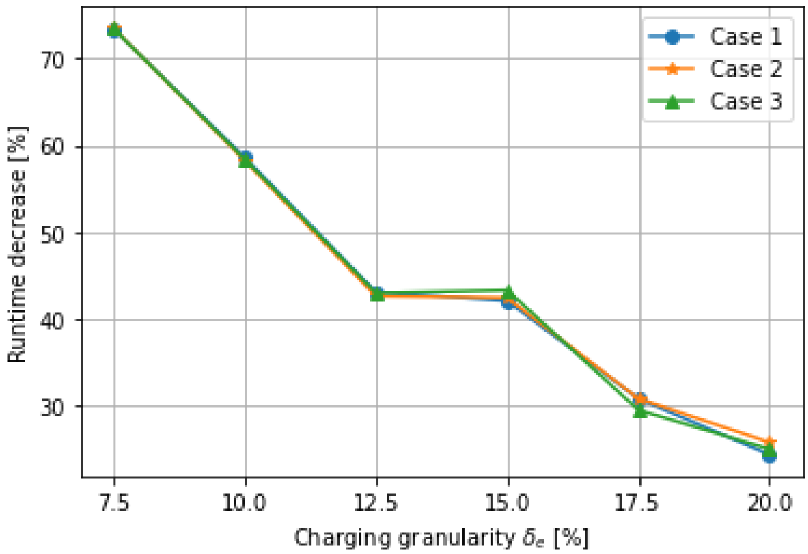

Figure 5-9: Percentile run time decrease compared to the parameter δ_{e} before.

that the mean outcome of the expected cost moves up if the charging granularity decreases. This is the price to pay for a faster running time of the algorithm.

5-2-3 Sensitivity to Charging Time Penalty

If the EV charges at a CS, a charging penalty, denoted by t_{p}, is added to the charging time. This charging penalty is present to capture the time required to leave the main road, to drive towards the CS, the setting up of the charging process and getting back on the main road. The charging time, including charging penalty, is given by:

$$\tau_{\mathrm{i}} = \begin{cases} 0, & \text{if } \Delta e_{\mathrm{k}} = 0, \\ \tau_{\mathrm{i}} + t_{\mathrm{p}}, & \text{otherwise.} \end{cases} \tag{5-13}$$

In the base case, it is assumed that the charging penalty is the same for the whole network. However, one can imagine that if a CS is not close to the main road, the charging penalty could be higher compared to a CS close to the main road. We will investigate the sensitivity of the proposed method to this charging penalty. It can be expected that if the charging penalty increases, the amount of charging occasions decreases. In order to test this, 100 simulations will be executed in which the charging penalty will be changed. In each simulation, the following charging penalties will be used:

$$t_{\mathrm{p}} = [0, 2.5, ..., 20.0] \text{ (min)}. \tag{5-14}$$

The link distances are randomly distributed between [100, 120] km in each simulation. The initial state, the charging granularity and the ambient temperature used in these simulations are described in Table 5-7.

Table 5-7: Parameters for simulations of the charging time penalty sensitivity.

Parameter	i [-]	e_0 [kWh]	t_0 [hr]	T_0 [°C]	$\mathrm{T}_{\mathrm{ambient}}$ [°C]	δ_{e} [%]
Value	Node 1	65	$\Omega \to [0, 20]$	20	20	5.0

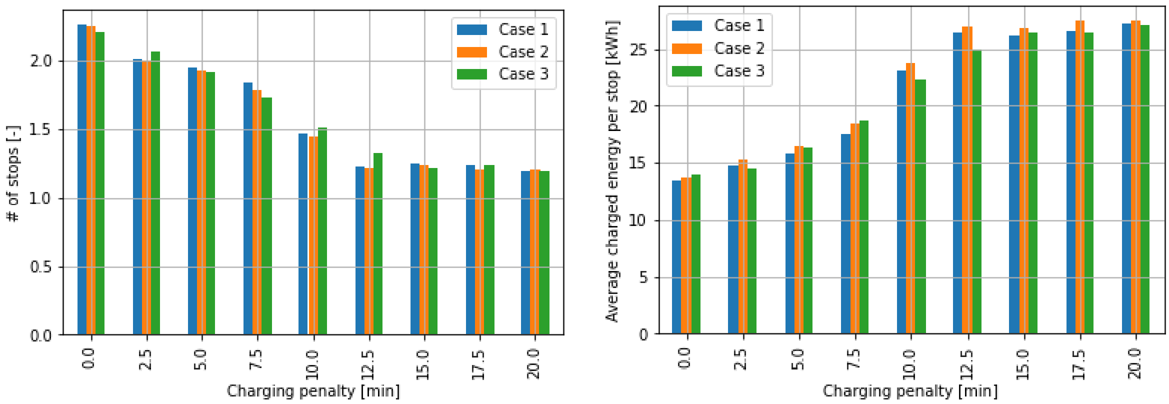

(a) Number of stops. **(b)** Average charged energy.

Figure 5-10: Number of stops and average charged energy for each simulated charging penalty.

In Figure 5-10a, the results for 100 simulations for each of the three cases with respect to the number of stops are shown. In this figure, we can see that the number of stops, as expected, decreases if the charging penalty increases. The same decreasing trend can be seen in Figure 5-10a for each of the three cases. The fact that the number of stops decreases if the charging penalty increases is logical. It becomes more expensive to charge since the charging penalty becomes higher. Therefore, at some point, it is more profitable to charge longer, which also gives more costs than to charge multiple times.

In Figure 5-10b, the results of the average energy that is charged per stop for each of the charging penalty is shown. A logical result of the fact that there are fewer stops for higher charging penalties is that more energy will be charged per stop. This can be seen in the figure, while a trend opposite to the number of stops is present for the average amount of charged energy per stop.

It can be concluded that the charging penalty has the desired influence on the proposed method. A high charging penalty is undesirable because it gives higher costs. However, a high charging penalty can not always be avoided, for example, if CS's are situated far from the main road.

5-2-4 Influence of the Battery Temperature and Ambient Temperature

The battery temperature is of importance for the expected cost. A battery temperature above 35 °C is not allowed due to safety reasons. The charging time will increase severely if the battery temperature is much below 25 °C at the start of the charging process. The ambient temperature influences the energy consumption for the cabin climate control. Therefore, it is interesting to test the sensitivity of the expected cost of the algorithm with respect to the battery temperature and the ambient temperature.

Table 5-8: Parameters for simulations of the temperature's influence.

Parameter	i [-]	e_0 [kWh]	t_0 [hr]	δ_{e} [%]
Value	Node 1	65	$\Omega \rightarrow [0, 20]$	5.0

In this thesis, we assume that two essential parameters influence the battery temperature: the initial battery temperature and the ambient temperature. The initial battery temperature is the battery temperature at the start of the route. This initial battery temperature can vary because the battery temperature can adapt to the ambient temperature, in case the EV is not used for a long time, and the battery is not charged for a while. However, the battery temperature can also be higher than the ambient temperature if the EV has just been used before the start of the route. The ambient temperature influences the energy consumed by the cabin climate control. For very low and very high temperatures, there is more energy consumed by the cabin climate control, and this has an impact on the amount of energy that has to be charged en route, which can influence the travel cost.

In order to test the influence of the initial battery temperature and ambient temperature on the expected cost for the EV, we will vary the ambient temperature between two extreme cases. These extreme cases are $-20\,°\mathrm{C}$ and $40\,°\mathrm{C}$. The set containing all of the ambient temperatures is given by:

$$\mathrm{T}_{\mathrm{ambient}} = [-20, -10, 0, 10, 20, 30, 40] \quad °C. \tag{5-15}$$

In each simulation, next to changing the ambient temperature, the initial battery temperature will be altered as well. This initial battery temperatures are given by:

$$\mathrm{T} = [0, 5, 10, 15, 20, 25, 30, 35, 40] \quad °C, \tag{5-16}$$

corresponding to a range of different possible initial battery temperatures. Next to the initial battery temperature, several other parameters describe the initial state of the system, given in Table 5-8. Here the initial battery temperature is left out since this is changed in each simulation.

Lastly, at the beginning of each simulation, the link distances are randomly distributed between [100,120] km. Now we can test the influence of the ambient temperature and the initial battery temperature on the expected cost of the route, which also influences the optimal route. While the expected cost is partly route-dependent, it might be beneficial to drive another route in terms of expected cost. It can be expected that very high, and respectively very low initial battery temperatures have higher costs than initial battery temperatures that are close to the desired range of $25\,°\mathrm{C}$ to $35\,°\mathrm{C}$. This is because the battery has to be heated or cooled relatively very much with these initial battery temperatures, and more energy is consumed due to the cabin climate control.

In Figure 5-11a, Figure 5-11b, and Figure 5-11c the results for network 1, network 2 and network 3 are shown. The figures show a contour plot with the initial battery temperature, ambient temperature and the expected cost, given by the colour. In the figures, we can see a relation between the expected cost, the initial battery temperature and the ambient temperature. This relation is present for each of the three cases.

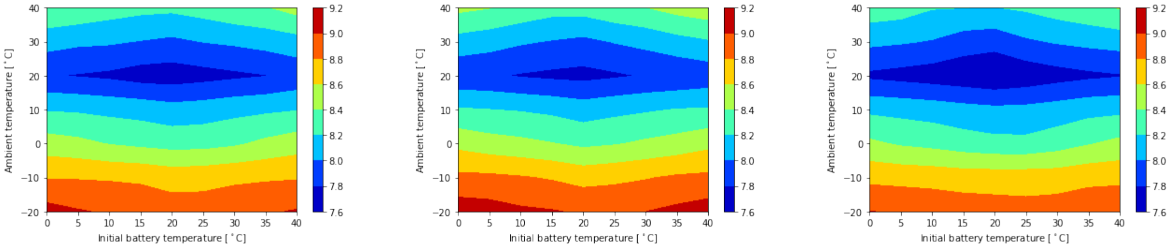

(a) Network 1. **(b)** Network 2. **(c)** Network 3.

Figure 5-11: Initial battery temperature and ambient temperature influence on the expected cost for the different networks.

First, looking at the influence of the ambient temperature, shown on the Y-axis of the figures, we can see that for each of the three cases, the highest expected costs are achieved for $-20\,°\mathrm{C}$. This can be explained due to the high energy consumption for the cabin climate control, causing the EV to charge more energy during the route, increasing the expected cost. For higher ambient temperatures, less energy is consumed due to cabin climate control. Therefore, it can be seen that the expected costs are lower for higher temperatures. However, higher temperatures also cause the fact that the battery has to be cooled more. Therefore, the optimal ambient temperature is $20\,°\mathrm{C}$.

The influence of the initial battery temperature shown on the X-axis shows a relationship between the expected cost and the initial battery temperature since the expected costs are higher for higher and lower initial battery temperatures. This can be explained because the battery has to be cooled or heated significantly more for these initial battery temperatures. Therefore, initial battery temperatures close to $20\,°\mathrm{C}$ give the optimal expected cost.

It can be concluded that there is a relation between the ambient temperature, the initial battery temperature and the expected cost. The ambient temperature and initial battery temperature influence the expected cost. This can cause the EV to spend more energy on the cooling or heating of the battery while driving, which in turn causes the fact that longer or possibly also more charging events have to take place. This impacts the amount of energy that has to be charged in total, but also on the arrival time of the EV, which both contribute to the expected cost of an EV.

5-2-5 Trade-off between Charging Cost and Journey Time

In this section, we will investigate the influence of parameter α. This α parameter is used in the stage cost and can be used in order to create a trade-off between the charging cost and the journey time. As explained in Section 4-2-5, this stage cost is given by:

$$g_{\mathrm{k}} = c_{\mathrm{charging}} + \alpha * c_{\mathrm{time}}. \tag{5-17}$$

By making α arbitrary large or small, a trade-off can be made between the charging cost or elapsed time. These different preferences can be referred to as an Economical route preference or the Fastest route preference. The Economical route preference minimises the charging cost, and the fastest route preference minimises the elapsed time. In this section, it will be

Table 5-9: Parameters for each simulation for the trade-off between charging cost and journey time.

Parameter	i [-]	e_0 [kWh]	t_0 [hr]	T_0 [°C]	T_{ambient} [°C]	δ_{e} [%]	t_{p} [min]
Value	Node 1	65	$\Omega \rightarrow [0, 20]$	20	20	5.0	5

investigated how this α parameter influences the solution and how this α must be chosen to find the economical or fastest route.

In order to test the influence of α, 100 simulations will be held. In each simulation, the parameter α will be changed. Other parameters, such as the initial battery temperature, the ambient temperature and the link distances, will be the same during a simulation. The link distances are randomly distributed between [100, 120] kilometres for each simulation. In Table 5-9, the used parameters for this simulations can be found.

The set describing the parameter α in each simulation is given by:

$$\alpha = 10^{\beta}, \tag{5-18}$$

where $\beta = [-5, -4, ..., 5]$. The results of the simulations are shown in Figure 5-12, where Figure 5-12a shows the influence of α on the total travel time from origin to destination. In this figure, the travel time is normalised such that the influence of parameter α between the three cases can easily be compared. In the figure, it is clear that a trend is present for each of the three cases. For $\alpha \leq 10^{-3}$, the total travel time remains unchanged, meaning that for these values of α, the economical route will be found. The same holds for $\alpha \geq 10^{2}$, where the total travel time also stabilises on a lower value compared to smaller values of α, meaning that these represent the fastest route.

This trend can be confirmed if we look at the total charging cost, shown in Figure 5-12b. Again, the total charging cost is normalised for ease of comparison in this figure. The figure shows that an opposite effect to the total travel time is present with the influence of parameter α. For values $\alpha \leq 10^{-3}$, the total charging cost remains unchanged, where these costs represent the minimum total charging cost. Which was the desired outcome for the Economical route. For values $\alpha \geq 10^{2}$, the total charging cost stabilises for the highest possible cost of the total charging cost. This cost is present for the fastest route, where the least travel time is achieved at a higher charging cost.

From Figure 5-12, it can be concluded that a different preference of route can be achieved by using the parameter α. Next to the economical and fastest route, a mixed route between the two can also be achieved for $10^{-3} < \alpha < 10^{2}$. This Mixed route preference generates a route that does not minimise the total drive time or the total charging cost. Resulting in a mixed route in which the travel time and charging cost are equally important, and a route will be found in which these two costs are balanced. The different preferences for the routes with the accompanying value of α are shown in Table 5-10.

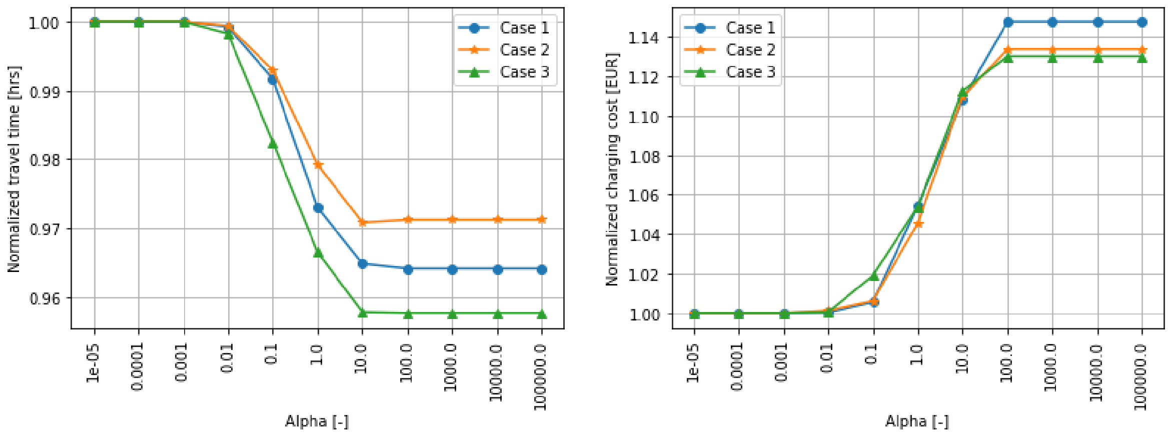

(a) Normalised drive time in hours.

(b) Normalised charging costs in Euro.

Figure 5-12: Normalised drive time and normalised charging costs for different values of α.

Table 5-10: Route preference with accompanied value of α.

Route preference	Value of α
Economical	$\alpha \leq 10^{-3}$
Mixed	$10^{-2} < \alpha < 10^{1}$
Fastest	$\alpha \geq 10^{2}$

5-3 Conclusions

In this chapter, it is verified that the proposed method functions for our problem and the simplification is valid. It was shown that the suggested simplification worked without influencing the outcome. Also, the influence and sensitivity of multiple parameters have been tested. Starting with the charging granularity, it can be seen that it influences both the run time and the expected cost of the method. How smaller the charging granularity how faster the proposed method will find a solution. However, this speed advantage comes with the price of a less accurate solution.

Then the algorithm was used for different ambient temperatures and different initial battery temperatures. The algorithm still functions with extreme conditions, such as $-20\,°\mathrm{C}$ and $40\,°\mathrm{C}$ ambient temperature, as well as very high and low initial battery temperatures. Although, the expected cost raises if more extreme temperatures are reached. In the tested temperatures, it was shown that the optimal ambient temperature is $20\,°\mathrm{C}$ and the optimal initial battery temperature is $20\,°\mathrm{C}$.

It was verified that the charging penalty has the desired influence. Since a high charging penalty is undesirable, it was shown that the number of charge events decreases for higher charging penalties. The higher charging penalties influence the charging cost, making it more appealing to have fewer charging events but a higher amount of charged energy.

Lastly, the influence of the parameter α was tested, which sets the trade-off between the optimal cost versus time. It became clear that it is possible to set a preference for an Economical route, which minimises the charging cost, a Mixed route that minimises the charging cost and the time cost, and the Fastest route, which minimises the time cost. The exact values of α to achieve this preference are found and stated.

Now that the proposed method is verified and its robustness to multiple parameters is shown, we can start with the case studies.

Chapter 6

Case Studies and Results

In this chapter, four case studies are performed. First, a case study will be conducted to test the performance of the proposed method compared with the conventional navigation systems for EVs. After which, a case study is performed to investigate the possibility of optimising the driving speed below the maximum allowed driving speed to improve travel costs. Then a case study is performed to optimise the charging platform selection to see how the travel costs can be optimised when there is a choice between charging platforms. Lastly, a case study is performed to investigate the influence of uncertainty on travel costs. These case studies are performed to investigate how the proposed method can be used to optimise the travel costs of an EV and to create new insights on how to optimise the travel costs of an EV.

6-1 Case study A - Comparison with Min Algorithm

In this section, the proposed method will be compared to a Min algorithm [5], which uses a strategy always to minimise the expected travel time and charging time. First, the simulation setup will be described. Then the Min algorithm will be explained, after which the performance between the proposed method and the Min algorithm will be compared.

6-1-1 Simulation Setup of Case Study A

For the simulation setup, to test the performance of the algorithm compared to the Min algorithm, the same simulation setup as in Section 5-1 will be used. This simulation setup has reasonable assumptions to test the performance of the two algorithms. Both algorithms should find an optimal policy with this simulation setup. Therefore the difference between the two algorithms can become visible using the simulation setup described in Section 5-1.

Again for each of the three networks, 100 simulations will be run. The link distances are randomly distributed between 100 and 120 kilometres in each simulation. Then in each simulation, both the proposed method and the Min algorithm are used to find an optimal

Table 6-1: Parameters for each comparison with Min simulation.

Parameter	i [-]	e_0 [kWh]	t_0 [hr]	T_0 [°C]	$\mathrm{T}_{\mathrm{ambient}}$ [°C]	δ_{e} [%]	t_{p} [min]
Value	Node 1	65	$\Omega \rightarrow [0, 20]$	20	20	10.0	5

policy. In order to generate more insights in the proposed method, the parameter α in Eq. (4-17) will be set on the three possible preferences: economical, mixed and fastest.

Next to α, other parameters, such as the initial battery temperature, are important. These parameters are given in Table 6-1.

6-1-2 Min Algorithm

Conventional navigation systems of EVs consists of algorithms that minimise the expected driving and charging time. However, in this travel time, there is no expected waiting time included. Therefore, simply the route with the shortest expected travel time between CSs is selected, disregarding the fact that there might be a waiting time when arriving upon a CS. This waiting time influences the total charging time, which influences the departure time at a CS. As explained, the expected driving speed, and thus the expected travel time, between two nodes depends on the departure time. Therefore, not considering the waiting time can lead to situations where a less favourable driving speed is expected.

Moreover, the strategy regarding the charging process is mostly relatively simple for conventional navigation systems. The policy is typically to charge at the closest CS when a SoC of 20 % or lower is reached. When the EV decides to charge, the departure SoC is always set to be equal to 80 %, independent of how long the route will continue.

The Min algorithm will also use SDP with the time-dependent stochastic model of the driving speed. The Min algorithm will not include the possibility of waiting time. Regarding the charging strategy of the Min algorithm, to prevent an extensive extra amount of energy from being charged to reach the destination, the Min algorithm includes the possibility to charge the expected energy consumption plus 15 % SoC at the last nodes before the destination. This is included to prevent the Min algorithm from charging up to 80 % SoC if, for example, a much lower SoC is required to reach the destination. This would give results that are not comparable to the proposed method because this may result in much longer charging times than required. Hence, the strategy used in the Min algorithm can be summarised as follows:

- Minimise the expected driving and charging time using SDP,
- Disregard possible waiting times,
- Charge at a node if SoC<20 %,
- Charge up to 80 % SoC for $k < N$,
- Charge $\bar{e}_{\mathrm{ij}} + 15\,\%$ SoC or up to 80 % SoC for $k = N$.

In order to compare the results of the Min algorithm with the proposed method, in the results, the waiting times from the selected optimal policy for the Min algorithm will be included.

In the remainder of this section, the results of the Min algorithm compared to the proposed method will be presented and discussed.

6-1-3 Results of Case Study A

The journey time of an EV is built up by the waiting time, the charging time and the driving time. For each of the three cases, we will discuss the results of the mean value for the waiting time, charging time, driving time, journey time and the charging cost.

In Table 6-2, Table 6-3, and Table 6-4, the results of a 100 simulations for network 1,2, and 3 respectively, are shown. If we look at the results presented in the tables, it can be seen that the Min algorithm expects the lowest waiting time compared to the other algorithm with different parameterisation. Followed by the Fastest preference, for which the waiting time is slightly higher than for the Min algorithm. The Mixed and Economical preferences have considerable higher waiting times. The waiting time of the Economical preference is the highest. This could be expected since this algorithm optimises the charging cost. Therefore, higher waiting times at a CS will be accepted if the charging cost is the lowest at the respective CS. The Mixed preference has a waiting time that is slightly lower than the Economical preference and higher than the Fastest preference. Also, this could be expected since the Mixed preference has a mixed objective for the charging and time costs. Interesting is the difference between the results of the Fastest preference and the Min algorithm. Since the waiting time of the Min algorithm is lower than the Fastest preference, even though the Min algorithm does not consider the waiting time in its cost function. However, the Fastest preference accepts more waiting time can be explained when we analyse the resulting charging time and the driving time of the two algorithms.

The charging time of the different algorithms shows a somewhat similar trend as the waiting time. The charging time of the Economical preference is the highest, which can be explained because the objective is to minimise the charging cost. The longer charging time can, for example, be the result of a longer charging event with a lower charging price. As explained, charging to higher SoCs has the disadvantage of a non-linear increase in the charging time. The Mixed preference and the Fastest preference have a comparable charging time. Again interesting to see is the fact that the Min algorithm has the lowest charging time of all of the algorithms.

The results of the higher waiting time and charging time of the Fastest preference compared to the Min algorithm can be explained with the driving time. As can be seen in the tables, the driving time for the Fastest preference is significantly lower than the other algorithms. This can be explained by the expected driving speed, and therefore the driving time, between two CSs, which depends on the departure time at a CS. It can be concluded that the Fastest preference optimises this departure time, in case it goes for charging, such that the lowest expected driving time is achieved. This also means that the Fastest preference can decide to break up a bigger charging event, where for example, the battery is recharged from 20 % to 80 %, in two smaller charging events, such that the optimal departure time at each CS can be achieved and thus the optimal journey time is reached.

Moreover, the Economical preference achieves the lowest charging cost. This explains the associated higher waiting time and driving time of this algorithm. What could also be expected is that the charging cost of the Mixed preference lies between the Economical and Fastest

Table 6-2: Results of the waiting time, charging time, driving time and journey time in minutes and charging cost in euros, for different algorithms for 100 simulations of network 1.

Algorithm	**Waiting time [min]**	**Charging time [min]**	**Driving time [min]**	**Journey time [min]**	**Charging cost [EUR]**
Economical	4.00	76.52	412.16	492.68	19.04
Mixed	3.81	73.54	404.30	481.65	19.45
Fastest	3.03	73.42	398.45	474.90	20.28
Min	2.36	70.45	407.19	480.00	20.31

Table 6-3: Results of the waiting time, charging time, driving time and journey time in minutes and charging cost in euros, for different algorithms for 100 simulations of network 2.

Algorithm	**Waiting time [min]**	**Charging time [min]**	**Driving time [min]**	**Journey time [min]**	**Charging cost [EUR]**
Economical	3.78	80.31	408.35	492.44	18.98
Mixed	3.61	74.61	398.99	477.21	19.66
Fastest	2.93	74.75	395.12	472.80	20.52
Min	2.30	71.91	400.81	475.02	20.33

preferences. Therefore, the Mixed preference results in more waiting, charging, and driving time compared to the Fastest preference. The charging cost of the Min algorithm and the Fastest preference is comparable and the highest of all algorithms. This can be explained because these algorithms minimise the time cost and accept higher charging costs to achieve lower time costs.

In order to show the difference between the optimal policies, i.e., the optimal route created by the proposed method and the Min algorithm, we will elaborate on some simulations of the networks. The difference between the policies will be shown and highlighted in these simulations. Since the most significant differences are achieved between the Fastest and Min algorithm, these two algorithms will be compared in the following.

We start with a simulation of network 1, for which the optimal policies for the two algorithms are shown in Figure 6-1. In this figure, the solid cyan coloured line represents the optimal policy created by the Fastest preference and the dashed red coloured line represents the optimal policy created by the Min algorithm. If the optimal policy includes charging at a particular node, the amount of charging is shown next to the node with the corresponding

Table 6-4: Results of the waiting time, charging time, driving time and journey time in minutes and charging cost in euros, for different algorithms for 100 simulations of network 3.

Algorithm	**Waiting time [min]**	**Charging time [min]**	**Driving time [min]**	**Journey time [min]**	**Charging cost [EUR]**
Economical	3.58	77.79	401.54	482.92	18.64
Mixed	3.41	73.49	391.21	468.11	19.21
Fastest	2.64	73.42	386.14	462.20	19.94
Min	2.12	72.25	394.02	468.39	20.32

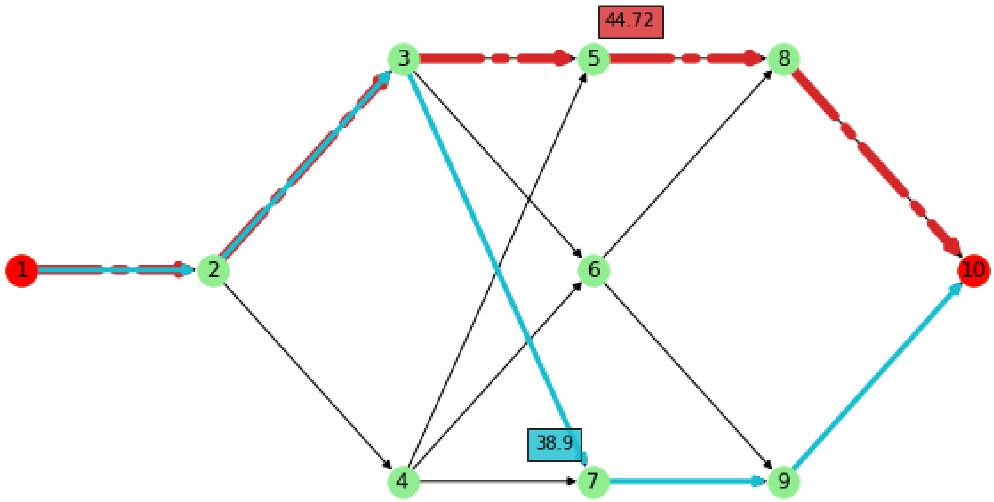

Figure 6-1: Optimal policies created by Fastest preference (cyan) and Min algorithm (red), with accompanied amount of charged energy, for one simulation of network 1.

Table 6-5: Detailed results of the waiting time, charging time, driving time and the journey time in minutes of one simulation of network 1.

Algorithm	**Waiting time** [min]	**Charging time** [min]	**Driving time** [min]	**Journey time** [min]
Fastest	1.20	51.84	319.20	372.24
Min	1.20	58.98	322.20	382.38

colour for the algorithm. It can be seen in Figure 6-1 that the optimal policy for the two algorithms is different. The chosen route, the amount of energy to be charged, and where this energy is charged are different.

The detailed parts of the optimal policy for this simulation are shown in Table 6-5, here we can see that the expected waiting time is the same for both policies. The most significant difference is achieved in the charging and driving times. These two are influencing each other. As described before, the departure time at a CS is essential for the expected driving speed, and thus driving time, between two CSs. Therefore, the Fastest preference decides to have a charging event at a different CS compared to the Min algorithm, such that a more favourable expected driving speed is achieved in another segment. Also, the amount of charged energy is slightly different such that the charging time for the Fastest preference is lower than for the Min algorithm. The choice of the CS and the amount of energy to be charged contribute to a lower journey time for the Fastest preference than the Min algorithm.

In Figure 6-2, a simulation is shown for network 2 where the advantage of splitting up a single charge event into two charging events is elaborated. In this simulation, the optimal policy of the Fastest and Min algorithm is substantially different. The Min algorithm uses only one very long charging event, while the Fastest preference uses two charging events to achieve the most favourable expected driving time.

In Table 6-6, the detailed results of the simulation presented in Figure 6-2 are shown. In this

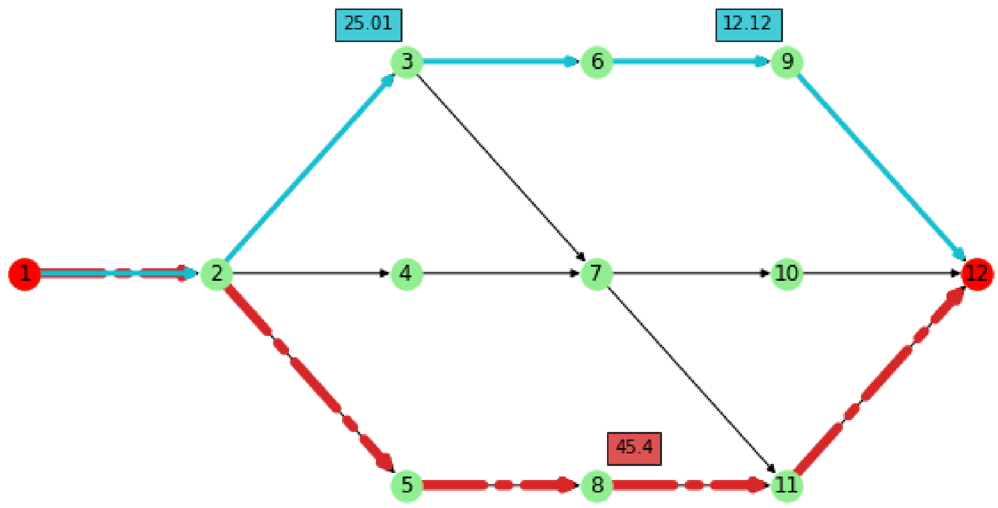

Figure 6-2: Optimal policies created by Fastest preference (cyan) and Min algorithm (red), with accompanied amount of charged energy, for one simulation of network 2.

Table 6-6: Detailed results of the waiting time, charging time, driving time and the journey time in minutes of one simulation of network 2.

Algorithm	**Waiting time** [min]	**Charging time** [min]	**Driving time** [min]	**Journey time** [min]
Fastest	3.60	55.20	422.40	481.2
Min	2.40	59.76	433.14	495.3

table, we can see that the journey time of the Fastest preference is significantly lower than the Min algorithm. This difference is achieved by using two charging events instead of one. Although more waiting and charging time is incurred, this is compensated by the driving time such that a more optimal journey time is achieved. The amount of charged energy is nearly the same. However, the charging penalty is incurred twice by using two charging events. Therefore, the charging time of the Fastest preference is higher than the Min algorithm even though the amount of total energy-charged is nearly the same.

In Figure 6-3, a very interesting simulation is shown for network 3. In this figure, it can be seen that for the Fastest and Min algorithm, the same optimal route is selected. However, the Fastest preference has chosen to undertake two charging events instead of one, favouring the journey time.

In Table 6-7, the detailed results for the simulation presented in Figure 6-3 are shown. This table shows that because the Fastest preference undergoes two charging events, a higher waiting and charging time is present for the Fastest preference compared to the Min algorithm. However, by optimising the departure time at the CSs, the driving time for the Fastest preference is lower than the Min algorithm. Therefore, the optimal policy created by the Fastest preference, which consists of two charge events, has a significant lower journey time than the Min algorithm.

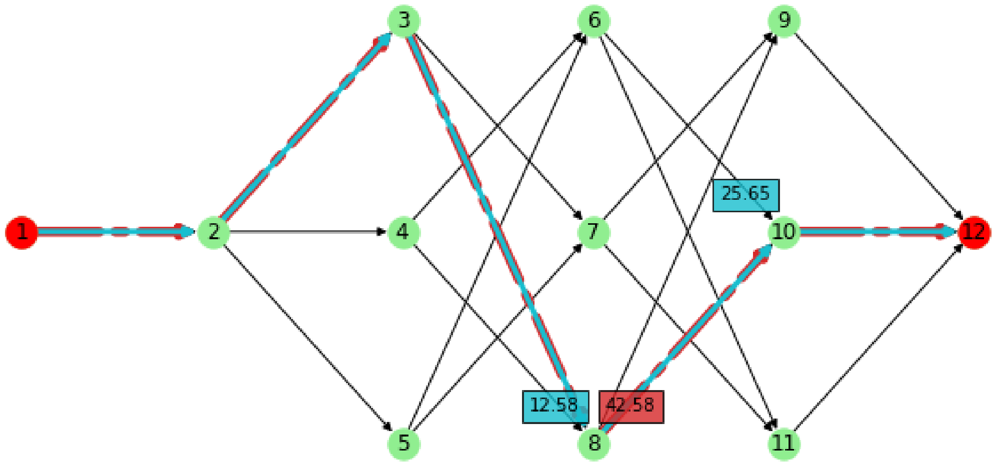

Figure 6-3: Optimal policies created by Fastest preference (cyan) and Min algorithm (red), with accompanied amount of charged energy, for one simulation of network 3.

Table 6-7: Detailed results of the waiting time, charging time, driving time and the journey time in minutes of one simulation of network 3.

Algorithm	**Waiting time [min]**	**Charging time [min]**	**Driving time [min]**	**Journey time [min]**
Fastest	4.80	55.20	459.24	519.24
Min	2.40	56.64	487.26	546.30

6-1-4 Conclusions of Case Study A

In this section, the proposed method has been compared with the conventional method for routing systems of EVs. This conventional method, referred to as the Min algorithm, consists of a method where only the expected driving time between CSs is considered. Waiting times are not considered, and the EV always charges up to the same SoC. Based on the results, it can be concluded that the proposed method in this thesis achieves a better performance than this conventional method. The Fastest preference of the proposed method achieves a significant lower journey time than the Min algorithm.

From elaborated simulations, it can be seen that the optimal policy created by the proposed method often prefers to split up a single charging event into multiple charging events. In this way, the proposed method can optimise both the charging cost and the departure time at CSs. The optimisation of this departure time at CSs incorporates the expected driving speed to find the optimal driving time.

6-2 Case study B - Speed optimisation

In this case study, in addition to the route and the amount of charging, we will look into the possibility of optimising the EV's driving speed. This can be seen as speed advice for the EV driver, which can have advantages for travel costs. With ICEV, it is conventional to drive the maximum allowable speed, while the refuelling process of ICEV is not impacted substantially by the energy consumption. However, multiple advantages can be achieved with driving at a slower speed than allowed with EVs.

The driving speed impacts the battery energy consumption, which impacts the amount of energy that has to be charged and thus the charging time and the charging cost. The driving speed also has an impact on the battery thermal heating. Therefore, driving slower than the speed limit can impact the rate at which the battery is heated by passive heat. This again influences the amount of cooling of the battery that is required, which has an impact on the battery energy consumption, the amount of energy to be charged and the charging time.

The downside of driving slower than the allowable speed, or the current driving speed of the traffic, is that the driving time between two CSs will increase. Therefore, the energy consumption for the cabin climate control increases since this depends on the ambient air temperature and the driving time.

As discussed, there are advantages and disadvantages of adopting a slower driving speed than the highway speed limit. How advantageous it is to adopt a lower driving speed and thus accept more driving time will be discussed in this section.

6-2-1 Simulation Setup of Case Study B

For the simulation setup, almost the same simulation setup as in Section 5-1 will be used. However, if we look at Figure 2-1, it can be seen that the energy consumption for the propulsive power demand increases especially for speeds higher than 100 (km/h). This results from the increased resistance, e.g., the air resistance. At speeds lower than 100 (km/h), the propulsive

Table 6-8: Parameters for each speed optimisation simulation.

Parameter	i [-]	e_0 [kWh]	t_0 [hr]	T_0 [°C]	δ_e [%]	t_p [min]
Value	Node 1	65	$\Omega \rightarrow [0, 20]$	20	10.0	5

energy consumption shows relatively small differences. Therefore, in this simulation setup, the maximum speed will be changed. For the maximum speeds that will be simulated, The Netherlands will be used as an example, where the maximum speed on highways varies between 100-130 (km/h). This simulation setup will use the same distribution for the expected speed for all possible time intervals during the day. This means that there is no difference in the expected driving speed during rush hours and non-rush hours. The maximum speeds that will be simulated are given by:

$$V_{\mathrm{max,ij}} = [100, 110, 120, 130] \text{ (km/h)}. \tag{6-1}$$

The maximum speed will be varied to investigate if there are certain maximum speeds for which it becomes interesting to drive a lower speed than the maximum speed. Next to driving speed, the ambient temperature also influences the energy consumption during the driving. The reason is that the ambient temperature determines how much energy is spent on the cabin climate control. The cabin climate control is present during the driving time. Therefore, the driving speed indirectly influences the amount of energy spent on the cabin climate control since the driving speed influences the driving time. The adaption of a lower driving speed also depends on the ambient temperature. While, for example, the energy consumption saved by driving at a slower speed might not compensate for the extra energy spent on cabin climate control due to the extra drive time. Therefore, the Speed Optimization (SPO) will be conducted for different ambient temperatures, given by:

$$\mathrm{T}_{\mathrm{ambient}} = [-20, 0, 20] \quad {}^\circ C. \tag{6-2}$$

Since we have seen that the results are not dependent on the network presented in Section 5-1, only network 1 will be used. This network will be simulated 50 times. The link distances are randomly distributed between 100-120 kilometres in each simulation. Also, in each simulation, the proposed method will create an optimal policy. The SPO is then used to optimise the driving speed for the path found with the proposed method. The SPO thus does not optimise the path, only the driving speed and optionally the amount of energy charged and the place where the charging event takes place. We are particularly interested in whether the SPO can have a positive influence on the journey time. Therefore, only the Fastest preference will be used, with $\alpha > 10^2$. Other parameters, such as the initial battery temperature, are given in Table 6-8.

The fact that the speed is also optimised and the next node is already determined by the optimal path created by the proposed method means that the control decision of the proposed method changes. We have to incorporate the advised speed in the control decision set, and we can leave out the choice of which node to travel next; this is given by:

$$u_k = (\Delta e_\mathrm{k}, q_\mathrm{k}, v_{\mathrm{a,ij}}), \tag{6-3}$$

where $v_{\mathrm{a,ij}}$ denotes the advised speed between CS i and CS j. This advised speed is chosen from a set given by:

$$v_{\mathrm{a,ij}} \in U_{v_{\mathrm{a,ij}}}(x_k), \tag{6-4}$$

this set depends on the state x_k, while the maximum advised speed is equal to the expected driving speed. Therefore the set $U_{v_{\mathrm{a,ij}}}(x_k)$ is given by:

$$U_{v_{\mathrm{a,ij}}}(x_k) = \{80 \leq \delta_{v_{\mathrm{a,ij}}} \leq V_{\mathrm{max,ij}}\} \text{ (km/h)}, \tag{6-5}$$

where 80 (km/h) means that this is the minimum driving speed and $\delta_{v_{\mathrm{a,ij}}}$ determines the granularity of this set. This minimum driving speed is used for safety reasons, while one can imagine that it is not safe to drive very slow on a highway. The maximum advised driving speed is given by $V_{\mathrm{max,ij}}$, which is the maximum driving speed between CS i and CS j and is changed in each simulation. For this case study, the granularity will be equal to 10 (km/h). Now that the simulation setup is explained, we can discuss the results.

6-2-2 Results of Case Study B

In this section, we will discuss the results of the SPO of the EV compared to the proposed method without SPO. We start with an ambient temperature of -20 °C. As can be seen in Figure 2-2, for this ambient temperature the energy consumption for the cabin climate control is the highest. Therefore decreasing the driving speed has a side effect of more energy consumption due to cabin climate control. Because the driving time increases and therefore also the required time to control the cabin climate. In Figure 6-4a, the mean journey time of 100 simulations for both the proposed method without SPO and the proposed method with SPO is shown. In the figure, it can be seen that the journey time generally decreases if the maximum speed increases. Also, it can be seen that the proposed method with SPO cannot optimise the driving speed such that a lower journey time is achieved. This can be concluded since the mean journey time for both methods is the same. The found journey time of the method without SPO represents an upper limit for the journey time, and therefore, if SPO is present, this can only positively influence the journey time.

In Figure 6-4b, the average driving speed during the journey of 100 simulations is shown. The driving speed of the method without SPO is the upper limit, while this method always uses the maximum allowable driving speed. It can, however, be seen that the method with SPO also decides to use the maximum allowable driving speed. It is, therefore, not optimal to adopt a lower driving speed with an ambient temperature of $-20\,°\mathrm{C}$. This would increase the driving time and therefore also the energy consumption due to cabin climate control. The increase in energy consumption for cabin climate control is too high compared to the decrease in energy savings due to the propulsive power demand.

In Figure 6-5a, the mean journey times of 100 simulations with different maximum speeds at $0\,°\mathrm{C}$ ambient temperature is shown for the method with SPO and without SPO. In this figure, it can be seen that it is beneficial to lower the driving speed below the maximum allowable driving speed for this ambient temperature. This can be seen due to the results shown in Figure 6-5a, where the journey time for the method with SPO is lower for speeds equal to

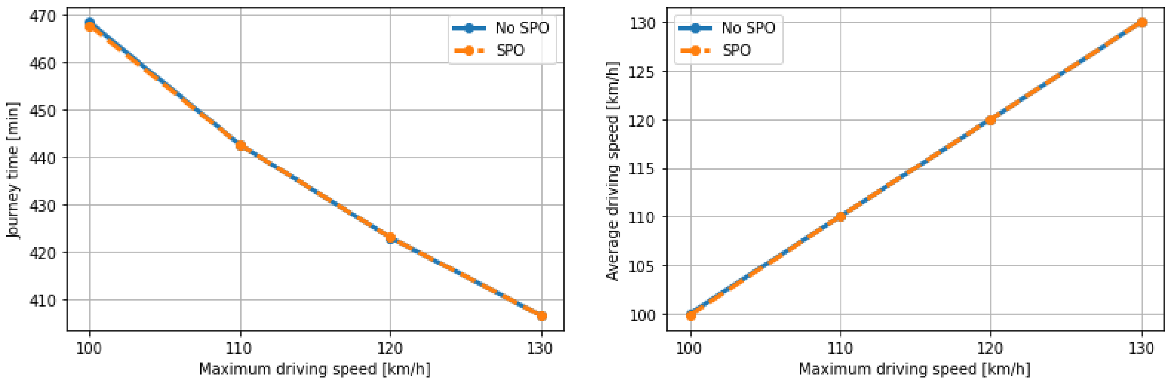

(a) Mean journey times.

(b) Average driving speeds.

Figure 6-4: Mean journey times and average driving speeds for different maximum speeds at an ambient temperature of $-20\,°\mathrm{C}$.

and higher than 110 (km/h). For a maximum speed of 100 (km/h), the journey time cannot be lowered by driving at a slower speed than the maximum allowable driving speed. This can be explained with Figure 2-1, where it can be seen that for speeds between 50 (km/h) and 100 (km/h) the energy consumption is almost similar. Therefore, it only becomes attractive to lower the driving speed for maximum speeds above 100 (km/h).

In Figure 6-5b, the results of the average driving speed during the journey of 100 simulations is shown. In this figure, it becomes clear that SPO is interesting for maximum speeds of 110 (km/h) and higher. For a maximum speed of 110 (km/h), the average driving speed of the SPO method is only slightly lower. However, looking at Figure 6-5a the gained advantage in journey time is present. This could, for example, be the case because, with a lower average speed, one less charging event is required to reach the destination. The EV, in that case, can charge upon arrival at the destination.

Looking at the average of the total energy that is charged during the journey of the 100 simulations, in Figure 6-5c, we can see that the total energy that is charged with SPO is lower than for the method without SPO. This is because lower energy consumption is achieved by adapting to a lower driving speed than the maximum allowable driving speed. Less energy has to be charged in total resulting in a slower charging time. If the decrease in charging time is higher than the increase in driving time, the journey time can be lowered by adopting a lower driving speed. In Figure 6-5d, the number of charging events for different maximum driving speeds for the method with SPO and the method without SPO is shown. In this figure, it can be seen that for the method with SPO, the number of charging events is generally lower than the number of charging events for the method without SPO. This, however, does not hold for a maximum speed of 100 (km/h).

In Figure 6-6, a bar chart is presented, which shows the charging time decrease versus the driving time increase for the different maximum allowable driving speeds at an ambient temperature of $0\,°\mathrm{C}$. This figure clarifies the advantage of adapting to a lower driving speed. If the decrease in charging time is more significant than the increase in driving time, speed adaption is profitable in terms of journey time decrease.

In Figure 6-7a, the result for the journey time of 100 simulations for the method with SPO and

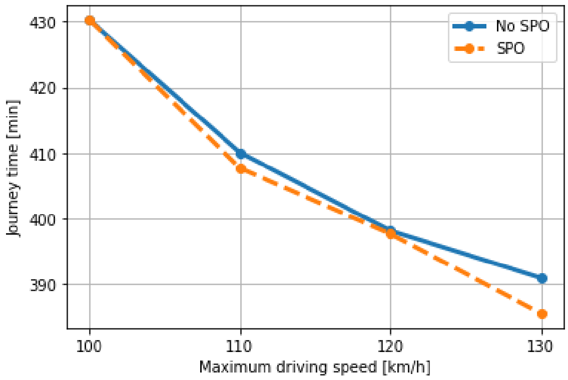

(a) Mean journey times.

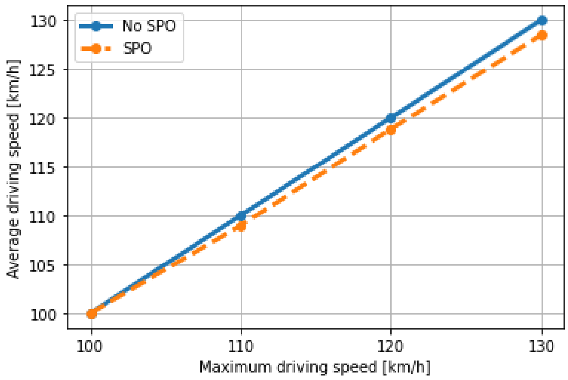

(b) Average driving speeds.

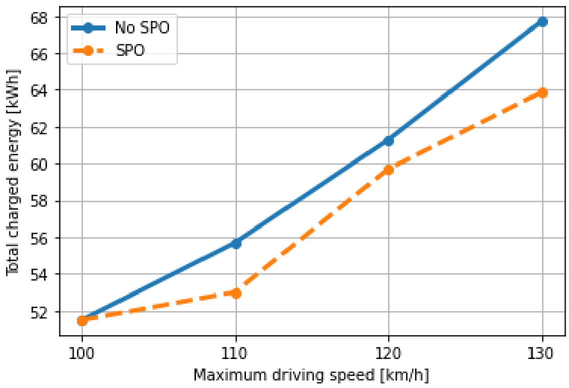

(c) Total charged energy.

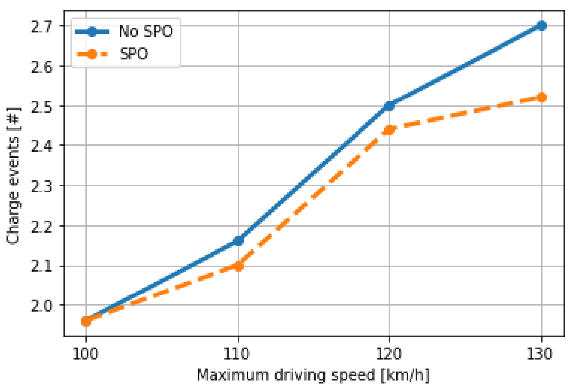

(d) Number of charging events.

Figure 6-5: Mean journey time, average driving speeds, total charged energy and the number of charging events for different maximum speeds at an ambient temperature of $0\,^{\circ}\mathrm{C}$.

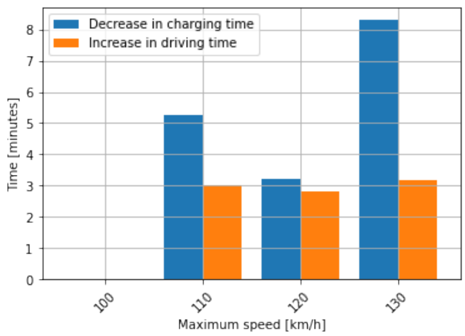

Figure 6-6: Average charging time decrease versus the average driving time increase with an ambient temperature of $0\,^{\circ}\mathrm{C}$.

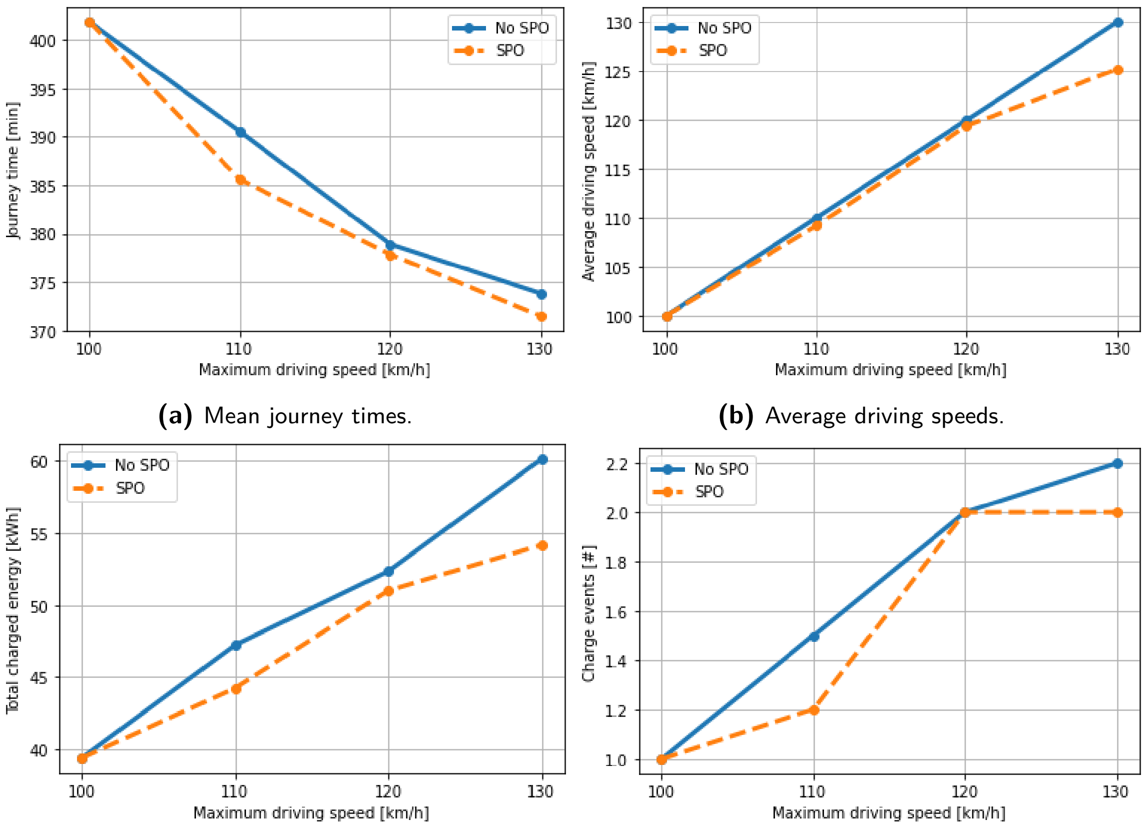

(a) Mean journey times.

(b) Average driving speeds.

(c) Total charged energy.

(d) Number of charging events.

Figure 6-7: Mean journey time, average driving speeds, total charged energy and the number of charging events for different maximum speeds at an ambient temperature of $20\,°\mathrm{C}$.

the method without SPO at an ambient temperature of $20\,°\mathrm{C}$ is shown. In this figure, it can be seen that the journey time decreases, for both the method with SPO and for the method without SPO, if the maximum allowable driving speed increases. However, the method with SPO can find an optimal policy that yields a lower journey time for all of the maximum allowable driving speeds. At an ambient temperature of $20\,°\mathrm{C}$, the energy consumption for the cabin climate control is the lowest. Therefore, lowering the driving speed can possibly have the highest impact on the journey time with this ambient temperature compared to higher or lower ambient temperatures.

In Figure 6-7b, the average driving speed for each of the maximum speeds with an ambient temperature of $20\,°\mathrm{C}$ for the method with SPO and the method without SPO is shown. In this figure, it can be seen that the most considerable driving speed adaption takes place for a maximum allowable driving speed of $130\,(\mathrm{km/h})$. Where the average driving speed for $110\,(\mathrm{km/h})$ and $120\,(\mathrm{km/h})$ is only slightly lower than the maximum allowable driving speed, this still results in a decrease in journey time. For a maximum allowable driving speed of $100\,(\mathrm{km/h})$, the method with SPO does not decide to adapt to a lower driving speed. An adaption of a lower driving speed will not result in a higher decrease in charging time than the increase in driving time for a maximum allowable driving speed of $100\,(\mathrm{km/h})$.

In Figure 6-7c, the mean of the total charged energy during a journey for 100 simulations at

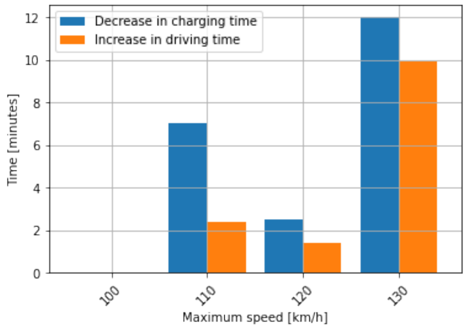

Figure 6-8: Average charging time decrease versus the average driving time increase with an ambient temperature of 20 °C.

an ambient temperature of 20 °C is shown. In this figure, it can be seen that the total charged energy increases with the increase in the maximum allowable driving speed, which was to be expected. However, the method with SPO can reduce the driving speed to achieve less total energy to be charged for all maximum driving speeds, resulting in a lower journey time for the method with SPO for all allowable maximum driving speeds.

In Figure 6-7d, the number of charging events for different maximum allowable driving speeds at an ambient temperature of 20 °C for the method without SPO and the method with SPO is shown. In this figure, we can see that, in general, the number of charging events increases if the maximum allowable driving speed increases as well. However, for the method with SPO at a maximum allowable driving speed of 130 (km/h), the number of charging events becomes larger than two, which means that in some cases with 130 (km/h) as maximum allowable driving speed, at least three charging events are required. With a maximum allowable driving speed of 130 (km/h), the method with SPO can lower the number of charging events to a maximum of two events. This is the result of SPO.

In Figure 6-8, a bar chart is presented, which shows the charging time decrease versus the driving time increase for the different maximum allowable driving speeds at an ambient temperature of 20 °C. This figure clarifies the advantage of adapting to a lower driving speed. If the decrease in charging time is more significant than the increase in driving time, speed adaption is profitable in terms of total journey time decrease. The most significant difference is achieved for a maximum allowable driving speed of 110 (km/h).

6-2-3 Conclusions of Case Study B

In this section, the advantage of optimising the driving speed has been investigated. Adapting to a lower driving speed can have multiple advantages. For example, driving slower generally means less energy consumption is required for the propulsive power demand. Therefore, driving slower has the advantage of less energy being consumed due to the propulsive power demand and possibly less charging time is required to reach the destination. However, by decreasing the driving speed, there is also an increase in the driving time. During the driving time, cabin climate control is applied to assure a pleasant cabin climate for the passengers of an EV. This means that with an increased driving time, also the energy consumption for the cabin climate control increases. The rate of cabin climate control depends on the ambient temperature. Therefore, the SPO has been tested for various ambient temperatures, varying from $-20\,°C$ up to $20\,°C$.

The results have shown that it can be advantageous to optimise the driving speed. While adopting a lower driving speed can possibly lower the overall journey time. This, however, depends on the ambient temperature. The decrease in charging time has to compensate for the increase in driving time. However, the decrease in charging time depends on the energy that is saved by adopting a lower driving speed. The charging time is not decreasing for very low ambient temperatures since large proportions of energy are spent on the cabin climate control. Therefore, for an ambient temperature of $-20\,°C$, it has no positive effect to adapt a lower driving speed than the maximum allowable driving speed. For ambient temperatures of $0\,°C$ and $20\,°C$, it does have a positive effect to adapt a lower driving speed in some parts of the journey. This is, however, also dependent on the maximum allowable driving speed. While for a maximum allowable driving speed of 100 (km/h), it has no positive effect to adapt a lower driving speed. This relates to the fact that for speeds between 50 (km/h) and 100 (km/h) the difference in energy consumption due to the propulsive power demand is limited. Therefore, only for maximum allowable driving speeds of 110 (km/h) and higher it is profitable, in terms of journey time, to adapt to a lower driving speed.

A side effect of optimising the driving speed is that less energy is charged in total. This can influence the total charging cost. Therefore, optimising the driving speed affects the journey time and possibly decreases the charging cost. Even though decreasing the charging cost is not included in the preference of the Fastest route.

6-3 Case study C - Charging Platform Selection

In the simulation setup in Section 5-1, it is assumed that at each node, there is only one CS present and that this CS delivers only one charging power, namely 50 kW. In reality, however, some chargers can give a much higher charging power, such as 350 kW provided by the Ionity charging network. Also, there is a possibility that multiple chargers are present at a particular location with different charging powers and different charging prices.

The charging power influences the length of the charging process. Therefore, it is desirable to optimise the choice of the type of charger to use. Also, the maximum effective charging power depends on the SoC, which means that higher charging power is not always faster. For example, Figure 2-3 depicts the charging profile of a Nissan Altra. In this figure, it can be seen that for higher SoCs, the maximum effective charging power decreases. For example, at a SoC of 80 %, a maximum charging power of approximately 26 kW can be reached. However, at a SoC of 20 %, approximately a maximum charging power of 48 kW can be reached. Therefore, for higher SoC, it is not advantageous to use a supercharger, which can charge with a charging power of 300 kW, instead of a fast charger, which can charge with a charging power of 50 kW.

In this section, it will be investigated how the presence of multiple choices for a charger can influence the travel cost. The question is whether it is always beneficial to use the charger that gives the highest charging power to reach the destination with the minimum journey time. Alternatively, is it, for example, cheaper to use a combination of lower charging power and a higher charging power during a trip while achieving the same charging time. First, it

Table 6-9: Different types of chargers with their accompanied charging power present in each node.

Charger Type	Charging Power [kW]	Electricity Price Multiplier [-]
Super Charger	150	2.0
Fast Charger	50	1.0

will be explained how the simulation setup to test this is constructed. Then the results will be presented.

6-3-1 Simulation Setup of Case Study C

For the simulation setup, almost the same simulation setup as in Section 5-1 will be used. However, a few minor changes will be important for this case study. These will be elaborated on in this section.

Instead of assuming that there is only one kind of charger present in each node, there will be multiple choices of chargers at each node. This can be interpreted in multiple ways. First, one can see this as a single CS, in a node, with multiple kinds of chargers. The second way to see this is that a node represents multiple CSs, where each CS has its specific charger with different charging power and price. This, however, only is a matter of perception. For this simulation setup, it is assumed that multiple chargers are present in each node. The type of chargers that are present in a node is given in Table 6-9, wherein the second column, the charging power for the specific charger type can be seen.

Moreover, in Section 5-1, it is assumed that for different time intervals namely t_{peak}, $t_{\text{intermediate}}$ and t_{base} different electricity prices are present. These are given by:

$$c_{\text{p}}(t_{\text{k}}) = \begin{cases} 0.42\,(\text{EUR/kW}), & \text{if } t_{\text{k}} \in t_{\text{peak}}, \\ 0.40\,(\text{EUR/kW}), & \text{if } t_{\text{k}} \in t_{\text{intermediate}}, \\ 0.35\,(\text{EUR/kW}), & \text{if } t_{\text{k}} \in t_{\text{base}}, \end{cases} \tag{6-6}$$

However, the electricity prices in Eq. (6-6) are on the basis that only one charger is present with 50 kW charging power. In this simulation setup, it is assumed that for the usage of a different charger, a different price is present. Therefore, the price given in Eq. (6-6) is multiplied with a particular factor for each specific charger. In Table 6-9, the specific electricity price multiplier for each charger can be seen in the third column.

Since the ambient temperature influences the energy consumption during driving, this can influence the number of charging events and the amount of energy charged. The ambient temperature thus also influences the charger selection. Therefore, the experiment will be conducted for different ambient temperatures, given by:

$$\text{T}_{\text{ambient}} = [-20, 0, 20] \quad ^{\circ}C. \tag{6-7}$$

In order to gain more insight, the Economical, Mixed and Fastest route preference will be used in the simulations. Next to α, other parameters are of interest for the simulations, such as the initial battery temperature and the ambient temperature, which are given in Table 6-10.

Table 6-10: Parameters for each CS selection simulation.

Parameter	i [-]	e_0 [kWh]	t_0 [hr]	T_0 [°C]	δ_e [%]	t_p [min]
Value	Node 1	65	$\Omega \rightarrow [0, 20]$	20	10.0	5

Table 6-11: Results of the waiting time, charging time, driving time and journey time in minutes and charging cost in euros, for different algorithms for 100 simulations of network 1 with CS selection with an ambient temperature of 20 °C.

Algorithm	**Waiting time [min]**	**Charging time [min]**	**Driving time [min]**	**Journey time [min]**	**Charging cost [EUR]**
Economical	2.81	80.53	412.59	495.93	13.98
Mixed	2.89	55.64	393.02	451.55	23.67
Fastest	2.90	45.41	394.34	442.65	29.30

6-3-2 Results of Case Study C

In Table 6-11, the mean waiting time, charging time, driving time, journey time and the charging cost for 100 simulations of network 1 are given for the Economical, Mixed and Fastest route preferences with an ambient temperature of 20 °C. This table shows that the journey time of the Economical route preference, as expected, is the highest. This is because this preference optimises the charging cost. Therefore, the charging cost is the lowest for the Economical route preference. On the other hand, the Fastest preference has the highest charging cost. This is the result of the preference of the algorithm, while it will optimise the time cost and the incurred charging costs are not of importance. It is, therefore, not surprising that the Fastest route preference finds the lowest journey time of all the algorithm preferences. Not surprisingly, the Mixed route preference has a journey time between the Economical and Fastest route preferences. The same holds for the charging cost.

In Figure 6-9, for each of the algorithms, the percentage of the type of charger that is used in the optimal policy is shown for an ambient temperature of 20 °C. The figure shows that the Economical route preference only uses the fast charger and never uses the supercharger. This was expected because the supercharger is twice as expensive as the fast charger. Therefore, the Economical route preference will always choose the cheapest charger, no matter how much extra time is incurred by making this choice. The Mixed route preference uses both the fast charger and the supercharger, but mostly the supercharger. Interesting to see is that the Fastest route preference does not solely use the supercharger. In fact, in some cases, the Fastest route preference uses both the fast charger and supercharger in an optimal policy. For example, this may happen when a charge event has to be undertaken at high SoC. In this case, the fast charger can give the same charging power as the supercharger and therefore, the Fastest route preference can use the fast charger without gaining more charging time than with the supercharger.

In Table 6-12, the mean waiting time, charging time, driving time, journey time and the charging cost for 100 simulations of network 1 are given for the Economical, Mixed and Fastest route preferences with an ambient temperature of 0 °C. In this table, the influence of the ambient temperature can be seen. Compared with Table 6-11, it can be seen that the charging time is much higher compared to the charging time for an ambient temperature of

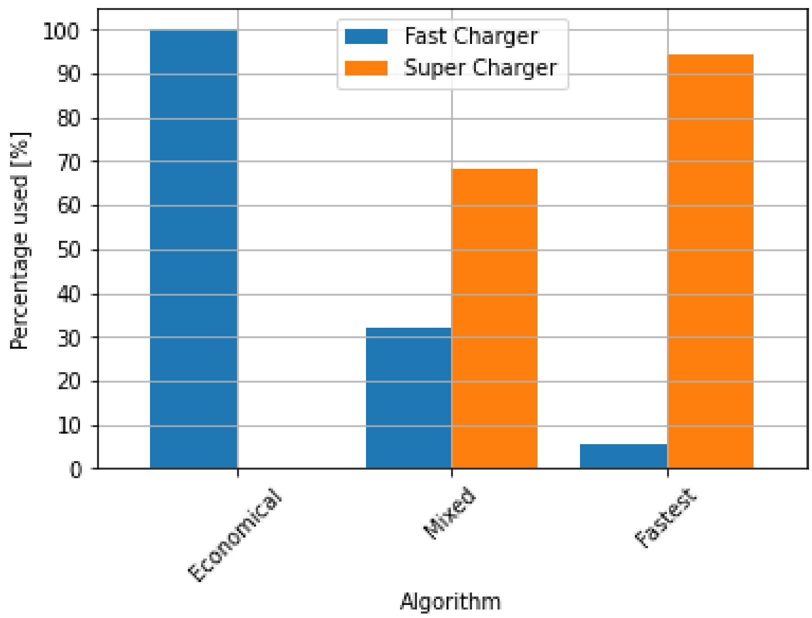

Figure 6-9: Percentage of type of charger that is used by the preference setting of the algorithm for 100 simulations of network 1 with an ambient temperature of 20 °C.

Table 6-12: Results of the waiting time, charging time, driving time and journey time in minutes and charging cost in euros, for different algorithms for 100 simulations of network 1 with CS selection with an ambient temperature of 0 °C.

Algorithm	**Waiting time [min]**	**Charging time [min]**	**Driving time [min]**	**Journey time [min]**	**Charging cost [EUR]**
Economical	3.91	106.97	415.01	525.88	18.96
Mixed	3.91	79.73	390.18	473.83	29.43
Fastest	3.95	59.48	396.03	459.46	39.06

20 °C. The reason behind it is that the ambient temperature influences the energy consumed due to the cabin climate control. The energy consumed due to this cabin climate control is higher for 0 °C ambient temperature than for 20 °C ambient temperature. Therefore, more energy has to be charged to reach the destination. This results in the charging time to increases severely with an ambient temperature of 0 °C compared to an ambient temperature of 20 °C.

In general, the same results as for the ambient temperature of 20 °C ambient temperature hold. The Fastest route preference can find the lowest journey time, with the highest charging cost. The Mixed route preference has a journey time between the Fastest and Economical route preference, the same holds for the charging cost. However, the Economical route preference has the lowest charging cost and the highest journey time.

In Figure 6-10, for each of the algorithm preferences, the percentage of the type of charger that is used in the optimal policy for an ambient temperature of 0 °C is shown. If this outcome is compared to the results shown in Figure 6-9, the influence of the ambient temperature concerning the charger selection can be seen. The Economical route preference, as expected, only

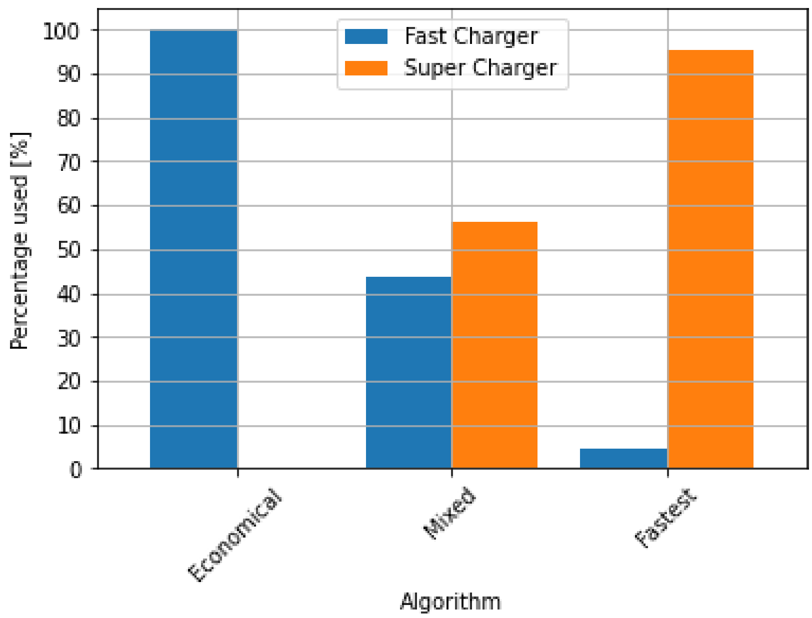

Figure 6-10: Percentage of type of charger that is used by the preference setting of the algorithm for 100 simulations of network 1 with an ambient temperature of 0 °C.

uses the fast charger since this yields the lowest charging cost. The Mixed route preference uses a mixed charger selection between the fast charger and the supercharger. There is still a preference for the supercharger. However, the fast charger now has a higher percentage of usage compared to an ambient temperature of 20 °C. This can be explained because more charging is required with an ambient temperature of 0 °C. However, the driving time is not increasing. This means that the charging time and cost are increasing, but the driving time is not. The objective of the Mixed route preference is to minimise the combination of the charging cost and the time cost. The charging cost will rise in a high proportion if the same percentage of super chargers is used as in Figure 6-9. Therefore, the Mixed route preference with an ambient temperature of 0 °C decides to use the fast charger more often.

The results in Figure 6-10 also show that for the Fastest route preference, the share of fast charger usage at an ambient temperature of 0 °C stays relatively the same compared to the results for an ambient temperature of 20 °C. It is, therefore, not always optimal to only use superchargers. This can, of course, be dependent on the SoC, while at higher SoCs, a higher charging power does not mean that this charging power can be used efficiently. Therefore, charging at high SoCs with superchargers does not speed up the charging process but does increase the charging cost.

In Table 6-13, the mean waiting time, charging time, driving time, journey time and the charging cost for 100 simulations of network 1 are given for the Economical, Mixed and Fastest route preferences with an ambient temperature of −20 °C. In this table, it can be seen that an ambient temperature of −20 °C has an even more significant impact on the travel cost. The charging time is higher because more energy is consumed for the cabin climate control, influencing the charging cost. More charging events are required, resulting in more waiting time. The general results are in line with the results for an ambient temperature of 20 °C

Table 6-13: Results of the waiting time, charging time, driving time and journey time in minutes and charging cost in euros, for different algorithms for 100 simulations of network 1 with CS selection with an ambient temperature of $-20\,°\mathrm{C}$.

Algorithm	**Waiting time [min]**	**Charging time [min]**	**Driving time [min]**	**Journey time [min]**	**Charging cost [EUR]**
Economical	4.16	133.93	410.21	548.31	23.89
Mixed	4.24	97.26	387.77	489.27	37.61
Fastest	4.46	74.84	390.91	470.21	49.89

and 0 °C.

If we look at the percentages of the type of charger that is used in the optimal policy for different preferences and an ambient temperature of $-20\,°\mathrm{C}$, it can be seen that a similar trend is present as for the ambient temperature of $0\,°\mathrm{C}$. For the Economical route preference, the fast charger is solely used to minimise the charging cost. The Mixed route preference shows a mixed preference between the fast charger and the supercharger. However, with an overall preference for the supercharger. If the percentage of the Mixed route preference is compared to an ambient temperature of $20\,°\mathrm{C}$, it can be seen that the share of fast charger usage is higher. This, again, has to do with the fact that the charging time and charging cost increase while the driving time remains the same. Therefore, the fast charger has to be chosen to balance the time cost and the charging cost more often.

For the Fastest route preference, it can be seen that the share of fast charger usage compared to the results shown in Figure 6-9 for an ambient temperature of $20\,°\mathrm{C}$ has become lower. Using the fast charger more frequently to achieve the lowest journey time with a lower ambient temperature becomes more interesting. This is most likely the result of the fact that more energy consumption takes place due to cabin climate control. This leads to more energy to be charged and possibly more charging events. These charging events most likely occur for high SoCs, and therefore, the fast charger can be used instead of the supercharger.

6-3-3 Conclusions of Case Study C

In this section, the influence of different chargers that can be present in a CS is investigated. In general, chargers with higher charging power are more expensive to use. However, the charging time can be reduced significantly due to the higher charging power. This has its restrictions, though, while for higher SoCs, a higher charging power does not necessarily lead to lower charging times. Therefore, this section investigated the different algorithm preferences, namely: Economical, Mixed and Fastest, which chargers the preference would use in their optimal policy. To test this, it was assumed that two chargers were present in each node; a fast charger and a supercharger. The fast charger can deliver a charging power of $50\,\mathrm{kW}$, while the supercharger can deliver a charging power of $150\,\mathrm{kW}$. However, the supercharger is twice as expensive as the fast charger. Since the ambient temperature has a significant influence on the energy consumption, and therefore also the charging events, the simulations were executed for different ambient temperatures, ranging from $-20\,°\mathrm{C}$ up to $20\,°\mathrm{C}$.

The results were partly predictable. For example, the Economical route preference only uses

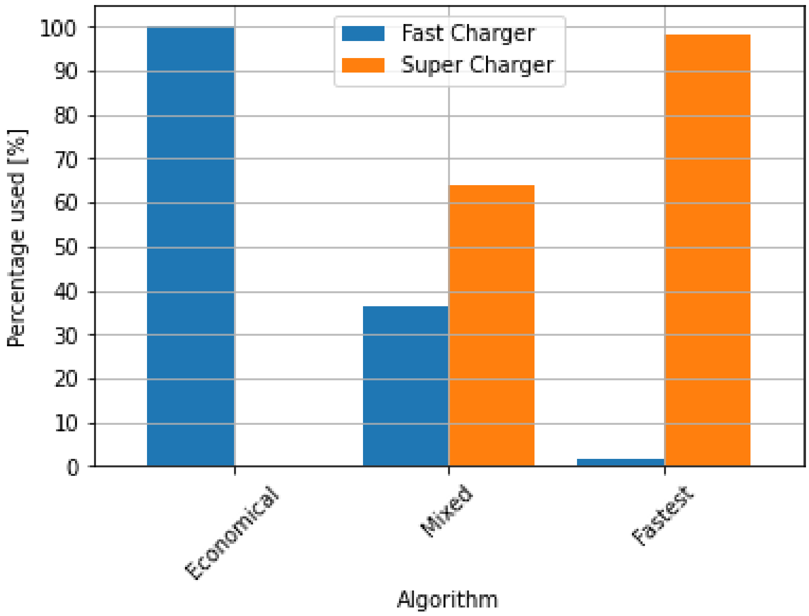

Figure 6-11: Percentage of type of charger that is used by the preference setting of the algorithm for 100 simulations of network 1 with an ambient temperature of $-20\,°\mathrm{C}$.

the fast charger, resulting in the lowest charging cost. That the charging time of the Economical route preference is much higher than the Mixed, and the Fastest route preference is not essential for the Economical route preference. Not surprisingly, the Mixed route preference uses a mixed charger preference, having a clear preference for the supercharger. However, the relative usage of the fast charger and the supercharger depends on the ambient temperature. While for lower ambient temperatures than $20\,°\mathrm{C}$, the share of fast charger usage increases compared to an ambient temperature of $20\,°\mathrm{C}$. Due to the lower ambient temperatures, the energy consumption for the cabin climate control increases. Therefore, the charging time and cost increase while the driving time remains the same. This results in more fast charger usage because the objective of the Mixed route preference is to balance the time cost and the charging cost.

Interesting are the results for the Fastest route preference. From the results, it can be seen that the Fastest route preference sometimes prefers the fast charger, while most likely, the charge events take place for high SoCs where the fast charger and the supercharger will result in the same charging time. However, using a supercharger gives much higher charging costs.

6-4 Case study D - Uncertainty

Due to the uncertainties in the driving speed and the waiting times, we calculate the expected value of the cost function. Furthermore, it was also assumed that the charging power at a CS could consistently deliver the stated charging power, which was, for example, 50 kW. However, this is an assumption, while in reality, there can be local grid capacity limitations causing the charging power delivered by the CS to be lowered than expected.

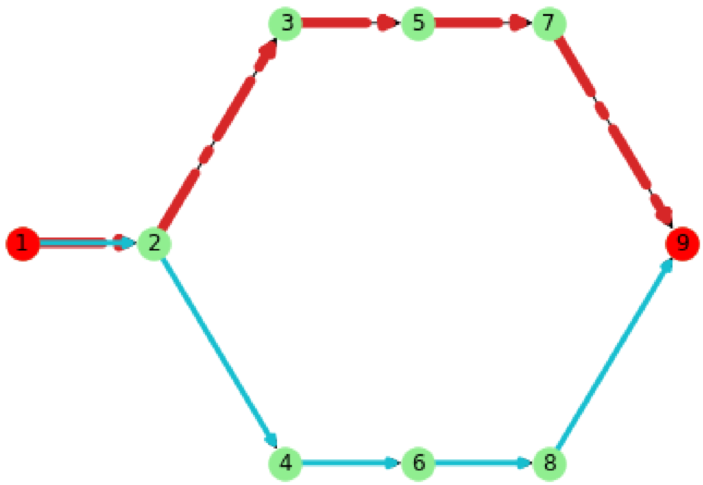

Figure 6-12: Network with motorway (cyan) and provincial-road (red).

In this case study, it will be investigated to which extent a certain faster path with higher uncertainty is favoured above a slower path with lower uncertainty. This can be seen as comparing a motorway with a provincial road where the average speed is higher than on the provincial road. However, the motorway is typically more sensitive to disruptions. In the following, the simulation setup will be discussed, followed by the results and conclusions drawn from the results.

6-4-1 Simulation Setup of Case Study D

The simulation setup will differ from the simulation setup described in Section 5-1. The biggest differences are present in the network, the probability distribution of the driving speed and the way the charging time is calculated. In the following, these changes will be discussed.

For this case study, a new network will be used. This network represents two possibilities: taking the motorway or using provincial roads to reach the destination from the origin. The network is given in Figure 6-12, here the cyan line represents the motorway, and the red line represents the provincial roads. The link distances in the network will all be equal to 120 km. In this way, the distance using the motorway from origin to destination is equal to the distance using the provincial roads from origin to destination. Moreover, it is assumed that the EV can only charge at nodes 3, 5, 7 for the provincial roads and nodes 4, 6, 8 for the motorway.

There are two essential differences between the motorway and the provincial roads. These are the average driving speed and the charging power that the CSs can deliver. For the driving speed, it is assumed that the motorway has an average driving speed of 90 (km/h); however, there is a high standard deviation attached to this average driving speed. This standard deviation will be increased during the simulations. The standard deviations for the motorway that will be used are given by:

$$\sigma^2_{\text{v,MW}} = [10, 15, 20] \text{ (km/h)}. \tag{6-8}$$

Therefore, there are three probability distributions that will be simulated one by one for the average driving speed on the motorway, which can be described by:

$$N_{\text{v,MW}}(\mu, \sigma^2) = N\Big(\mu = 90, \sigma^2 = \sigma^2_{\text{v,MW}}\Big), \tag{6-9}$$

for $\sigma^2_{\text{v,MW}} \in$ Eq. (6-8).

Having a higher standard deviation means higher uncertainties attached to the expected driving speed on the motorway. This could, for example, mean that there is a chance of having a really low average driving speed, resulting in a very high driving time. For the average driving speed on the provincial roads, it is assumed that the mean average driving speed is equal to 80 (km/h), with a very low standard deviation attached to it, which means that the uncertainties on the provincial roads are lower. However, in general, the driving time using provincial roads will be higher than the motorways due to the difference in the mean speed. The probability distribution for the provincial-roads can be described as follows:

$$N_{\text{v,PR}}(\mu, \sigma^2) = N(\mu = 80,\ \sigma^2 = 1). \tag{6-10}$$

The second difference between the motorway and the provincial roads is the power that can be delivered at a CS and the waiting time that can be present. This case study assumes that CSs at motorways will have a higher maximum charging power available. However, the chance of local grid limitations and higher waiting times at CSs on motorways is higher compared to the provincial roads. Therefore, the high standard deviation of the available charging power will manifest both the limitations on the grid level and the possible waiting times. Lower available charging power results in a higher charging time. This symbolises local grid limitations or high waiting times, increasing the charging time. To model this in the simulations, it is assumed that a mean charging power of 100 kW is available on the motorways. The standard deviation of the probability distribution of the available charging power will be altered during the simulations. The standard deviations of the available charging power are given by:

$$\sigma^2_{p_{\text{cs}},\text{MW}} = [25, 30, 35, 40, 45, 50] \text{ kW}. \tag{6-11}$$

The probability distributions that will be simulated one by one, describing the available power at the CS on motorways, can be described as follows:

$$N_{p_{cs},MW}(\mu, \sigma^2) = N\Big(\mu = 100,\ \sigma^2 = \sigma^2_{p_{\text{cs}},\text{MW}}\Big), \tag{6-12}$$

for $\sigma^2_{p_{\text{cs}},\text{MW}} \in$ Eq. (6-11).

The high standard deviations present in the available charging power at CSs on the motorways mean a big distribution on the possible charging times that can occur. It is assumed that negative charging powers cannot occur. Therefore, negative parts of the probability distributions are assumed to be equal to zero. The available charging power is lower than on the

Table 6-14: Parameters for each uncertainty simulation.

Parameter	i [-]	e_0 [kWh]	t_0 [hr]	T_0 [°C]	δ_e [%]	t_p [min]
Value	Node 1	65	$\Omega \to [0, 20]$	20	5.0	5

motorways for the provincial roads. However, the standard deviation in this available charging power is assumed to be much lower. This means that the chance of local grid limitations or waiting times at CSs on provincial roads is minimal. Therefore, it is assumed that the probability distribution describing the available charging power at CSs on provincial-roads is given by:

$$N_{p_\mathrm{cs},\mathrm{PR}}(\mu, \sigma^2) = N(\mu = 50,\ \sigma^2 = 1). \tag{6-13}$$

The charging time is not a deterministic value anymore. The expected charging time depends on the probability distribution for the charging power, for either the provincial-road or the motorway. Therefore, the charging time is given by:

$$\tau_\mathrm{i} = \frac{\Delta e_\mathrm{k}}{E\{P_\mathrm{cs}\}}, \tag{6-14}$$

where $E\{P_\mathrm{cs}\}$ is the expected charging power of a realisation from the present charging power probability distribution given in Eq. (6-12) and Eq. (6-13). In other words, to summarise the case study, the provincial road represents a slower route with lower uncertainty. The motorway represents a fast route but with higher uncertainty. In this case study, we will investigate with how much uncertainty the route with low uncertainty will be preferred over the route with high uncertainty. Other important parameters, such as the initial battery temperature, are given in Table 6-14.

In the simulations, the Fastest route preference of α will be used. Since we have seen that the ambient temperature has a big influence on the energy consumption of the EV and with this on the optimal policy that is created. The simulations will be held for various ambient temperatures, which are given by:

$$\mathrm{T}_\mathrm{ambient} = [-20, 0, 20] \quad {}^\circ C. \tag{6-15}$$

For each ambient temperature, 100 simulations are run. In the remainder of this section, the results of the simulations will be discussed. After which, conclusions from the results will be presented.

6-4-2 Results of Case Study D

In Figure 6-13, the mean of the expected costs, with respect to the standard deviation of the charging power, of the provincial-road and the motorway, with different standard deviations of the driving speed at an ambient temperature of 20 °C are shown. As can be seen in the figure, the expected cost of the provincial road remains the same while the standard deviation of the charging power of the motorway increases. This was expected since the standard deviation of

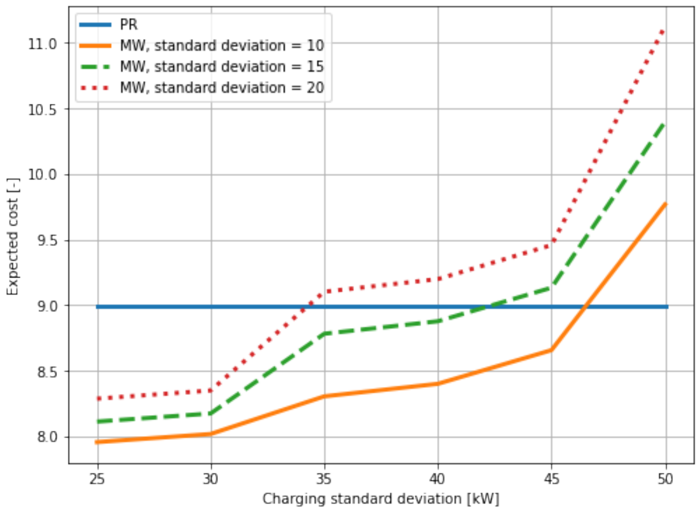

Figure 6-13: Results of the expected costs of the provincial-roads and the motorway, with different standard deviations of the driving speed for an ambient temperature of $20\,°\mathrm{C}$.

the charging power on the motorway has no effect on the charging power at the CSs on the provincial road. The expected costs of the motorway are increasing with the increase of the standard deviation of the charging power; this is the result of much higher charging times due to local grid limitations or lower charging powers. If the standard deviation of the driving speed also increases, the motorway's expected costs are increased. This can result from much higher driving times or the possibility of running out of energy due to higher driving speeds than expected.

At the moment, the expected costs of the motorway cross the line of the expected costs of the provincial road, then it becomes favourable to choose the provincial road instead of the motorway. In Figure 6-13, it can be seen that this point differs for the present standard deviation of the driving speed. In Table 6-15, the different cross over points for the different driving speed standard deviations is shown. It can be seen that the cross over point decreases if the driving speed standard deviation increases.

In Figure 6-14, the mean of the expected costs, with respect to the standard deviation of the charging power, of the provincial-road and the motorway, with different standard deviations of the driving speed at an ambient temperature of $0\,°\mathrm{C}$ are shown. Compared with the case for an ambient temperature of $20\,°\mathrm{C}$, it can be seen that for an ambient temperature of $0\,°\mathrm{C}$, the expected costs for the provincial-road is higher. This can be explained due to the energy consumption associated with cabin climate control. As explained in Section 5-2-4, this energy consumption is higher for certain ambient temperatures. Resulting in higher expected costs. The mean driving speed on the provincial road is lower than on the motorway, therefore compared to the motorway, the driving time on the provincial road is higher. This results in higher energy consumption, due to the cabin climate control, on the provincial road compared to the motorway. This causes the fact that compared to an ambient temperature of $20\,°\mathrm{C}$, the expected costs for the provincial-road have risen substantially. This fact causes the cross over points to shift as well, which means it becomes only favourable for higher charging standard deviations to use to provincial-road instead of the motorway.

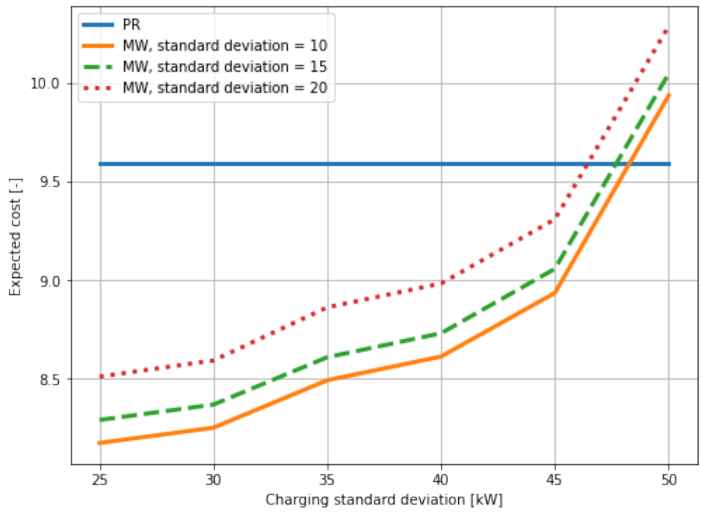

Figure 6-14: Results of the expected costs of the provincial-roads (PR) and the motorway (MW), with different standard deviations of the driving speed for an ambient temperature of $0\,^{\circ}\mathrm{C}$.

In Table 6-15, the cross over points for an ambient temperature of $0\,^{\circ}\mathrm{C}$ are shown. Comparing Table 6-15 and Table 6-15, it is clear that the ambient temperature has a big influence. Since the cross over points are a lot closer to each other right now. This results from the expected cost of the provincial road that has increased. While at the same time, for high charging standard deviation, the expected costs for the different standard deviations in the driving speed are closer to each other. Therefore the cross over points are closer to each other as well as higher compared to the cross over point in Table 6-15. Meaning that much uncertainty on the motorway is required before the provincial road is preferred over the motorway.

In Figure 6-15, the mean of the expected costs, with respect to the standard deviation of the charging power, of the provincial-road and the motorway, with different standard deviations of the driving speed at an ambient temperature of $-20\,^{\circ}\mathrm{C}$ are shown. Again, in this figure, it can be seen that the expected costs for the provincial-road have become higher compared to the results presented in Figure 6-13 and Figure 6-14. This results from even more energy consumption for the cabin climate control due to the lower ambient temperature. The effect on the higher energy consumption due to the cabin climate control can also be seen in the expected costs for the motorway for all of the three driving speed standard deviations. However, because the speed is higher on the motorway, the higher energy consumption has less effect on the expected costs.

In Table 6-15, the cross over points for an ambient temperature of $-20\,^{\circ}\mathrm{C}$ are shown. If these cross over points are compared to the cross over points for an ambient temperature of $0\,^{\circ}\mathrm{C}$, shown in Table 6-15, it can be seen that the cross over points have moved up a bit more. However, the difference is minimal. The biggest difference is present if the cross over points are compared to an ambient temperature of $20\,^{\circ}\mathrm{C}$.

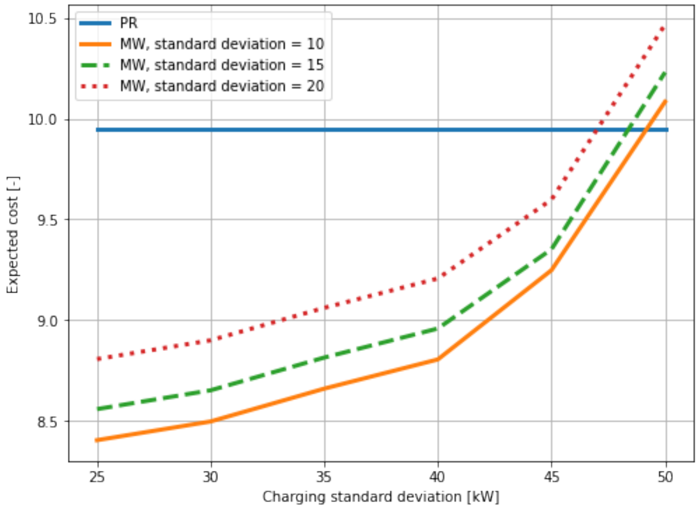

Figure 6-15: Results of the expected costs of the provincial-roads (PR) and the motorway (MW), with different standard deviations of the driving speed for an ambient temperature of $-20\,^{\circ}\mathrm{C}$.

Table 6-15: Cross over point, in terms of the charging standard deviation, when the provincial-road is preferred over the motorway at an ambient temperature of $20\,^{\circ}\mathrm{C}$, $0\,^{\circ}\mathrm{C}$ and $-20\,^{\circ}\mathrm{C}$.

Driving speed standard deviation	**Cross over point [kW]**		
	$20\,^{\circ}\mathrm{C}$	$0\,^{\circ}\mathrm{C}$	$-20\,^{\circ}\mathrm{C}$
$\sigma^2_{v,MW} = 10$	46.0	48.0	49.0
$\sigma^2_{v,MW} = 15$	42.5	47.5	48.5
$\sigma^2_{v,MW} = 20$	34.0	46.0	47.0

6-4-3 Conclusions of Case Study D

The nature of our problem includes uncertainties. However, in previous case studies, the uncertainty was not altered, and there is no insight, this far, how this uncertainty influences the optimal policy. The question is how high the uncertainty can become before a fast route with high uncertainty is not favoured over a slower route with lower uncertainty. The uncertainty can cause the EV to have a much higher driving time than expected or arrive at a CS while the available charging power is much lower than expected.

Therefore, in this case study, the amount of uncertainty required to favour a more reliable but slower route over a faster route with more uncertainty is investigated. This amount of uncertainty is obtained for various ambient temperatures, while we have seen in previous case studies that the ambient temperature significantly influences energy consumption. Therefore, different ambient temperatures can have different optimal policies as a result.

The results show that a substantial amount of uncertainty in the fast route is required before the slower route with low uncertainties is favoured as the optimal solution. The probabilities of having a higher driving time or very high charging times become relevant only at these higher standard deviations.

The ambient temperature significantly influences the amount of charging standard deviation that has to take place to favour the slower route with low uncertainties above the faster route with high uncertainties. This is a result of the fact that on the slower route, the driving time, and therefore the amount of time that cabin climate control takes place, is higher than on the faster route. This impacts the expected costs of the route on the provincial-road, because it causes these expected costs to become higher. The effect of the ambient temperature is also visible on the route on the motorway. However, this impact is not as significant as on the provincial-road route. The ambient temperature has relatively more impact on the provincial road than on the motorway. It is increasing the expected cost for the provincial road more than the expected cost for the motorway. This causes the cross-over points, where choosing the provincial road above the motorway becomes favourable, to shift to higher values for low ambient temperatures.

6-5 Conclusions

In this chapter, the proposed method has been used to investigate possibilities to reduce the travel costs of EVs by conducting four case studies.

In the first case study, the proposed method was compared with the conventional way to optimise the travel costs of EVs. From the results, it became clear that the proposed method, with the Fastest route preference, performs better in finding a route with a lower journey time. This does not necessarily mean that the proposed method has lower waiting times, charging times, and charging costs. In general, it was seen that the proposed method suggests optimal policies with higher waiting times and comparable charging times. The improvement in journey time was achieved by a much lower driving time. This driving time depends on the departure time at a CS, which the proposed method can optimise. The Economical route preference can find a route that has a much lower charging cost than the conventional EV navigation systems. This is, however, at the expense of a much higher journey time.

In the second case study, the possibility of optimising the driving speed was explored. Lowering the driving speed has several advantages, as well as disadvantages. The advantage of lowering the driving speed is that the energy consumption for the propulsive power will also decrease. However, this does not hold anymore for certain speeds, or the difference is relatively small. Also, by lowering the driving speed, the battery heats itself less due to less energy losses. This can cause the fact that less energy has to be spent on heating the battery. Lower energy consumption means that, in potential, less energy has to be charged at a CS, which means lower charging times, which can benefit the travel cost. However, by lowering the driving speed, the driving time increases. With the increase of the driving time, the energy spent on the cabin climate control increases, nullifying the energy savings due to lower driving speed. From the results, it is shown that for an ambient temperature of $0\,^{\circ}\mathrm{C}$ and $20\,^{\circ}\mathrm{C}$, the journey time can be decreased if the driving speed is lowered below the maximum allowable driving speed. This only holds if the maximum allowable driving speed is 110 (km/h) or higher, with a maximum of 130 (km/h).

In the third case study, the possibility of selecting a charger with different quantities at a CS was investigated. The different chargers offer different charging powers. However, for higher charging powers, more charging costs are present. In the case study, a fast charger with 50 kW charging power and a supercharger with 150 kW charging power was used. The supercharger was set to be twice as expensive as the fast charger. The results showed that using the supercharger is not always faster, even for the Fastest route preference. This has to do with the fact that the SoC can limit the maximum effective charging power. Therefore, it also depends on the SoC which charger type is optimal.

The fourth case study investigated the amount of uncertainty required to favour a slow route with low uncertainty over a fast route with high uncertainty. The uncertainty present in, e.g., the driving speed causes a significant deviation of the actual driving time from the corresponding expected value. The fourth case study measured how high this uncertainty has to become before a solution with high reliability is preferred over a solution with high uncertainties. From the results, it became clear that this also depends on the ambient temperature, while the ambient temperature influences the energy consumed due to the cabin climate control. In general, it can be concluded that a relatively high uncertainty is required to favour the slower and more reliable route above the fast and uncertain route.

Chapter 7

Conclusions and Discussion

In this thesis, SDP is used to optimise the travel cost of an EV on long-haul trips when there exists uncertainty in waiting time and driving speed. SDP offers a good methodology to optimise the policy for EVs moving through a network with stochastic travel costs present. In the thesis, a simplification is used to improve the computation time of the SDP algorithm while having the same optimal policy as a result. In four extensive simulation-based case studies, the possibility of optimising the travel cost of an EV using the proposed method have been investigated. In this chapter, the research questions are answered, conclusions are drawn, and recommendations for future research are given.

7-1 Conclusions

The main research question of the thesis is:

> How can the travel cost of an Electric Vehicle on long haul trips, with historical charging occupancy information and historical average road network travel speeds, be minimised?

To answer the main research question, the two sub-questions will be answered first:

1. *What factors influence the travel costs of the Electric Vehicle on long-haul trips?*

   Many aspects influence the travel costs of an EV on long-haul trips. First, there is the edge cost, which consists of the driving time and the energy consumption. The driving time is dependent on the driving speed and the link distance. The driving speed is modelled using a probabilistic approach in this thesis. By modelling the driving speed in a probabilistic way, the chance of disturbances in the traffic is incorporated in the probabilistic model.

   The energy consumption of an EV is also an important component. Several factors influence this energy consumption.

(a) The driving speed and driving distance. In general it holds that the higher the driving speed, the higher the energy consumption due to the propulsive power demand. Also, the longer a driving segment, the more energy has to be used to travel this segment.

(b) Active cooling or heating of the battery. The battery temperature is important for safety and charging efficiency. The battery temperature cannot become too high while driving since this could impose danger to the passengers. Furthermore, the battery temperature is of importance during the charging process. Low battery temperatures negatively influence the charging efficiency and should therefore be avoided upon arrival at a charging station.

(c) The ambient temperature. Due to the fact that the cabin climate has to be pleasant for the passengers. There is cooling or heating required for the cabin based on the ambient temperature. This energy consumption due to the cabin climate control can significantly influence the overall energy consumption while driving.

(d) The base auxiliary load. A certain amount of energy is required for all of the electronics on board of an EV. The longer the driving time, the more energy is spent on the auxiliary load.

The node cost significantly influences the total travel cost of an EV, while the node cost consists of the waiting time, the charging time, and the charging cost. In this thesis, the waiting times at a CS have been modelled using a time-dependent stochastic model. The waiting times can influence the travel cost, due to that EVs cannot start directly with charging upon arrival at a CS. Therefore, waiting times can influence travel costs without achieving any advantage.

The charging time has a very substantial impact on the travel cost. First, the EV will have to leave the main road to enter the CS. This CS could be next to the main road or, possibly the EV has to drive a substantial amount of time to reach the CS. After the charging process, the EV has to enter the main road again. Therefore, if an EV decides to have a charging event, travel costs are already incurred without having gained any SoC. Then, there is the charging event itself. The charging time is dependent on the amount of energy to be charged, the available charging power, the SoC, and the battery temperature. The amount of energy influences the charging time; however if the same amount of energy is charged, this does not necessarily imply that the same amount of charging time is incurred. The SoC can limit the maximum effective charging power that can be achieved. While the battery temperature below certain temperatures can negatively affect the charging time as well. Another factor that influences the charging time is the charging power. In general, higher charging power gives faster charging times; however, the SoC can limit this charging power.

Lastly, there is the charging cost. This corresponds to the cost to be paid for the received service and energy. The charging cost is dependent on the type of charger that is used. Higher charging power chargers can be more expensive than lower charging power chargers and the amount of energy that is charged, while mostly there is a price to pay per kW. A time-dependent charging price model was used in this thesis to capture price dynamics during the day.

2. *How can Stochastic Dynamic Programming be used in order to optimise the travel costs of an Electric Vehicle?*

   In the first case study, the proposed method was compared to one of the conventional methods for the route guidance of EVs. This case study showed that the proposed method can decrease the travel cost compared to the conventional method. A lower journey time can be achieved if one prefers the Fastest route. However, a more economical route, saving charging cost, can be achieved than the conventional method by using an Economical route preference.

   In the second case study, the possibility of optimising the driving speed below the maximum allowable driving speed was exploited. The results showed promising insights. It was observed in some situations that a lower journey time can be achieved if a lower driving speed than the maximum allowable driving speed is adapted. The driving speed influences energy consumption, and by adapting to a lower driving speed, the energy consumption can be reduced. This relates to the fact that by finding a good combination of the driving speed and the arrival time, either the charging time decreases or fewer charging events are required. If the decrease in charging time is bigger than the increase in driving time, it is profitable to adapt to a lower driving speed. From the results, it is also became clear that adapting to a lower driving speed is only appealing for certain ambient temperatures. There is high energy consumption for very low ambient temperatures due to the cabin climate control. Hence, it may not be appealing to lower the driving speed since energy consumption would only increase instead of decrease.

   In the third case study, the model incorporated the possibility of choosing between two types of chargers: a super charger with a very high charging power and high charging cost and a fast charger with medium charging power and lower charging cost. The fact that the effective charging power depends on both the temperature and the SoC results in the fact that the super charger is not always the faster in terms of charging time. This is also what was seen in the result. It was observed that for the Fastest route preference, the fast charger was used in some cases. This means that, in some cases, it is at least as fast to use the fast charger instead of the super charger.

   In the fourth case, the sensitivity to uncertainty in the driving speed and the charging events has been investigated. Dealing with uncertainties is important for EVs, while it can be devastating for an EV if a CS has very high waiting times or can not deliver the expected charging power. This can possibly have a high impact on the travel costs of the EV and the choices that are made at the start of the journey. Therefore, it was investigated how high the uncertainties have to become to favour a more reliable but slower route over a faster route with high uncertainties.

Now that both the sub-questions are answered, the main research question of this thesis can be addressed. It is not simple to formulate a concrete answer on how the travel costs of an EV can be minimised. In the research, it became clear that many aspects influence the travel costs of an EV. Prominent in the first place is the energy consumption of an EV. The energy consumption determines all aspects of the EV, the amount of energy to be charged, the place to charge, and even the type of charger to use. It is, therefore, essential to be able to model the energy consumption of an EV with high precision. However, this is difficult while the energy consumption consists of many parts, such as the energy consumption for the cooling and heating of the battery, the energy consumption due to the cabin climate control and the energy consumption due to the propulsive power demand.

From the results, it became clear that to optimise the journey time, it is in some cases faster to split up a big charging event into two smaller charging events. Conventional route guidance methods for EVs use a charging strategy that does not allow these smaller charging events. However, it has multiple advantages. For example, in low range SoC, the battery can be charged with a higher power, while in contrast, high SoC results in a reduced power to charge the battery. Therefore, it can be advantageous to have multiple charging events in low SoC ranges instead of a big charge event covering both low SoC ranges and high SoC ranges. This positively affects the charging time, even though the charging penalty is incurred multiple times instead of once. Another advantage is the possibility to optimise the departure time at a CS. The departure time at a CS influences the expected driving speed in the following segments. For example, by having two small charging events, the EV can have its first charging event at a CS such that when it leaves the CS, there is a low possibility of congestion, and when the EV has passed the segment with a high chance of congestion, the second small charging event can be held.

Moreover, from the case studies, multiple conclusions can be drawn. Since the energy consumption of EVs is very determinative for the travel cost, the possibility of adopting a lower driving speed than the maximum allowable driving speed showed promising results. By lowering the driving speed, in the right ambient conditions, energy can be saved such that a faster journey time can be achieved.

Also, the selection of the charger type has shown interesting results. Since the super charger delivers a much higher charging power, one would easily assume that this also gives the fastest charging time. Therefore, a person who has the Fastest route preference might be tempted to always use the super charger instead of the fast charger. The result, however, showed that also for the Fastest route preference, in some situations, using the fast charger rather than the super charger may be a better option. While in some cases, due to the SoC, the fast charger is at least as fast as the super charger. Hence, it may result in an equal charging time as the super charger, while paying less for the charge, as the super charger is generally more expensive than the fast charger.

In general, electric driving will need a change of mindset for people. Letting go of the old habits and beliefs that have been created using ICEV. The travel costs of EVs can be reduced using the right insights, compared to conventional methods to optimise the routes of EVs, it is, however, a very delicate problem.

7-2 Future Work

Although this thesis showed some promising results, there are some suggestions for future work:

More detailed energy consumption model

The proposed method includes all aspects of the energy consumption related to an EV. Nonetheless, the used energy consumption models use, for example, the average driving speed of the EV to calculate the energy consumption required for the propulsive power. However, during the acceleration phases of driving with an EV, the energy consumption due to propulsive power demand can be higher than the energy consumption assumed for the average driving speed. Since the energy consumption is of very high importance for the travel cost of the EV, it would be interesting to use more detailed energy consumption models. For example, instead of using a fixed energy consumption based on the ambient temperature, a more sophisticated model that could incorporate how many persons there are in the car or likewise can be used for the cabin climate control.

More detailed battery thermal model

To model the battery temperature, a lumped capacity model was used. Although this model is quite accurate, some assumptions were made modelling the battery temperature. For example, it was assumed that the battery could be seen as a single mass with a uniform temperature distribution. Nonetheless, the battery consists of various components, each having its own mass with a non-uniform temperature distribution. Incorporating a more detailed battery thermal model could improve the model's performance.

Realistic charging station characteristics

Numerous CS characteristics are of importance. For the simulations, probabilistic waiting times have been used. Because there is very limited to no data available on the waiting times at CSs, these probabilities are just a mere estimation. For the model's accuracy, it would be desirable to have more realistic waiting time probabilities. Also, the available charging power in the model, except for case study D, was assumed to be a fixed value. However, it would be interesting to incorporate a realistic prediction of the charging power received, which can have a spatial and time dependency, since this is very important to calculate the expected charging time. In the simulations, also, it was assumed that there were no spatial dependencies, for example, for the charging price. Although this does not influence the working of the model, it does influence the model's outcome. To create a more realistic outcome, spatial dependencies could be added to the model.

Real-time traffic information

In the simulations, probabilistic models are used for the driving speed. It would be interesting to include the possibility of real-time traffic information to influence the probabilistic distributions of the driving speed. This would increase the accuracy of the model and give more realistic outcomes. Also, this would open up the option of re-optimising during the driving, which is favourable for long-haul trips.

More realistic traffic networks

During the simulations, fictional traffic networks were used. To increase the model's accuracy, more realistic traffic networks should be used. For example, altitude differences in segments could be included and the length of segments. However, the inclusion of realistic networks is not problematic with the model.

Bibliography

[1] D. P. Bertsekas. *Reinforcement learning and optimal control.* Athena Scientific, 2019.

[2] S. A. Birrell, A. McGordon, and P. A. Jennings. Defining the accuracy of real-world range estimations of an electric vehicle. *17th IEEE International Conference on Intelligent Transportation Systems, ITSC 2014*, pages 2590–2595, 2014.

[3] S. Cheon and S. J. Kang. An electric power consumption analysis system for the installation of electric vehicle charging stations. *Energies*, 10(10), 2017.

[4] T. Conway. On the Effects of a Routing and Reservation System on the Electric Vehicle Public Charging Network. *IEEE Transactions on Intelligent Transportation Systems*, 18(9):2311–2318, 2017.

[5] M. De Weerdt, S. Stein, E. H. Gerding, V. Robu, and N. R. Jennings. Intention-Aware Routing of Electric Vehicles. *IEEE Transactions on Intelligent Transportation Systems*, 17(5):1472–1482, 2016.

[6] E. Figenbaum. Analysis of fast charger usage. *TØI Report*, pages 1–79, 2019.

[7] Q. Guo, S. Xin, H. Sun, Z. Li, and B. Zhang. Rapid-charging navigation of electric vehicles based on real-time power systems and traffic data. *IEEE Transactions on Smart Grid*, 5(4):1969–1979, 2014.

[8] C. Huber and R. Kuhn. *Thermal management of batteries for electric vehicles.* Elsevier Ltd, 2015.

[9] E. Jafari and S. D. Boyles. Multicriteria stochastic shortest path problem for electric vehicles. *Networks and Spatial Economics*, 17(3):1043–1070, 2017.

[10] C. Ji, Y. Liu, L. Lyu, X. Li, C. Liu, Y. Peng, and Y. Xiang. A personalized fast-charging Navigation strategy based on mutual effect of dynamic queuing. *IEEE Transactions on Industry Applications*, 56(5):5729–5740, 2020.

[11] A. W. F. Kemp. The discrete half-normal distribution. In *Advances in mathematical statisctical modeling*, pages 353–360. Birkhäuser, Boston, 2006.

[12] Y. Kobayashi, N. Kiyama, H. Aoshima, and M. Kashiyama. A route search method for electric vehicles in consideration of range and locations of charging stations. In *IEEE Intelligent Vehicles Symposium, Proceedings*, number I, pages 920–925. IEEE, 2011.

[13] W. Lee, L. Xiang, R. Schober, and V.W.S. Wong. Analysis of the behavior of electric vehicle charging stations with renewable generations. *IEEE International Conference on Smart Grid Communications, SmartGridComm*, pages 145–150, 2013.

[14] X. Li, H. Kan, X. Hua, and W. Wang. Simulation-based electric vehicle sustainable routing with time-dependent stochastic information. *Sustainability*, 12(6), 2020.

[15] C. Liu, M. Zhou, J. Wu, C. Long, and Y. Wang. Electric Vehicles En-Route Charging Navigation Systems: Joint Charging and Routing Optimization. *IEEE Transactions on Control Systems Technology*, 27(2):906–914, 2019.

[16] H. Liu, Z. Wei, W. He, and J. Zhao. Thermal issues about Li-ion batteries and recent progress in battery thermal management systems: A review. *Energy Conversion and Management*, 150(August):304–330, 2017.

[17] C. Luo, Y. F. Huang, and V. Gupta. Stochastic dynamic pricing for EV charging stations with renewable energy integration and energy storage. *arXiv*, 9(2):1494–1505, 2018.

[18] K. B. Naceaur and J. Gagné. Global EV outlook. *International Energy Agency (IEA)*, 2016.

[19] J. Neubauer and E. Wood. Thru-life impacts of driver aggression, climate, cabin thermal management, and battery thermal management on battery electric vehicle utility. *Journal of Power Sources*, 259:262–275, 2014.

[20] W. B. Powell. *Approximate Dynamic Programming*. Wiley & Sons, Hoboken, New Jersey, 2011.

[21] Z. Rezvani, J. Jansson, and J. Bodin. Advances in consumer electric vehicle adoption research: A review and research agenda. *Transportation Research Part D: Transport and Environment*, 34:122–136, 2015.

[22] K. Sarrafan, K. M. Muttaqi, D. Sutanto, and G. E. Town. An Intelligent Driver Alerting System for Real-Time Range Indicator Embedded in Electric Vehicles. *IEEE Transactions on Industry Applications*, 53(3):1751–1760, 2017.

[23] S. Schoenberg and F. Dressler. Planning Ahead for EV: Total Travel Time Optimization for Electric Vehicles. *IEEE Intelligent Transportation Systems Conference, ITSC 2019*, pages 3068–3075, 2019.

[24] B. Shabani and M. Biju. Theoretical modelling methods for thermal management of batteries. *Energies*, 8(9):10153–10177, 2015.

[25] G. van der Poel. De ontwikkeling van snelladers in Nederland t/m 2025. Technical report, ElaadNL, 2019.

[26] Q. Wang, B. Jiang, B. Li, and Y. Yan. A critical review of thermal management models and solutions of lithium-ion batteries for the development of pure electric vehicles. *Renewable and Sustainable Energy Reviews*, 64:106–128, 2016.

[27] Y. Wang, J. Bi, W. Guan, and X. Zhao. Optimising route choices for the travelling and charging of battery electric vehicles by considering multiple objectives. *Transportation Research Part D: Transport and Environment*, 64(3):246–261, 2018.

[28] Z. Yi and P.H. Bauer. Optimal stochastic eco-routing solutions for electric vehicles. *IEEE Transactions on Intelligent Transportation Systems*, 19(12):3807–3817, 2018.

Glossary

List of Acronyms

EV	Electric Vehicle
SoC	State of Charge
ITS	Intelligent Transportation Systems
CS	Charging Station
PDF	Probability Density Function
DP	Dynamic Programming
ICEV	Internal Combustion Engine Vehicles
SDP	Stochastic Dynamic Programming
HVAC	Heat, Ventilation and Air Conditioning
SPO	Speed Optimization